INAUGURAL DISSERTATION

submitted to the

Combined Faculties for the Natural Sciences and for Mathematics

of the Ruperto-Carola University of Heidelberg, Germany

for the degree of

Doctor of Natural Sciences

presented by

Dominik Dorer

Diplom Molekular Mediziner

born in: Stuttgart, Germany

Date of oral examination: ……

DEVELOPING NOVEL STRATEGIES FOR ONCOLYTIC ADENOVIRUS THERAPY BY HOST CELL GENE EXPRESSION PROFILING AND ARMING WITH THERAPEUTIC ANTIBODIES.

This work was carried out at the
German Cancer Research Center (DKFZ), Applied Tumor Virology

First referee: PD. Dr. Suat Özbek
Faculty of Biosciences, Heidelberg University

Second referee: PD Dr. Dirk M. Nettelbeck
Helmholtz University Group "Oncolytic Adenoviruses", DKFZ and
Department of Dermatology, Heidelberg University Hospital

THESIS DECLARATION

Hereby, I declare that the submitted work has been completed by me, the undersigned, and that I have not used any other than permitted reference sources or materials nor engaged in any plagiarism. All references and other sources used by me have been appropriately acknowledged in the work. I further declare that the work has not been submitted for the purpose of academic examination, either in its original or similar form, anywhere else.

Heidelberg, 10.02.2011

Dominik Dorer

“Time is a companion that goes with us on a journey. It reminds us to cherish each moment, because it will never come again. What we leave behind is not as important as how we have lived.”

Jean-Luc Picard

ABSTRACT

Oncolytic adenoviruses are promising candidates for treatment of various cancer entities with a favorable safety profile and therapeutic efficacy in individual cases. However, it has been neglected so far to investigate whether the observed varying efficacy in clinical trials could be due to differences in the cellular environment, between tumor cells and the virus's natural host cells, which may influences successful virus replication. My aim was to analyze wild type adenovirus 5 infections in primary human bronchial epithelial cells and various tumor cells by microarray analysis in order to reveal pathways that differentially affect oncolytic adenovirus replication. Kinetics of early viral gene expression and DNA replication together with cytotoxicity assays showed that primary bronchial epithelial cells optimally supported adenovirus infection. In contrast, infection of the two melanoma cell lines SK-MEL-28 and Mel624 revealed delayed early viral gene expression and slower DNA replication and decreased cytotoxicity. Microarray analysis of these melanoma cells versus primary bronchial epithelial cells led to the identification of differentially expressed genes and activated cellular pathways. The most prominent one, called the G1/S-phase transition pathway, was strongly activated in the primary bronchial epithelial cells but not in melanoma. The data helped to develop a strategy which enhanced viral replication in SK-MEL-28 cells by combining chemotherapy using temozolomide and viral oncolysis.

Another aim of my work was to enhance therapeutic efficacy of oncolytic adenoviruses by combining viro- and antibody therapy. Therefore, I armed tumor-selective adenoviruses with a gene encoding a recombinant single-chain antibody directed against the well-established carcinoembryonic antigen. As effector domain the constant domain of immunoglobulin type G 2a was selected which is able to mediate anti-tumor immune cell activation by antibody-mediated cytotoxicity. First, different tools to facilitate efficient antibody production via the adenoviral major late promoter were compared, identifying an internal ribosomal entry site and a splice acceptor from the human adenovirus 40 as the most potent ones. Then, antibodies expressed after infection with recombinant adenoviruses were analyzed by Western Blot, ELISA, and flow cytometry. These assays demonstrated that the recombinantly produced antibodies were fully functional regarding their ability to bind the carcinoembryonic antigen *in-vitro* and on living tumor cells.

ZUSAMMENFASSUNG

Die virale Onkolyse oder Virotherapie ist ein vielversprechender Ansatz zur Behandlung von Krebserkrankungen und wurde unter anderem klinisch getestet für onkolytische Adenoviren. Jedoch schwankt die therapeutische Wirksamkeit von Fall zu Fall, was daran liegen könnte, dass Krebszellen nicht die natürlichen Wirtszellen von Adenoviren sind. Ziel meiner Doktorarbeit war es Adenovirus 5 Infektionen in ihrem natürlichen Umfeld primärer Bronchialepithelzellen und verschiedener Krebszellen zu untersuchen, um Gene und zelluläre Signalwege zu finden, die einen Einfluss auf die adenovirale Replikation haben. Unter anderem konnte ich zeigen, dass in Bronchialepithelzellen die frühe virale Genexpression und DNA Replikation sehr schnell einsetzt, verbunden mit einer hohen Zytotoxizität. Dagegen war die frühe virale Genexpression als auch die DNA Replikation in zwei Melanomzelllinien stark verlangsamt, verbunden mit einer geringen Zytotoxizität. Genexpressionsanalysen mittels Microarray in infizierten Bronchialepithelzellen und jener Melanomzelllinien konnten zeigen, dass in den jeweiligen Zelltypen unterschiedliche Expressionsmuster einzelner Gene und zellulärer Signalwege vorlagen. Der am stärksten beeinflusste Signalweg reguliert den Eintritt in die S-Phase des Zellzyklus und war in den primären Bronchialepithelzellen aktiviert, aber nicht in den Melanomzelllinien. Anhand der Daten konnte eine Strategie zur verbesserten Onkolyse in einzelnen Melanomzelllinien entwickelt werden. Dafür wurden Adenovirus infizierte Melanomzellen zusätzlich mit dem Chemotherapeutikum Temozolomid behandelt.

Ein weiteres Ziel meiner Arbeit war es, die Wirksamkeit onkolytischer Adenoviren durch die Expression von therapeutischen Antikörpern zu verbessern. Dafür habe ich tumor-spezifische Adenoviren mit einem rekombinanten „single-chain“ Antikörper-Gen ausgerüstet. Die Antikörper erkennen das Tumor-assoziierte karzinoembryonale Antigen und verfügen außerdem über die Effektordomäne des Typ G Immunglobulins 2a, um eine Antikörper vermittelte Immunantwort gegen Krebszellen zu richten. Zuerst wurden verschiedene Expressionskonstrukte für eine optimale Antikörperproduktion mit dem adenoviralen „major late promoter“ getestet. Dabei wurden zwei effiziente Expressionskonstrukte identifziert, die sogenannte „internal ribosomal entry site“ und ein Spleiß-Akzeptor des humanen Adenovirus 40. Anschließend wurden die rekombinant hergestellten Antikörper im Western Blot, ELISA und mittels Durchflusszytometrie auf ihre Funktionalität geprüft. Eine erfolgreiche Antikörper-Antigen Reaktion konnte *in-vitro* als auch anhand lebender Tumorzellen gezeigt werden.

TABLE OF CONTENTS

ABBREVIATIONS

40SA	human adenovirus 40 long fiber gene splice acceptor
ACTB	β-actin
APS	ammonium persulfate
AraC	arabinosyl-cytosine
BCL2	B cell lymphoma 2 protein
bp	base pairs
BPSA	human beta globin splice acceptor
$CaCl_2$	calcium chloride
CAR	coxsackie adenovirus receptor
CBP	CREB binding protein
CCND	cyclin D
CCNE	cyclin E
CD	cluster of differentiation
CDC25A	cell division cycle 25 A homologue
CDK	cyclin dependent kinase
cDNA	complementary deoxyribonucleic acid
CEA	carcinoembryonic antigen
CFSE	carboxyfluorescein diacetate succinimidyl ester
CMV	cytomegalovirus
CR	conserved region
CREB	cyclic adenosine monophosphate responsive element-binding
cRNA	complementary ribonucleic acid
DAVID	Database for Annotation, Visualization and Integrated Discovery
DKFZ	German Cancer Research Center
DMEM	Dulbecco's Modified Eagle Medium
DNA	deoxyribonucleic acid
dNTP	deoxyribonucleotide triphosphate
DPBS	Dulbecco's phosphate buffered saline
EDTA	ethylenediaminetetraacetic acid
ELISA	enzyme linked immunosorbent assay
FACS	flow cytometry activated cell sorting

Fc	crystallizable fragment
G1-phase	gap or growth phase 1
G2-phase	gap or growth phase 2
GAPDH	glyceraldehyde-3-phosphate dehydrogenase
gfp	enhanced green fluorescent protein
GO	gene ontology
HAdV	human adenovirus
HBEC	primary human bronchial epithelial cells
HER2/neu	human epidermal growth factor receptor 2, neuregulin
HFF	human foreskin fibroblasts
HHV	human herpes virus
HPV	human papilloma virus
HSPG	heparan sulfate proteoglycan
hTK	human thymidine kinase
IgG	immunoglobulin G
IMAC	immobilized metal affinity chromatography
IPA	Ingenuity Pathway Analysis
IRES	internal ribosomal entry site
kb	kilo base pairs
KCl	potassium chloride
KH_2PO_4	potassium dihydrogen phosphate
LB	Luria Bertani medium
M-CHiPS	Multi-Conditional Hybridization Intensity Processing System
MDM2	murine double minute 2
MEM	Minimal Essential Medium
MeV	Multi-Experiment Viewer
$MgCl_2$	magnesium chloride
$MgSO_4$	magnesium sulfate
MLP	major late promoter
MOI	multiplicity of infection
M-phase	mitosis phase
MRE11	meiotic recombination 11 homolog
MRN	complex of MRE11/RAD50/NBS1

mRNA	messenger ribonucleic acid
MUC1	mucin 1
MWCO	molecular weight cut off
Na_2HPO_4	sodium dihydrogen phosphate
NaCl	sodium chloride
NaN_3	sodium azide
NBS1	Nijmegen breakage syndrome protein 1
ORF	open reading frame
PCR	polymerase chain reaction
PHK	primary human keratinocytes
PI	propidium iodide
pIIIaSA	human adenovirus 2 L1 pIIIa splice acceptor
PMSF	phenylmethylsulfonyl fluoride
pRB	retinoblastoma protein
qPCR	quantitative real time polymerase chain reaction
RAD50	DNA repair protein RAD50 homologue
RGD	arginine-glycine-aspartate
RNA	ribonucleic acid
RPMI	Roswell Park Memorial Institute 1640
$scFv_{CEA}$-Fc	single-chain antibody against the carcinoembryonic cancer antigen fused to the mouse heavy chain gamma 2 constant region
SDS	sodium dodecyl sulfate
SDS-PAGE	discontinuous sodium dodecyl sulfate polyacrylamide gel electrophoresis
siRNA	small interfering ribonucleic acid
S-phase	synthesis phase
SV40	simian virus 40
$TCID_{50}$	tissue culture infectious dose 50
TP53	tumor suppressor protein 53
v/v	volume / volume
v-cyc	viral cyclin
w/v	weight / volume
wt	wild type
YB1	Y-box binding protein 1

I INTRODUCTION

1 History of cancer

Cancer is a leading cause of death worldwide responsible for about eight million deaths in 2007 according to the World Health Organization [1]. Furthermore, numbers are expected to rise to twelve million deaths by the year 2030, most of them occurring in countries with low or moderate income. The disease may affect any part of the human body and can be defined as abnormal growth of cells which eventually invade neighboring tissue or spread throughout the body, referred to as metastasis. Nevertheless, primary tumor sites are most frequently found in lung, stomach, liver, colon and breast depending on sex and age.

Mankind has long been suffering from cancer which is evident in fossilized bone tumors, mummies, and ancient manuscripts. The oldest description of tumors dates back to about 1550 B.C. and was discovered in an Egyptian papyrus believed to contain parts of a 3000 year old textbook on trauma surgery [2]. Despite the medical knowledge gained over centuries, it was not before the 19th and early 20th century that major breakthroughs in surgery were made allowing the resection of primary tumors. Along with the discovery of X-rays in 1895 and radium in 1898 [3], physicians experimented with radiation therapy which led to a cure for some inoperable cancers and established diagnostic imaging, additionally. Later during World War II, it was noted that soldiers exposed to mustard gas suffered from loss of white blood cells. Less toxic compounds like nitrogen mustard were discovered and found to be effective against lymph node cancers, which gradually led to the development of chemotherapy [4,5]. Over the following decades, considerable progress in cancer prevention and diagnosis has been made. Even so, the majority of malignancies nowadays remain refractory to current treatment regimens including various combinations of surgery, radiation, and chemotherapy. Moreover, established therapies often cause severe side-effects along with insufficient anti-tumor efficacy because they lack specificity for malignant cells. Especially disseminated tumors appear to be invincible due to incomplete eradication of the tumor burden and eventual re-growth resulting in unacceptable high mortality rates. Thus, there is a tremendous need for new, more effective but yet less toxic, treatment modalities to successfully fight cancer.

With the advent of molecular biology, our understanding of genes and proteins, as well as their regulation, synthesis, structure, and function within cellular networks has vastly improved. As a consequence, this knowledge helped scientists to identify and dissect molecular switches causative for diseases in humans, particularly for diseases with a complex etiology like cancer. Together with the rapidly developing fields of molecular techniques including recombinant DNA technology, therapeutic protein engineering, and pharmaceutical chemistry they often provide drug targets for novel, more specific and effective therapies. The last decades have witnessed several innovations which have found entry into clinical practice. Among them, therapeutic antibodies which bind to cell surface molecules aberrantly expressed on tumor cells, like the humanized monoclonal antibody Herceptin™ directed against the epithelial growth factor receptor 2 (*HER2/neu*) thereby mediating tumor cell death [6,7]. Lately, researchers and clinicians gained support from a yet unexpected side as several viruses, previously well known as causal agents for devastating diseases in humans, have emerged on the horizon as promising tools for cancer therapy.

2 Gene therapy and viral oncolysis

Upon the introduction of genetic engineering, scientists proposed a novel approach for the curative treatment of inherited genetic defects, which became known as gene therapy depicted in **Figure 1**. The idea is to replace a defective gene by implanting a functional one and thus correct mutations causing severe hereditary disorders. This requires the precise characterization of genetic malfunctions as well as the ability to engineer and introduce a correct gene copy into a target cell where it can be stably produced for an extended time. Regarding the gene transfer, several viruses are currently investigated as vectors. In general, viruses are intracellular parasites that depend on infection of a host cell to amplify and create progeny virions, referred to as the viral life cycle (*see below*). The viral particle basically consists of the viral genome, encoding regulatory and structural proteins, and an outer protein shell also known as capsid. This structure is typical for so-called naked viruses or enveloped viruses which have an additional lipid membrane surrounding the capsid. At the end of the viral life cycle, viral particles spontaneously assemble by packaging amplified viral genomes into newly synthesized capsids that are subsequently released from the infected cell. Since viruses have an inherent

ability to efficiently enter a cell and establish viral or, in case of gene therapy, therapeutic gene expression they are optimal tools for gene delivery [8]. Therefore, researchers usually engineer viruses devoid for their ability to replicate and cause toxic effects by replacing some essential or even all viral genes through a gene expression cassette containing the therapeutic gene of choice. Further, it is possible to exploit distinct properties of different viruses like adenoviruses that feature an episomal genome usually resulting in transient transgene expression or retroviruses that integrate their genome into the host cell's genome and provide long-term expression of a therapeutic gene.

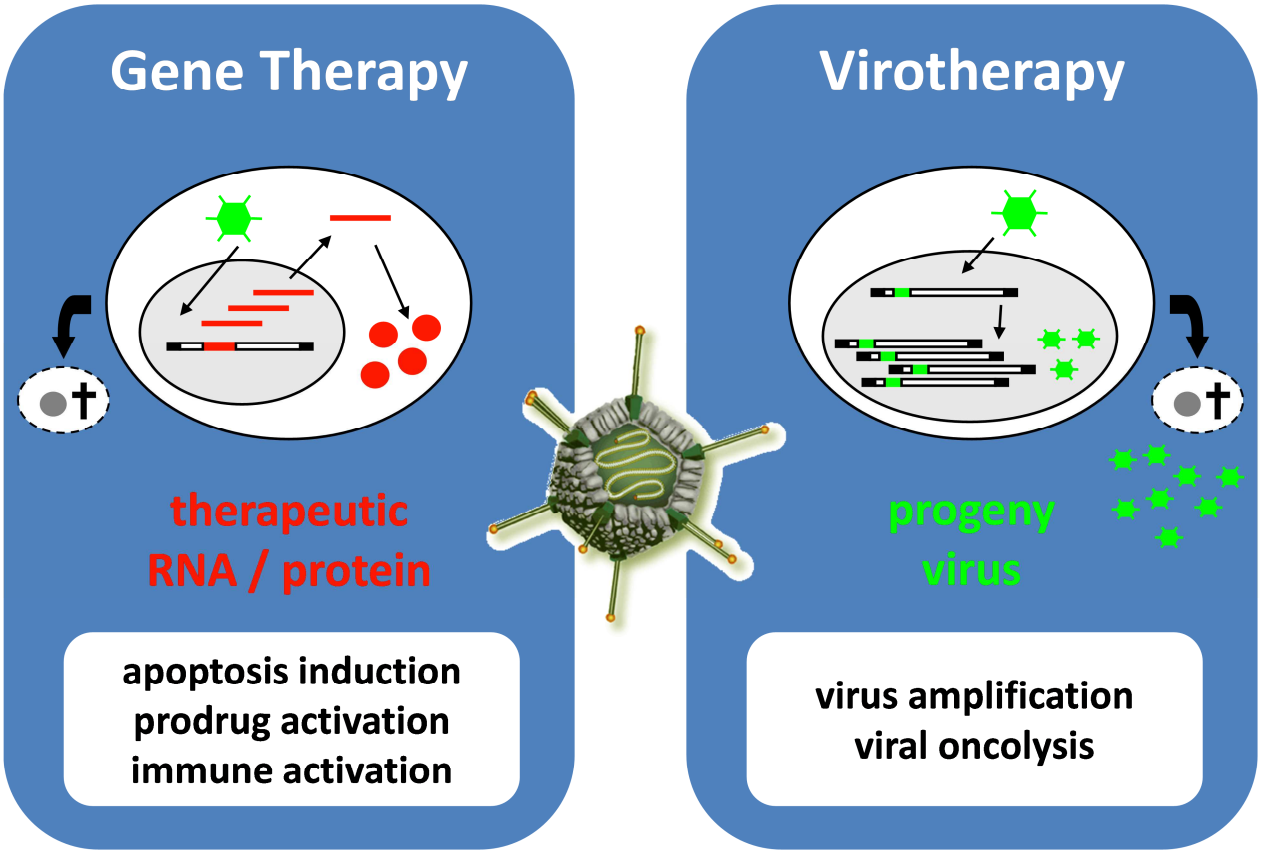

Figure 1| comparison of gene- and virotherapy: in cancer gene therapy, replication-deficient viruses or non-viral tools are being exploited as vectors for transfer of therapeutic genes which replace essential viral genes (*red, left panel*). For virotherapy, viruses feature replication-competency that is restricted to tumor cells and allows virus replication and generation of progeny (*green, right panel*). Thus, the major difference between both approaches is that for cancer gene therapy either therapeutic proteins or RNAs have to be introduced in order to kill tumor cells whereas in virotherapy the oncolytic virus directly is the antitumoral agent. *Modified from Dorer et al., Advanced Drug Delivery Reviews, 2009* [9].

Such a gene correction approach, however, is probably not ideal for cancer therapy for two reasons. For one, cancer is a complex genetic disease resulting from the accumulation of multiple mutations and thus correction of single genes would most likely not provide a clinical benefit. Nevertheless, the Chinese Food and Drug administration approved Gendicine for the treatment of head and neck cancers in 2003 [10,11]. This drug represents a replication-deficient adenovirus containing the wild type tumor suppressor protein 53 (*TP53*) gene, one of the most frequently mutated genes in all cancers therefore known as the guardian of the genome [12,13]. A similar gene therapy approach from Introgen, called Advexin, was turned down by the United States Food and Drug administration in 2008 [14,15]. The second reason is that successful therapies need to eradicate all cancer cells in the patient's body, but gene transfer into each cancer cell is technically extremely challenging if not impossible. In this regard, a promising approach is the transfer of genes encoding therapeutic proteins, which also affect the larger percentage of malignant cells that do not obtain the transgene, an activity called "bystander effect". Ideally, this manifests in direct or indirect activation of a specific program which forces the cancer cell to commit suicide, known as programmed cell death or apoptosis. Examples are transgenes encoding secreted, apoptosis-inducing proteins such as human tumor necrosis factor related apoptosis-inducing ligand [16], stimulatory factors for systemic anti-cancer immune activation such as granulocyte macrophage colony-stimulating factor [17], or genes encoding prodrug-activating enzymes like yeast cytosine deaminase able to convert a systemically applied non-hazardous drug precursor into its toxic form [18]. Genetic prodrug-activation, if spatially restricted to tumors, should result in high local drug concentrations able to kill the tumor cells which otherwise cannot be reached by systemic application of the drug because of its limiting side-effects on healthy tissue. Since the mechanism of action for most of such therapeutic gene encoded proteins is not tumor-specific, targeted gene therapy must result from selective transfer/expression of the therapeutic gene [9]. Consequently, strategies to deliver the genetic payload to a target cell in a selective manner by a vector are pivotal for cancer gene therapy (*refer to I, 3.3*).

Besides conventional gene therapy, recombinant viruses have been intensively investigated in the past two decades for yet another strategy of targeted cancer treatment, namely viral oncolysis (*also termed virotherapy, **Figure 1***) [19]. Viral oncolysis can be defined as the killing of tumor cells by selective viral infection, replication, cell lysis, and spread of progeny

viruses in the tumor. Thus, as opposed to gene therapy where viruses are used as tools for gene transfer, the virus itself is the therapeutic agent. Anti-cancer activity of viruses has been investigated for almost 100 years [20]. The renaissance of this field in recent years resulted from advances in knowledge about the interplay between viruses and hosts on the molecular level, combined with the ability of genetic engineering in order to specifically tailor viruses for applications in viral oncolysis. A growing arsenal of different viruses, which feature differences in their natural tropism, lytic properties, pathogenicity, and opportunities for genetic engineering, has been investigated for this application [21-23].

3 Human adenoviruses and their application for cancer therapy

Since the first isolation of more than 50 years ago by Rowe and Hilleman [24,25], many different variants of adenoviruses have been identified that are distinguished into four genera, of which the genus Mastadenovirus primarily infects mammals including humans. To date, more than 50 serotypes of human adenoviruses (*HAdV*) have been identified and sub-grouped into species A to F based on their DNA sequence homology, serological profile, and hemagglutination properties [26]. Most of the HAdVs cause acute respiratory (*species B1 and C*), gastrointestinal (*species A, F, and G*), ocular (*species D and E*), or urinary tract (*species B2*) infections which usually are self-limiting [27]. However, they may also cause severe complications in immunocompromised individuals especially in patients receiving liver transplants [28]. During the 1960's, researchers discovered that small DNA viruses including human adenoviruses can transform primary rodent cells *in-vitro* and induce tumors in rodents [29,30]. However, only cells that were transformed by species A or B adenoviruses were oncogenic in animals. In following studies, the event of transformation has been attributed to abortive infections of cells from non-host species and random genomic integration of viral DNA [31-33]. Moreover, the vast majority of primary human tumors lack any HAdV DNA suggesting that there is most likely no etiological link to cancer in humans [34]. In early stages of molecular biology research, adenoviruses have proven extremely useful as model system for revealing basic aspects of cell biology such as transcription initiation, messenger RNA (*mRNA*) splicing, and cell cycle regulation [35-37]. Overall, the HAdV serotypes 2 and 5 of the species C as well as oncolytic viruses derived from them are by far the most intensively characterized ones in terms of their

genome, structure, and biology and thus they serve as prototype for all other species. The following paragraphs focus on diverse aspects of their structure, life cycle, and use in cancer virotherapy.

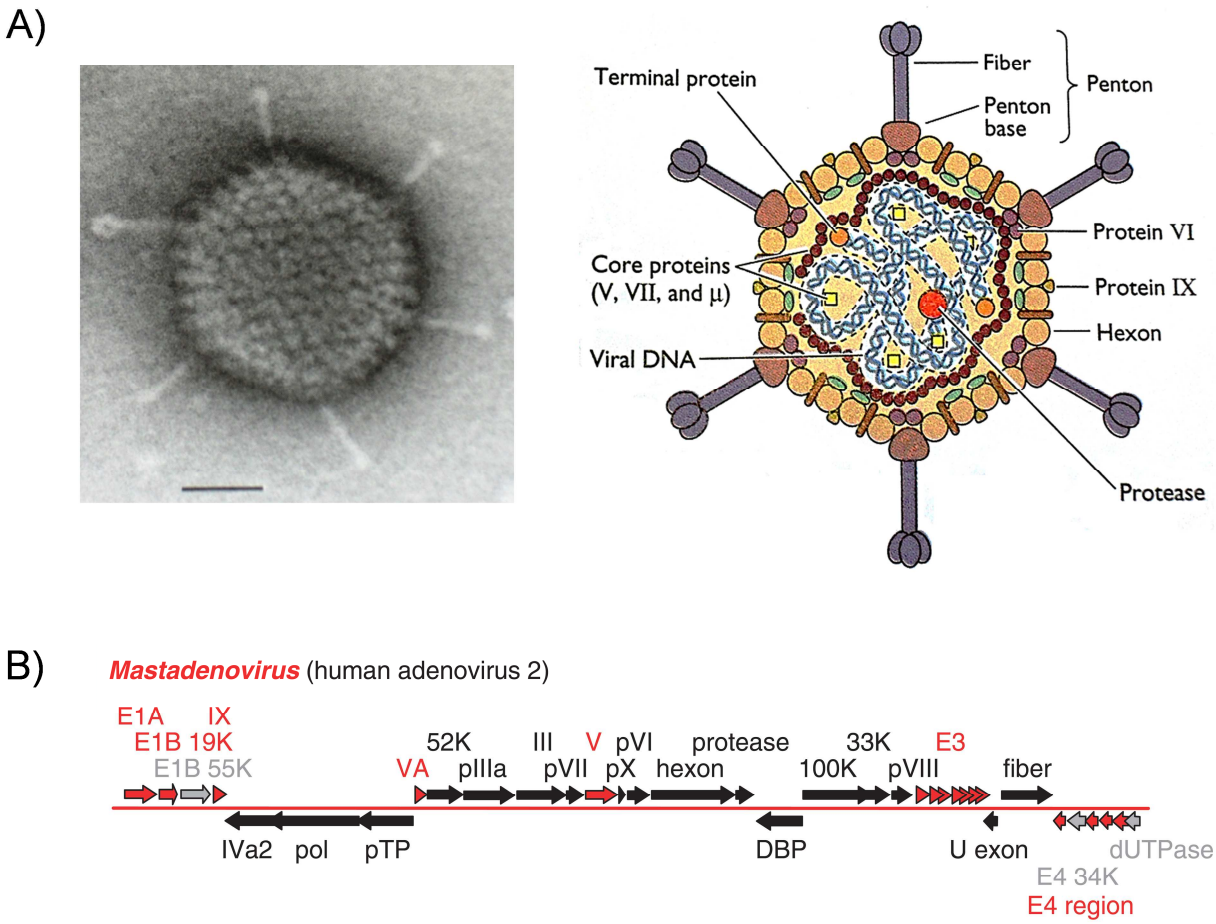

Figure 2| general structure & genome organization of human adenoviruses: A) electron micrograph (*left*) from a HAdV-5 capsid showing the triangular faces built of hexon trimers which constitute the icosahedral shell, antenna like fibers protrude from the vertices, bar = 50 nm. Diagram (*right*) shows the virus capsid composed by various major (*hexon, penton and fiber*) and minor structural proteins (*VI and IX*). Located inside is the viral DNA associated with the core proteins (*V, VII, and μ*) and the viral protease. The adenovirus genome is inside encapsidated by the core proteins. *Modified from Flint's "Principles of Virology", second edition.* **B)** schematic drawing of the linear HAdV-2 genome, which is identical to HAdV-5 regarding the genome organization. Black arrows depict conserved genes in all adenovirus genera, grey arrows show genes known to exist in more than one genus, and red arrows are unique for Mastadenoviruses. *Modified from Harrach's Encyclopedia of Virology, 2008.*

3.1 Structure and genome organization

Adenoviruses possess a double stranded, linear genome of about 36 kilo base pairs (*kb*) which is tightly associated with the core proteins V, VII and µ (*see* ***Figure 2***) [38,39]. At each end of the viral genome inverted terminal repeats are located which are covalently joined to the terminal proteins. Furthermore, the viral genome is encased in an icosahedral protein capsid of about 70-90 nm in diameter which is not covered by a lipid membrane. Hence, adenoviruses are classified as naked or non-enveloped viruses. The capsid consists of three major structural components, the hexon, penton, and fiber and some accessory minor capsid proteins [40]. The most abundant protein is the hexon forming 240 trimers that constitute twenty equilateral triangular faces converging into twelve vertices. At each vertex, a pentameric complex of penton base proteins is located. These complexes provide a scaffold for the antenna like fiber proteins which give adenoviruses their typical look. The fiber is a homotrimeric glycoprotein consisting of three domains, the tail which binds to the penton bases, a long flexible shaft and the knob domain. Both, penton and fiber proteins play important roles in cell binding and entry of the virus (*refer to I, 3.2*) [39].

The adenoviral genome is organized in several independent transcriptional units which are active in a timely defined cascade (*see* ***Figure 2***). Upon infection the early genes (*E1A, E1B, E2A, E2B, E3, and E4*) are the first to be transcribed and expressed. Among them are several distinct E1A isoforms named 13S, 12S, 11S, 10S, and 9S according to their sedimentation coefficient measured by the Svedberg unit [41]. They mainly act as transcriptional activators on adenoviral and cellular genes but also fulfill various functions in repression of cellular genes, regulation of the cell cycle, and apoptosis [41-44]. The other early adenoviral genes encode mainly proteins needed for prevention of apoptosis (*E1B*), viral DNA replication (*E2A, E2B, and E4*), host cell protein synthesis shut off (*E1B and E4*), and suppression of the immune response (*E3*) as discussed in the next section. Moreover, four intermediate transcription units are known containing the IX gene, encoding a regulatory and minor capsid protein, as well as the IV2a gene which codes for an essential protein for packaging and capsid assembly [40,45]. Besides, two genes of the VA locus are transcribed into non-coding RNAs of approximately 200 base pairs (*bp*) by the cellular RNA Polymerase III which act on mRNA translation and counteract the host defense [46,47]. With the onset of viral genome replication, the major late

promoter (*MLP*) drives expression of five late mRNA transcripts (*L1, L2, L3, L4, and L5*) resembling mostly diverse structural proteins like the penton, hexon, and fiber but also a few regulatory proteins like the L4-100k protein, all of which are alternatively spliced and polyadenylated [48,49].

3.2 Adenoviral life cycle

The first step in adenovirus infection, schematically shown in **Figure 3**, is binding of the virus particle to its host cell. Therefore, the virus attaches to ubiquitously expressed cellular heparan sulfate proteoglycans (*HSPG*) which function as co-receptors [50,51]. Despite some controversy about the function, it was found that HAdV serotypes 2 and 5 possess a HSPG binding motif in the fiber shaft domain. Whereas many other serotypes, for example the HAdV-3 and HAdV-35, engage HSPGs either by the knob domain, the penton base, or a yet undefined binding site [52-54]. Subsequently, the virus keeps floating on the cellular surface until it comes in contact with its primary receptor. For most adenovirus serotypes including HAdV-5 this receptor is a transmembrane protein known as coxsackie adenovirus receptor (*CAR*), expressed in many human tissues including heart, lung, liver, and brain [55-57]. In contrast, species B adenoviruses lack a conserved CAR binding sequence in their fiber and were found to interact with the ubiquitously expressed cluster of differentiation (*CD*) molecule CD46 (*species B1*) or desmoglein-2 (*species B2*) [58,59]. Following interaction with CAR, cellular integrins bind to the penton base complex via an arginine-glycine-aspartate (*RGD*) motif found in all HAdV, except HAdV-40 and HAdV-41 [60,61]. This event triggers clathrin-dependent endocytosis of the adenovirus capsid and shedding of fiber proteins on the cell surface [62,63]. Inside the cell, the environment in early endosomes becomes acidic which leads to destabilization of the capsid structure and partial disassembly [62,64]. Thus, a predicted N-terminal amphipathic helix of the internal capsid protein VI is exposed and released, eventually, leading to membrane disruption and escape of the adenovirus capsid from the endosome [65]. Next, the metastable capsid is actively transported along microtubules towards the nuclear periphery where it docks onto the nuclear pore complex [66]. This event then leads to a complete disassembly of the capsid freeing the viral genome for import by the cellular machinery into the nucleus [67].

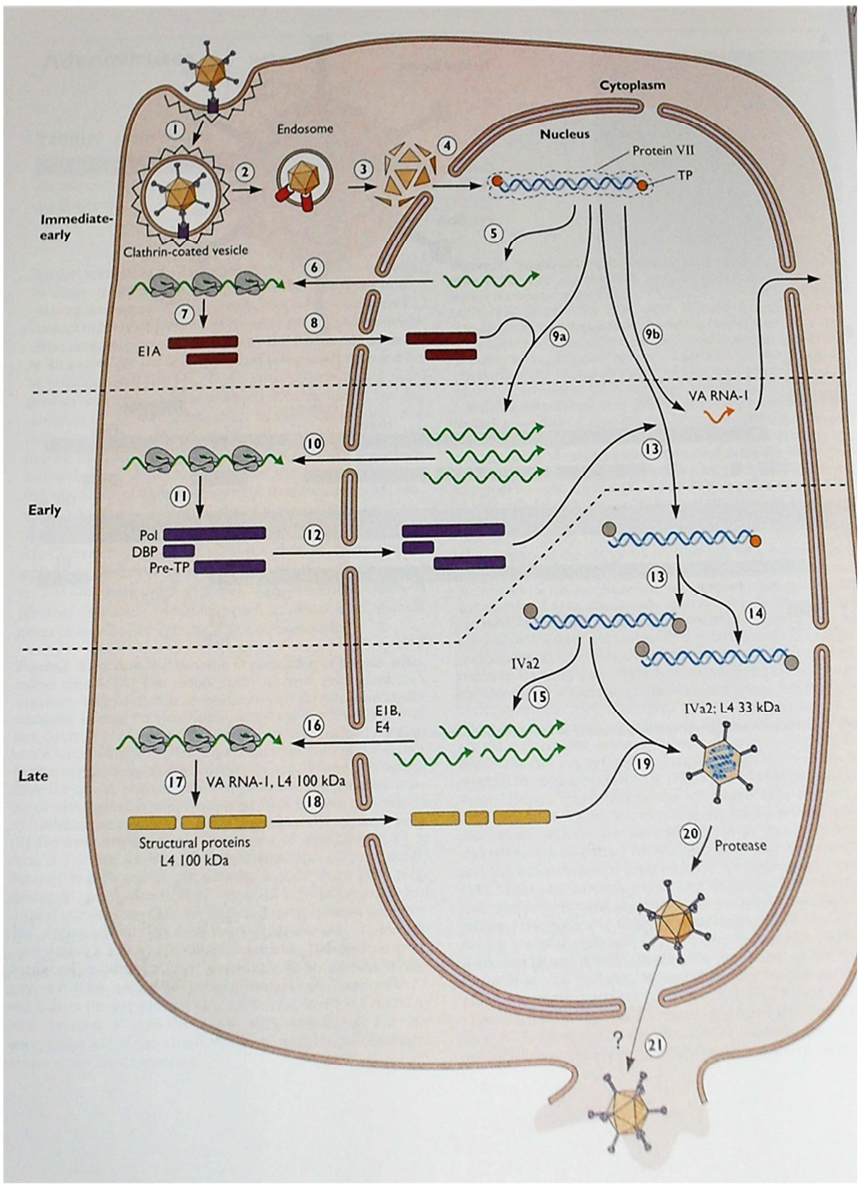

Figure 3| life cycle of human adenoviruses: upon binding of the HAdV-5 particle to the cellular CAR receptors (*1*), clathrin dependent endocytosis is triggered (*2*). Inside the cell, the capsid partially disassembles and escapes from acidic endosomes (*3 and 4*). Then, the viral genome is transported into the nucleus where the early gene E1A is transcribed (*5*). The E1A proteins in turn stimulate expression of further early genes and facility S-phase entry of the host cell (*6-12*). This leads to replication of the adenovirus DNA and expression of late structural genes (*13 and 15-18*). Progeny virus particles spontaneously assemble inside the nucleus and are filled with virus genomes (*19*). Finally, mature progeny particles leave the nucleus via an unknown mechanism and are released from the cell through disruption of the outer cellular membrane, a process called lysis (*20 and 21*). *Modified from Flint's "Principles of Virology", second edition.*

At this stage adenovirus infection is manifested through gradual expression and translation of the early genes. The most prominent one is the E1A gene which becomes differentially spliced to give rise to five distinct isoforms. The major variants 13S and 12S can be detected early on during infection and are the largest E1A proteins consisting of several conserved regions (*CR*) [41]. The smaller isoforms 11S, 10S, and 9S are expressed late during infection and their function is no fully understood yet. Whereas the 13S and 12S proteins share the CR1 and CR2 domain, they differ in the zinc finger containing CR3 domain required for transcriptional activation of adenoviral or cellular genes [42,43]. The latter is absent in the

12S isoform. Furthermore, the CR1 regions binds proteins involved in chromatin structure control like p300 or CREB binding protein (*CBP*) which are highly related and contain histone acetyl transferase activity. In uninfected cells, p300/CBP interact with several DNA-binding transcription factors and activate expression of cellular genes [68]. Thus, binding by E1A can either repress or redirect transcriptional activity of p300/CBP which is still a controversial topic [44,69]. However, it is clear that E1A/p300/CBP causes acetylation of retinoblastoma protein (*pRB*) and association with the murine double minute 2 (*MDM2*) protein homologue which consequently inhibits TP53 [70]. Most importantly, CR1 and CR2 fulfill essential functions in cell cycle stimulation and entry into the synthesis phase (*S-phase*) of infected cells where DNA replication occurs. This is a fundamental aspect as adenoviruses, like the majority of viruses, are obligate intracellular parasites and therefore they depend on the cellular replication machinery in order to amplify their genome and create infectious progeny virions. In quiescent cells, the hypophosphorylated retinoblastoma protein normally sequesters and keeps E2F transcription factors, bound to promoter sequences, inactive. Upon a mitogenic stimulus, like binding of growth factors to relevant cell surface receptors, cells start to express cyclins (*overview in **Figure 4***) [71]. At the beginning of gap or growth phase 1 (*G1-phase*), the dominant family member is cyclin D (*CCND*) which binds to the cyclin dependent kinases (*CDK*) 4 and 6. In turn, the kinase activity leads to hyperphosphorylation of pRB. As a consequence, pRB undergoes a conformational change thereby E2F transcription factors, consisting of eight family members with activating and inhibiting properties, are released leading to expression of multiple cellular S-phase genes involved in cell cycle regulation, nucleotide metabolism, and DNA replication [37,72,73].

Two prominent examples are the cellular phosphatase cell division cycle 25 A homologue (*CDC25A*) and cyclin E (*CCNE*), which are necessary at late G1-phase to overcome a cellular restriction point and facilitate S-phase entry [74,75]. In S-phase, DNA replication occurs after which the cells reach the gap or growth phase 2 (*G2-phase*) and prepares to undergo cell division called mitosis (*M-phase*). During adenovirus infection, S-phase entry is triggered by binding of the 13S and 12S E1A proteins to hypophosphorylated pRB, mainly via the CR2 domain, and subsequent displacement of E2F from the binding pocket through competition of CR1 [76,77]. In addition, the E2F transcription factors, first discovered as trans-activating factors for the adenoviral early gene E2 promoter, activate early viral gene expression [78]. The

latter is complemented through E4 open reading frame (*ORF*) 6/7-19k and E1A proteins [79-81]. Hence, due to the pleiotropic effects of the E1A proteins on cellular and viral promoters they are often referred to as master regulators of adenovirus infection.

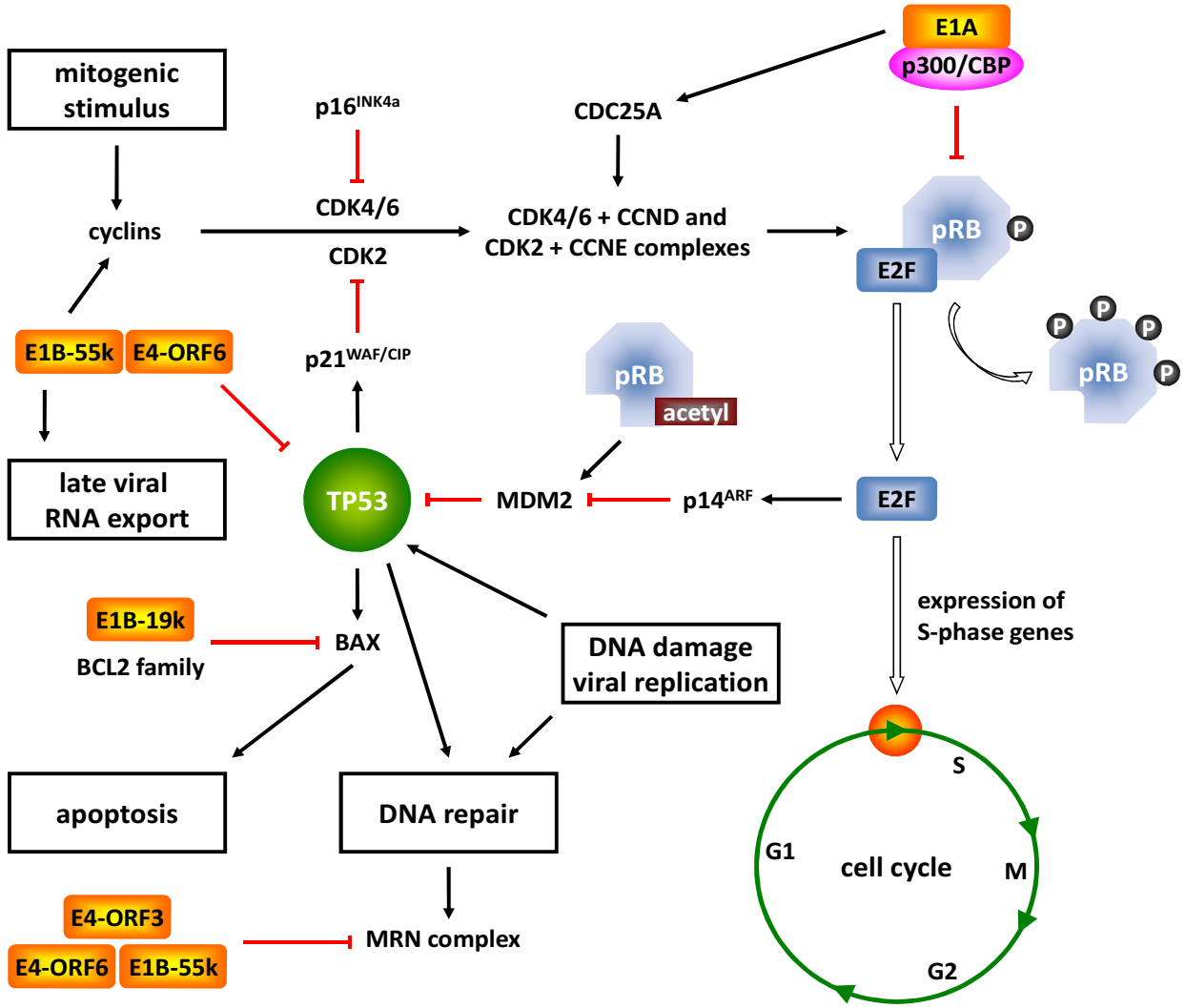

Figure 4| interactions of viral early proteins with cellular host factors for cell cycle regulation: in quiescent cells, the retinoblastoma protein pRB is hypophosphorylated and sequesters E2F transcription factors. Upon a mitogenic stimulus, cyclins become expressed and associate with CDKs which in turn phosphorylate pRB. Consequently, E2F is released, stimulates expression of S-phase genes, and promotes G1/S-phase transition. Unscheduled S-phase entry normally triggers cell cycle arrest via the tumor TP53 and $p21^{CIP/WAF}$, activation of DNA repair, or apoptosis. During adenovirus infection, E1A disrupts pRB/E2F complexes leading to S-phase entry and viral DNA replication. The expression and catalytic activity of the phosphatase CDC25A is also enhanced. Further, E1A binds p300/CPB proteins leading to acetylation of pRB which inhibits TP53 through MDM2. Premature cell death is counteracted by the early E1B proteins either by direct degradation of TP53 (*E1B together with E4-ORF6*) or by inhibiting pro-apoptotic proteins and TP53 independent apoptotic signals (*E1B-19k*). Replication of linear viral DNA elicits a cellular DNA damage response. The relevant double strand repair complex MRN is destructed by concerted actions of the viral E4-ORF3, E4-ORF6 and E1B-55k proteins which prevent concatemeric ligation of viral DNA. *Modified from Wong, Viruses, 2010* [71].

Nevertheless, unscheduled S-phase entry would normally lead to accumulation of TP53 and p21CIP/WAF, eventually resulting in cell cycle arrest and apoptosis (*refer to* ***Figure 4***). Instead, expression of the adenoviral E1B and E4 genes prevents premature cell death by mainly two strategies. On the one hand the E1B-55k isoform and E4-ORF6 sequesters and degrades TP53 [82-84], thus repression of the cell cycle is relieved and transcription of pro-apoptotic genes is diminished. On the other hand the smaller E1B-19k isoform, a viral homologue to the cellular anti-apoptotic B cell lymphoma 2 protein (*BCL2*), is produced which additionally counteracts TP53 independent apoptotic signals [85,86]. Besides cell cycle regulation and prevention of apoptosis, HAdVs have evolved various countermeasures to divert the host anti-viral immune response. Among them, two non-coding RNAs VAI and II are transcribed which form hairpin-loop like structures and inhibit the protein kinase R, a cellular sensor for viral infections [87]. In addition, the VAII RNA is required for efficient mRNA translation in late stages of adenovirus infection [46,47,88]. To counteract the innate and adaptive immune response, the early E3 genes are expressed. The glycoprotein E3-19k prevents viral antigen presentation via interaction with major histocompatibility complex I molecules [89]. This leads to endosomal retention of the complexes rather than transport to the cell surface where viral antigens would be accessible for natural killer cells and cytotoxic T cells [90]. Furthermore, E3 receptor internalization and degradation proteins α and β form a complex to block extrinsic cellular death pathways triggered through the FAS ligand or tumor necrosis factor related apoptosis-inducing ligand [91,92]. Both factors are readily expressed and/or secreted by cytotoxic T cells or monocytes, respectively [93]. While the cell cycle is progressing into S-phase, the linear viral genome is replicated by an adenovirus encoded polymerase and several other viral and cellular factors including the adenoviral DNA binding protein, nuclear factor I and III, as well as topoisomerase I [94]. First, the terminal proteins join through interaction of the adenoviral polymerase and nuclear factor III forming the circular pre-initiation complex. Then, protein priming by the terminal proteins and nuclear factor I enables DNA synthesis of the nascent strand. Thereby HAdVs solve the problem of replicating molecular ends found in linear genomes. Normally, linear DNA elicits a cellular DNA damage response which, if not inhibited by viral proteins, would lead to concatemeric ligation and inactivation of viral genomes by non-homologous end joining. Hence, the cellular MRN sensor complex consisting of

MRE11/RAD50/NBS1 proteins is relocalized to the cytosol by E4-ORF3 proteins where it is degraded through actions of E4-ORF6 and E1B-55k [95,96].

With initiation of viral genome replication, the major late promoter is strongly activated by increasing levels of the adenoviral IV2a protein and in turn drives expression of late genes through a yet unidentified cis-acting switch, presumably involving L4-22k and L4-33k proteins, meaning that late gene transcription takes place only from newly synthesized DNA [97,98]. At the same time, most gene expression from early promoters is diminishing. This results in accumulation of structural components within the cytoplasm and self-assembly of virus capsomers from individual hexons and penton proteins. These are eventually transported into the nucleus where replicated genomic DNA is condensed by viral core proteins and packaged into immature adenovirus capsids through the L1-52/55 kDa and IV2a proteins [99]. Accumulation of progeny virions gives rise to so-called inclusion bodies that can be visualized by histochemical staining in microscopy. Prolonged infection eventually leads to swelling and rounding up of the host cell due to virus mediated disruption of the cytoskeleton and subsequent cell lysis. This may be facilitated by the E3-11.6k adenovirus death protein capable of inducing apoptosis [100]. Finally, the adenovirus life cycle is completed with release of progeny virions from the infected cell and maturation of the capsid by the L3-23k protease [100,101].

3.3 Targeting human adenoviruses for cancer therapy

As previously mentioned, viruses can be generally used to fight cancer by therapeutic gene transfer or viral oncolysis. Therefore, tumor targeting represents an inherent and fundamental requirement for both treatment modalities which makes it a key consideration for the development of therapeutic viruses. The following principles generally apply for cancer gene therapy and virotherapy but will be discussed with a special focus on oncolytic adenoviruses. Some of the viruses under investigation have been reported to be naturally oncotropic such as parvoviruses, Vesicular Stomatitis Virus, or Newcastle disease virus [21,23,102]. Other candidates like adenovirus, herpes simplex virus or measles virus require genetic modification to be truly cancer specific [22]. In theory, tumor selectivity of oncolytic viruses can be achieved at multiple levels. Therefore, researchers could interfere either during virus cell binding

and entry (*entry targeting*) or after virus uptake (*post-entry targeting*). Diverse strategies and a plethora of cell type specific markers have been exploited to achieve tissue- or even tumor-specific viral transduction and infection, respectively.

Initial clinical trials showed that the overall efficacy of oncolytic adenoviruses in patients remained limited despite an encouraging safety profile [103,104]. One possible explanation therefore was soon after proposed, namely the inability of the virus for widespread tumor transduction and destruction. Indeed, the results from independent studies have shown that freshly isolated tumor cells, unlike their *in-vitro* counterparts, are resistant to adenovirus infection due to absent CAR receptor expression [105-107]. Consequently, this finding propelled the field of cell entry targeting. Towards this goal, modifications of the capsid are necessary which ablate native receptor binding on the one hand, and confer binding to new cancer cell surface molecules on the other [8]. Ablation of the native tropism has been achieved by chemical modification of the virus, by mutating amino acid motifs, physical interaction with adaptor proteins, and by replacing domains of viral capsid proteins that interact with cellular virus receptors [108-110]. The same is true for interactions with blood factors that mediate indirect cell binding [111,112]. Subsequently, receptor blind adenoviruses have been retargeted to cells after complexing with adaptor proteins and by chemical or genetic insertion of ligands into the capsid [8,113]. Usually genetic insertion strategies exploit ligand incorporation into the protruding fiber knob domain although other capsid proteins like the penton can be used accordingly [114,115]. Prominent examples for fiber engineered oncolytic adenoviruses are the HAdV-5 RGD, carrying an arginine-glycine-aspartate motif [116], an poly-lysine bearing fiber mutant [117], and the HAdV-5/3 chimera where the fiber knob domain has been replaced by the serotype 3 knob [110]. The latter strategy where tropism of adenoviruses is altered by replacing the knob or even larger parts of the fiber domain with those from other serotypes is also referred to as pseudotyping of the virus. Further examples are chimeric HAdV-5/35 and HAdV-5/41 [51,118,119]. All of these recombinant adenoviruses show CAR independent cell entry, which is however not tumor-specific as the target receptors are ubiquitously expressed integrins, HSPGs, CD46, or the desmoglein-2 molecule [27,59]. Nevertheless, the transduction efficiency in case of HAdV-5 RGD or HAdV-5/3 infection of freshly isolated primary cancer cells, established cell lines, and tumor xenografts could be strongly enhanced depending on the relevant receptor expression profile [120-124]. Alternatively, tropism can be restored by

complexing virions with various adapter molecules like bi-specific antibodies [125,126]. Nonetheless regarding the approach of adaptor molecules, successful entry targeting of viruses for applications in oncolysis ultimately requires genetic strategies of virus modification to ensure that also the virus progeny generated in the patients' tumors is targeted. As to date, entry targeting has been successfully implemented for enveloped viruses such as measles but remains the Holy Grail for the field of oncolytic adenovirus research [127,128]. This circumstance is owed to several obstacles. First, entry targeting requires a detailed understanding of the molecular interactions between the virus and its host. Second, for several tumor entities suitable cell surface targets are not known or suitable ligands for established targets are not available. Finally, the insertion of ligands into viral capsid proteins has been frequently shown to be difficult as recombinant proteins often fail to assemble into functional virions or because they lose their cell binding ability due to improper folding. Moreover, biosynthesis of ligands and virus capsid proteins is not always compatible. For example, recombinant antibodies representing targeting moieties of high interest are synthesized in the endoplasmatic reticulum whereas viral capsid proteins are synthesized in the cytosol.

Post-entry targeting of therapeutic genes or infection to cancer can exploit a panel of cellular genetic control mechanisms [9,129]. The two most established strategies in this regard are transcriptional targeting of transgene or essential viral gene expression as well as mutation of regulatory viral genes. More recently, gene expression was further regulated through translation efficiency or mRNA stability by insertion of microRNA target sites [130-132]. Transcriptional targeting capitalizes on cellular regulatory DNA sequences that control transcription initiation and can be used to generate promoters which are specifically, or at least preferentially, active in a certain tissue or tumor cell type. These "cancer-selective promoters" can then be used to control expression of essential adenoviral genes such as the master regulator E1A. The first oncolytic HAdV that was targeted in such a way carries the prostate-specific antigen promoter to restrict adenovirus replication to prostate cancer cells [133]. Many other examples followed thereafter using the alphafetoprotein promoter for hepatocellular carcinomas, the human tyrosinase promoter for malignant melanomas, or the mucin 1 (*MUC1*) promoter for breast and ovarian cancer [134-136]. Moreover, tumor selectivity of oncolytic adenoviruses could be dramatically increased by specifically expressing two rather than one early viral gene. Towards this end, researchers utilized either two specific promoters, a

bidirectional promoter or a bi-cistronic transcription unit expressed from a single specific promoter [135,137-140]. Nevertheless, it has been shown that cryptic transcription initiation sites or enhancers found in upstream adenoviral sequences of the left inverted terminal repeat or the adenoviral packaging sequence can interfere with cellular promoters [141-144]. As a consequence, promoter regulation becomes leaky allowing non-specific viral replication. To overcome this, various approaches have been pursued to shield the cancer-selective promoters from upstream elements such as polyadenylation transcription termination signals, insulator sequences, or inversion of the promoter/transgene cassette [145-149]. However, within a tumor mass, which is vastly inhomogeneous, it is unlikely that all cells express a specific tumor marker. Therefore, researchers had focused on identifying pan-cancer promoters that are ideally active in all tumor cell types. The human telomerase reverse transcriptase (*hTERT*) promoter is a widely used representative of such promoters and has been utilized to target oncolytic adenoviruses to various cancers [139,150]. Even before viruses could be restricted to cancer cells by transcriptional targeting, scientists engineered so-called conditionally replicating viruses. Studies in recent years created mutants with crippled replication potential in normal cells but not in cancer cells. For this approach gene mutations in key regulators of viral replication, like the E1 genes, are introduced and efficient replication is rescued in tumor cells through complementation by overactive growth factor signaling cascades, aberrant cell cycle control checkpoints, or absence of cellular antiviral factors [21-23]. One of the first and most prominent examples, was the development of an adenoviral deletion mutant dl1520 ONYX-015 lacking the early E1B-55k gene, which binds and inactivates the tumor suppressor TP53 [151]. Therefore, adenoviral replication was thought to be restricted to cancer cells with a mutated TP53 pathway. Although later the precise mechanism of action was found to relate to altered mRNA export in tumor cells as opposed to normal cells [152,153]. Nevertheless, a genetically similar virus termed H101 became the first licensed oncolytic virus in China for treatment of recurrent head and neck cancers [10,11]. Other examples are adenoviruses bearing a 24 bp deletion in the CR2 domain of the E1A-13S and 12S isoforms (*termed HAdV-5 Δ24*) [154]. As a result, these proteins are no longer able to interact with the retinoblastoma protein in order to induce cell cycle entry via release of E2F transcription factors (*see above*).

The major focus of targeting strategies for cancer therapy using oncolytic adenoviruses, however, lies on the HAdV-5 serotype which currently provides the scaffold for most adenovirus

based drugs in clinical trials. Although, they showed great promise several limitations to oncolytic virotherapy still remain.

3.4 Limitations and implications for adenoviral oncolysis

The last decade has witnessed considerable progress in the field of oncolytic adenovirus research resulting in numerous pre-clinical and clinical trials. Despite revealing clinical benefit in some patients combined with an outstanding safety profile and no dose limiting toxicity, the overall therapeutic efficacy in humans is generally insufficient [103,104]. However, animal models using human xenografts or tumor biopsies usually show up to complete eradication of the tumor mass. These converse observations can be attributed to several hurdles encountered in virotherapy and emphasize the need to optimize oncolytic adenoviruses. First, the primary tumor mass is usually highly heterogeneous containing cancer cells surrounded by stroma cells, vasculature, and extracellular matrix which can act as anatomical barriers to virus spread [155,156]. This is combined with insufficient expression of viral receptors on target tumors as described previously. Furthermore, some tumor areas are necrotic or under a high interstitial pressure [157]. Taken together, these aspects severely affect the initial virus distribution and transduction efficacy. As a consequence, eradication of the whole tumor mass or distant metastases cannot be achieved due to scarce spread of progeny virions beyond these anatomical barriers. Second, there is a narrow time window for therapeutic viruses until the host immune response will start to counteract the infection [158-160]. On the one hand, viruses are rapidly inactivated by, mostly pre-existing but also newly formed, neutralizing antibodies and cytotoxic T cells that clear infected cells. On the other, healthy tissues such as the liver sequester therapeutic viruses resulting in loss of efficacy and toxicity [161,162]. The latter often caused by mounting of a strong cytokine mediated inflammatory response [163]. Third, the lytic efficacy of mutated or targeted viruses can be reduced compared to wild type viruses due to improved tumor specificity. Thus, viral replication may become restricted to fewer tumor cells, out of a heterogeneous tumor mass, which are capable to provide the necessary environment for virus growth [103,104]. In conclusion, some of these limitations constitute major hurdles whereas others can be overcome by further genetic engineering or modification of the virus.

The first limitation of insufficient virus infectivity and distribution in the tumor can be overcome by tropism modification of oncolytic adenoviruses as discussed for entry targeting above. In addition, the lytic effect can be increased by different administration routes and procedures currently evaluated. These include multiple intratumoral injections, pre-treatment with matrix-modifying agents like collagenase [164,165], or systemic injections combined with local application of vasoactive compounds such histamine as to increase the blood vessel permeability inside the tumor [166]. Several approaches to circumvent the second limitation, namely the immune system, have also been proposed. Therefore, researchers investigated plasmapheresis to remove neutralizing antibody from the blood or temporary immunosuppression by through short-term exposure to cyclophosphamide to inhibit their *de-novo* formation [167,168]. Alternatively, mutations or exchange of antigenic determinants in the hexon proteins with other less prevalent serotypes can hide the virus from pre-existing immunity [169,170]. In the same line, chemical modifications of the capsid have also proven to be successful [113]. Last but not least, the limiting lytic efficacy of adenoviruses for cancer therapy needs to be enhanced. To this end, mutations affecting adenovirus induced apoptosis showed increased antitumoral effects in some cancer entities. Examples are HAdVs bearing a deletion of the viral anti-apoptotic E1B-19k gene which did not reduce the infectious particle yield but increased oncolysis in some but not all cancer cells [171-174]. Alternatively, the adenoviral death protein can be overexpressed resulting in a similar phenotype [175,176]. Yet, a potentially far more powerful approach is the combination of viral tumor cell lysis with established treatment regimens like radiation and chemotherapy which can be amplified by concomitant delivery of therapeutic genes. These so-called “armed” oncolytic adenoviruses amplify and spread by replication and tumor cell lysis while the encoded therapeutic protein should exert a toxic effect on surrounding uninfected cancer cells, an activity called “bystander effect” (*exemplified in **Figure 5***). The feasibility of this combination therapy approach was first demonstrated in 1998 when Chase and colleagues equipped an oncolytic human herpes virus type-1 with a rat cytochrome P450 enzyme responsible for bioactivation of cyclophosphamide or ifosfamide into toxic compounds [177]. Later, similar strategies have been adopted for replication-competent oncolytic adenoviruses by deleting non-essential viral genes, like the E3 region, and incorporation of sequences encoding the thymidine kinase able to metabolize its respective prodrug ganciclovir [178]. Similarly, expression of the sodium iodide

symporter gene theoretically allows combination of virotherapy with local enrichment of toxic radioisotopes [179]. Importantly, the arming approach is not restricted to prodrug-activating enzymes as also other proteins can be exploited like the immunomodulatory granulocyte macrophage stimulating factor or interleukin-12/B-Lymphocyte Activation Antigen B7-1 [180,181], the cell death inducing ligands such as the tumor necrosis factor related apoptosis-inducing ligand [182], or the extracellular matrix degrading relaxin resulting in enhanced virus spread [183].

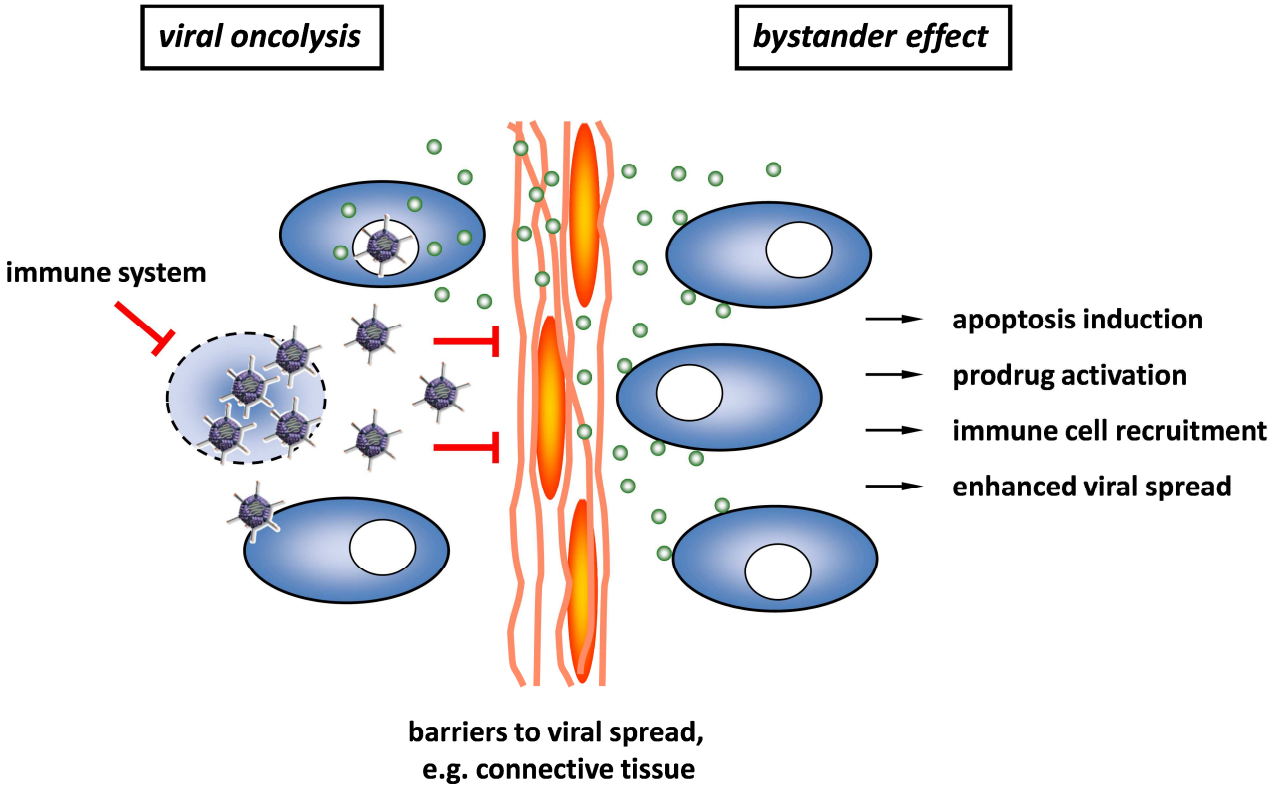

Figure 5| arming of oncolytic adenoviruses: anatomical barriers including tumor stroma cells, vasculature, necrotic areas, and extracellular matrix (*orange*) inhibit virus spread throughout the tumor mass (*dark blue*). Thus, viral oncolysis (*shown on the left side*), leading to tumor cell killing and release of progeny virions, is spatially restricted. In addition, the immune system counteracts the viral infection eventually. Arming of viruses leads to production of therapeutic molecules (*green orbs*) from infected cells. In turn, the secreted or released molecules are able to penetrate anatomical barriers and subsequently kill uninfected tumor cells by various means (*shown on the right side*). This effect, called bystander effect, is a widely accepted strategy to enhance or combine virotherapy with established treatment regimens such as chemo-, radiation, and monoclonal antibody therapy.

Recently, an oncolytic Newcastle disease virus has been equipped with an antibody against a vascular tumor marker [184]. This intriguing approach combined virotherapy with the widely accepted concept of monoclonal antibody therapy. After establishment of the hybridoma technology, antibodies quickly emerged as priceless diagnostic tools and eventually found entry into the clinic for autoimmune disease and cancer treatment [185]. In general, antibody therapy combines several advantages over other treatment modalities as they can be virtually generated against every available cellular surface target with high specificity and affinity [186]. The most renowned example, is the humanized monoclonal antibody Herceptin™ directed to the HER2/neu receptor thereby mediating tumor cell death which was licensed in 1998 [6,7]. Herceptin™ similar to other G type immunoglobulins have the intrinsic ability of the crystallizable fragment (*Fc*) to activate the classical complement cascade resulting in formation of a membrane attack complex and cell killing as well as activation of antibody-dependent cellular cytotoxicity by natural killer cells after Fc receptor engagement [187]. Moreover, downstream signaling events are blocked by binding of the monoclonal antibody to the HER2/neu receptor leading to apoptosis [7]. In addition to these first generation antibodies, several studies showed the feasibility to couple antibodies to immunotoxins, radioisotopes, prodrug converting enzymes, or cytokines for targeted delivery and local accumulation at the tumor site (*for a comprehensive review see* [188,189]). In 2002, the Food and Drug administration of the United States licensed the immunoconjugate ibritumomab tiuxetan which can be coupled to the radioisotope yttrium-90 [190]. This recombinant antibody, like the unmodified rituximab antibody, confers toxicity towards CD20 positive cells in non-Hodgkin lymphoma but additionally features local toxicity due to radiation via the conjugated radioisotope.

In conclusion, more potent but yet cancer-specific oncolytic adenovirus are urgently needed to provide a useful weapon in the battle against cancer. Therefore, the principles of entry and post entry targeting as well as efficacy enhancement provide different points of attack for recombinant adenoviruses. Towards the goal of therapeutically enhanced virus drugs, arming with therapeutic antibodies is attractive as viral-mediated delivery may lead to high local concentrations of the antibody in the tumor potentially achieving synergistic effects of tumor cell killing caused through virus and antibody-mediated cell lysis.

4 Gene expression profiling of adenovirus infections

Over the past decade, microarrays have grown in popularity as they provide the tool for a comprehensive study of genome-wide gene expression in cells. Every cell type expresses a unique set of RNAs, also referred to as transcriptome, which determines the cells' phenotype and function. In addition, the cellular transcriptome is able to respond to various intrinsic and extrinsic stimuli including changes in metabolite levels, signaling pathways, or bacterial and viral infections. Thus, microarray approaches offer an attractive tool to analyze genome-wide responses in gene expression under diverse experimental conditions. In contrast to most other established techniques, they enable specific detection and quantification of mRNA copies from all known genes in different species. Due to considerable progress in the technology, microarrays are now broadly utilized due a relatively low cost/benefit ratio and increasing development of sophisticated computational software which allow interpretation of the enormous amounts of generated data.

Today, several miscellaneous array platforms with different advantages and drawbacks exist. The Illumina Sentrix-8 V2 technology, used in this study, enables researchers to analyze eight samples in parallel for the expression of over 24.000 genes derived from the RefSeq database. Besides, these arrays show a high-quality performance resulting in high reproducibility and strong correlation of the results with those obtained from routinely used approaches like quantitative polymerase chain reaction. This is largely owed to the array design which utilizes beads carrying several thousand copies of covalently attached oligonucleotides probes (*see **Figure 6***). They bind labeled complementary RNA (*cRNA*) copies and facilitate identification as well as quantification of the respective transcripts. Moreover, they are assembled into over 1.6 million pits, each with a diameter of 3 µm, resulting in an average of 30-fold redundancy for each represented transcript [192]. Thus, each reading for a certain transcript is taken multiple times over the array and measurement accuracy can be strongly increased. The microarray approach seems particularly useful to identify changes in single gene expression or even complete cellular pathways which are disturbed through adenovirus infection.

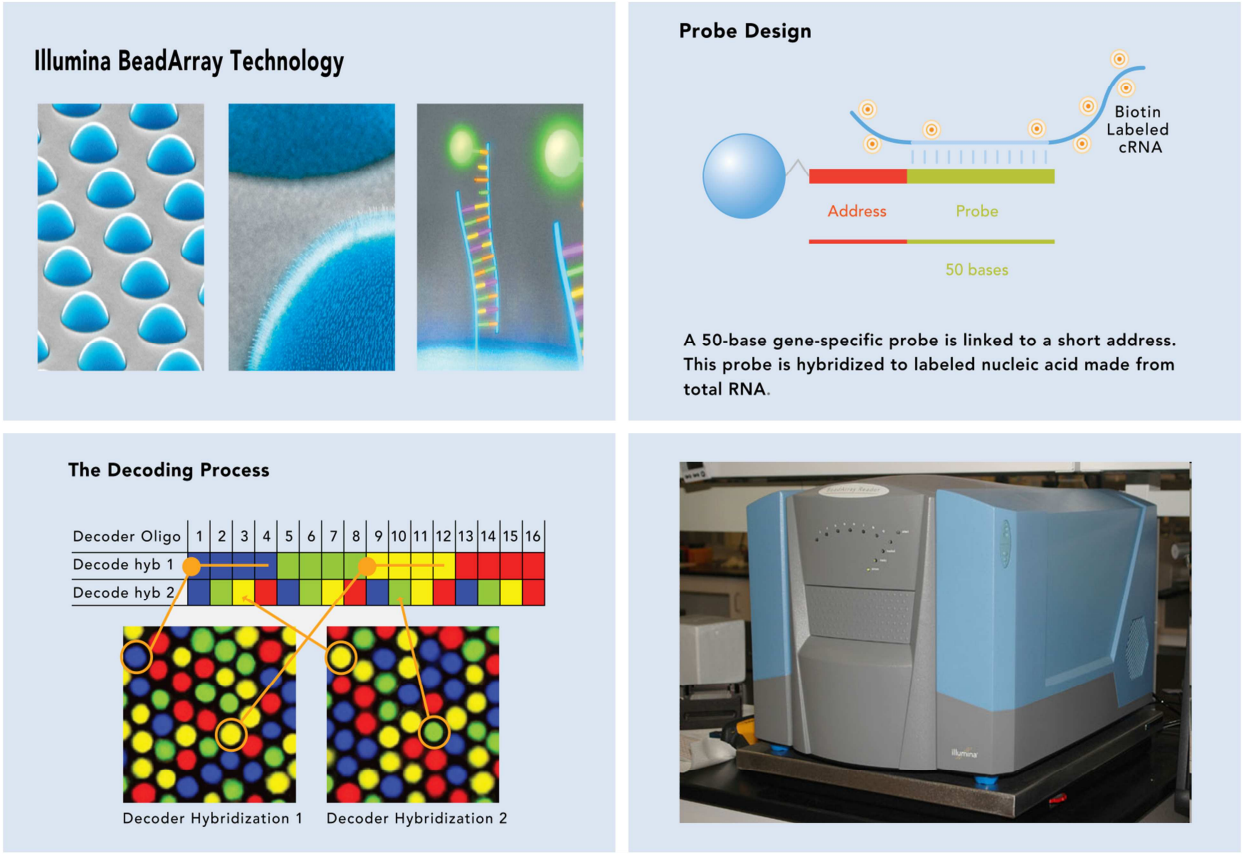

Figure 6| Illumina Human Sentrix technology: small silica beads carry thousands of covalently attached oligonucleotides that can bind to fluorescently labeled RNAs (*upper left panel*). Each oligonucleotide consists of and address (*red*), allowing identification of the transcript, and a probe sequence (*green*) that specifically hybridizes to the cRNA. (*upper right panel*). Single beads are identified through sequential hybridization of sixteen fluorescently labeled decoder oligonucleotides (*lower left panel*). Scanning and read out of the array is performed in an Illumina BeadStation array scanner (*lower right panel*). *Modified from the Illumina's "Product Guide 2009"* [191] *and the Core Facility for Nucleic Acid Research, Alaska.*

Over the last decade, several microarray studies investigated the impact of adenovirus infection on cellular gene expression in human fibroblasts and different cancer cells. Amongst other things it has been shown what happens on a genome-wide level after adenovirus binding and entry and how numerous E2F responsive promoters of S-phase genes were activated during forced cell cycle progression [193-195]. Also the antiviral response was inhibited early on by downregulation of respective genes including pro-apoptotic proteins as well as pro-inflammatory cytokines and chemokines [196]. At late stages, the cytopathic effect of

adenovirus on the cell was assisted by downregulation of various genes involved in controlling the cytoskeleton architecture such as filamentous actin and microtubule organizing proteins [197]. Regarding clinical applications, the impact on cancer cells by adenovirus mediated therapeutic gene transfer of TP53, E2F1, and others have been a focus of scientific research [198-200]. More recently this data was complemented by studies of oncolytic adenovirus infection of permissive and resistant cancer cells or after concomitant treatment with radiation therapy [201,202]. Therefore, insights gained from these and future comprehensive microarray data will help to identify genes and molecular pathways supporting or counteracting virotherapy. This seems an extremely appealing approach as oncolytic adenoviruses have not evolved to specifically replicate and kill cancer cells. Most importantly, all previous studies used cell types that do not appropriately reflect the natural host cell environment for HAdV-5. In addition, gene expression profiles of adenovirus infected normal cells have not been compared alongside with cancer cells

5 Objectives

Recent clinical trials show that the overall antitumoral efficacy of oncolytic adenoviruses is insufficient indicating the need for new virus generations with improved potency. For most therapeutic applications the HAdV-5 serotype has been used which is evolutionary adapted to infect and replicate in native host cells of the respiratory epithelium. Nonetheless, the fact that the cellular environment in most tumor cells, especially in malignant melanoma, might be suboptimal for HAdV-5 replication has been neglected so far. However, efficient virus replication in cancer cells is crucial for successful virotherapy. Furthermore, tumor cell killing can be increased by arming oncolytic viruses, for example, with a therapeutic antibody gene. Consequently, this study aimed to identify how adenovirus replication, lysis, and antibody expression in tumor cells can be modulated in order to create more potent virotherapeutics.

The main objectives are:

(1) Comparison of HAdV-5 infection in various cell types

Primary bronchial epithelial cells representing the native host cells for HAdV-5 will be compared versus various cancer cell lines. Kinetics of viral gene expression, replication, and cytotoxicity will be assessed in infected cell types.

(2) Analysis of host cell gene expression after HAdV-5 infection

Genes and cellular pathways that potentially influence adenovirus genome replication will be investigated by microarray as well as computational analyses and verified in further assays.

(3) Identification of strategies to enhance HAdV-5 replication in cancer cells

Knowledge gained from microarray analysis will be used as a rationale to engineer oncolytic adenoviruses with an increased replication potential.

(4) Arming of oncolytic adenoviruses with therapeutic antibodies

A recombinant single-chain antibody directed against the tumor-associated carcinoembryonic antigen will be used for proof of principle. This part includes analyses of the oncolytic capacity, antibody expression, as well as functional studies.

II RESULTS

1 Comparison of HAdV-5 infection in various cell types

1.1 Analysis of lung cells as model system

Currently the majority of oncolytic adenoviruses in use are derived from the wild type HAdV-5. This serotype is normally infecting epithelial cells lining the respiratory tract but it is also able to infect a wide range of cells *in-vitro* and *in-vivo* [27]. However, cancer cells are not target cells for natural adenovirus infections and might differ in several aspects of complex virus host interactions. Thus, the virus potentially encounters unappreciated obstacles that could be limiting in a virotherapy setting. To test this hypothesis, I investigated wild type HAdV-5 infections in a panel of different target cell types including natural host cells and established cancer cell lines.

For that reason my experiments were conducted with primary human bronchial epithelial cells (*HBEC*) representing a cell type of the most natural environment for HAdV-5. They are frequently isolated and purified from healthy human donors and can be purchased from Promocell, Heidelberg. Subsequently, HBEC were characterized by immunofluorescence staining for expression of epithelial markers in close collaboration with Werner Franke's lab at the DKFZ, Research Program Cell Biology and Tumor Biology. The results were then compared to the closely related lung squamous carcinoma cell line SK-MES-1, which originated from an epithelial lesion in the respiratory tract. As summarized in **Table 1**, both the primary HBEC as well as the SK-MES-1 tumor cell line expressed a high degree of acidic and basic cytokeratins, especially cytokeratin 18. Further, vimentin which can be considered as a major subunit of intermediary filaments was also highly produced in both entities. Besides, HBEC and tumor cells were positive for desmoplakins that are usually found in tight junctions of epithelial tissues and they were negative for expression of synaptophysin, a transmembrane protein found in neuroendocrine cells. Last but not least, analysis of the glycoprotein MUC1 specific for glandular and ductal epithelial cells revealed a low grade expression in HBEC in contrast to high and uniform expression in tumor cells.

These immunofluorescence data of HBEC as well as the closely related lung carcinoma cell line SK-MES-1 strongly favored an epithelial origin as they shared several characteristic

markers. First, they expressed typical cytokeratins and the tight junction proteins desmoplakin which differentiated them from mesenchymal cells, which give rise to the connective tissue, bones and cartilage. Both can be considered as key features of a functional epithelium. Second, they did not express synaptophysin, normally expressed by discrete non-epithelial neuroendocrine cells throughout different tissues, which therefore is typically associated with a different type of lung malignancy termed small cell lung carcinoma. Additionally, the vast majority of HBEC did not express MUC1 which is usually found only in secretory cell types. However, MUC1 can be strongly upregulated in a variety of tumors, typically in breast cancers, which I could also confirm in the lung squamous carcinoma cell line. Vimentin which is normally expressed only in mesenchymal cells but not epithelial cells was found in both primary as well as tumor cells. Yet, this protein is frequently produced in cultured cells and therefore could represent an artifact. Overall, I validated that HBEC provide a good *in-vitro* model for the study of HAdV-5 infections in native host cells.

Table 1| analyzed markers

antibody	description	primary lung epithelial cells	tumor cells
pan-cytokeratin Lu-5	specific for acidic (*type 1*) & basic (*type 2*) cytokeratins, found in epithelial & mesothelial cells	100 %	80 %
cytokeratin 18	acidic keratin, expressed in simple epithelia lining the respiratory and gastrointestinal tract	95 %	100 %
desmoplakin	obligate component required for functional desmosomes in epithelia	positive	positive
vimentin	major subunit protein of intermediate filaments, specific for mesenchymal cells	90 %	100 %
synaptophysin	transmembrane glycoprotein found only in neuronal and neuroendocrine cells	negative	negative
MUC1	transmembrane glycoprotein expressed by most ductal and glandular epithelial cells, associated with various cancers	5 %	100 %

1.2 Cytotoxicity assays of primary cells and established tumor cell lines

The efficiency of HAdV-5 based oncolytic adenoviruses to successfully infect cells, produce progeny virions and trigger host cell lysis, and thereby spread to neighboring uninfected tumor cells is known to be cell type-dependent. For instance, epithelial cells including lung adenocarcinoma cells A549 or cervical cancer cells HeLa are usually highly permissive whereas cells of mesenchymal origin like fibroblasts prolong adenovirus infection [203]. In the latter, the adenovirus infection efficiency can be reduced and/or the time for completion of the lytic virus life cycle is significantly extended. Thus, some or the majority of cancers that do not originate from epithelial cells, like malignant melanoma for example, might be more resilient to HAdV-5 based virotherapy.

In initial experiments, I investigated the ability of wild type HAdV-5 to infect and cause cytotoxicity in a set of different human target cell types (***Figure 7***). To this end, primary HBEC were infected alongside with the two squamous lung cell carcinoma cell lines (*SK-MES-1, SW900*), and two malignant melanoma cells lines (*SK-MEL-28, Mel624*) using serially diluted HAdV-5. In addition, the highly permissive lung adenocarcinoma cell line A549 served as positive control, as it is well characterized and routinely used in oncolytic adenovirus applications. Other primary cells including primary human keratinocytes (*PHK*) and foreskin fibroblasts (*HFF*) were also included. To rule out replication-independent cytotoxic effects from viral particles, cells were infected in parallel with a serially diluted replication-deficient HAdV-5 CMV-gfp variant. The assay was incubated for eight days and cells stained by a crystal violet solution which binds non-specifically to cellular proteins. After a gentle washing, the cytopathic effects of HAdV-5 infection became apparent as infected or lysed cells detach. Almost every cell line of lung origin (*A549, SW900, and HBEC*) allowed a rapidly progressing infection spreading throughout the monolayer as indicated by advanced cell lysis at a low tissue culture infectious dose 50 (*$TCID_{50}$*) of 10^{-3} $TCID_{50}$/cell. PHKs, isolated from the epidermis, matched this phenotype shown by similar adenovirus cytotoxicity and spread. The only exception was the lung squamous carcinoma cell line SK-MES-1, which was at least two orders of magnitude less susceptible indicated by an almost intact monolayer at 10^{-1} $TCID_{50}$/cell. In strong contrast to this, the HFFs did not show cytopathic effects as the cell monolayer was not destroyed even at the highest adenovirus titer and both melanoma cell lines SK-MEL-28 and

Mel624 were only killed with a very high multiplicity of infection (*MOI*) between 1-10 $TCID_{50}$/cell at this time. Finally, infection with the replication-deficient HAdV-5 CMV-gfp did not cause noticeable toxicity in any of the tested cell lines demonstrating that toxicity by wild type HAdV-5 was truly replication-dependent.

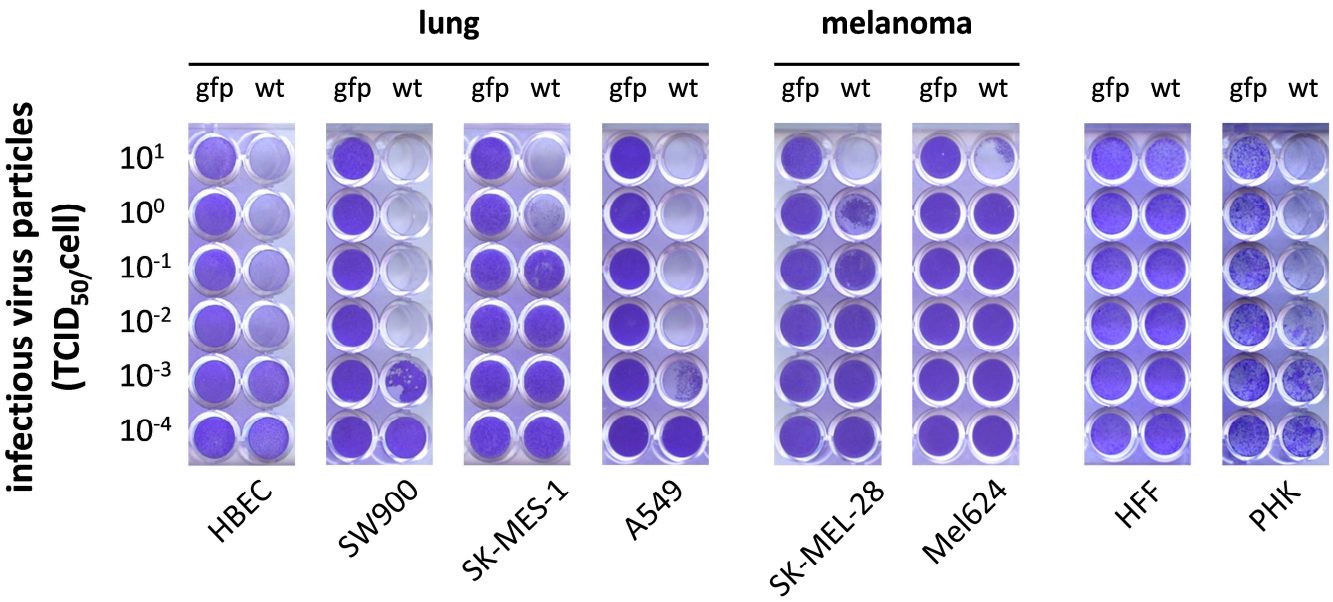

Figure 7| comparison of HAdV-5 cytotoxicity in primary cells and tumor cell lines: various cell types were infected at decreasing MOI of 10^{1} to 10^{-4} $TCID_{50}$/cell with either the replication-deficient HAdV-5 CMV-gfp (*gfp, left lane, negative control*) or the wild type HAdV-5 (*wt, right lane*). After incubation for eight days, surviving cells were fixed and stained with crystal violet. Lung cells (*left panels*) showed overall stronger cytotoxicity compared to melanoma cells (*middles panel*) and primary HFFs.

In line with other publications, the wild type HAdV-5 resulted in cell type-dependent cell killing which can be considered as direct consequence from adenovirus infection. So far, there is no available literature comparing adenovirus infection of tumor cells to primary HBEC. Hence, it was of interest to see that they sustained HAdV-5 infection to an at least equivalent extent as A549 cells, which usually serve as reference cell line. The presented data showed that most cells derived from an epithelium, especially from the respiratory tract, were highly permissive for adenovirus infection and lysis compared to both malignant melanoma cell lines and fibroblasts. However, crystal violet based cytotoxicity assays allow only comparison of virus dependent cytopathic effects and spread but not precise conclusions about the HAdV life cycle itself as

many critical steps, including virus binding and entry, DNA replication, and generation of progeny cannot be evaluated per se. Hence, I addressed these points in the following chapters.

1.3 Transduction capacity of HAdV-5

One reason for varying efficacy of adenovirus infection *in-vitro* as well as *in-vivo* is different expression levels of cell surface receptors such as CAR, HSPGs, and integrins which facilitate virus binding and cell entry. Afterwards, the virus has to overcome several intracellular hurdles, such as escape from early endosomes, cytoplasmatic trafficking, and nuclear import in order to establish an infection (*see I, 3.2*). Therefore, when comparing virus host cell interactions between different cell types it is essential to standardize the infection conditions and apply titers that result in a homogenous rate of adenovirus infected cells. This can be achieved by a virus carrying a reporter gene or by immunofluorescence staining of intracellular capsid proteins.

Towards this goal, I first standardized cell culture conditions for all cell types including media formulations with low serum content and maintenance at similarly low passage numbers before freezing stocks for future experiments. Then, I established a cell seeding protocol using frozen aliquots to ensure higher reproducibility throughout my experiments and a similar cell density and state of proliferation between different cell types (*data not shown*). To determine adenovirus titers leading to high but comparable infection rates, I transduced different cell types with increasing MOI of HAdV-5 CMV-gfp. This virus is derived from wild type HAdV-5 but cannot replicate inside cells as the essential E1 genes have been replaced by the enhanced green fluorescent protein reporter gene (*gfp*). Therefore, gfp expression is a direct consequence of nuclear adenovirus genomes reaching the nucleus. After one hour, the inoculums were removed to enable a more synchronized infection. Following incubation for 48 hours, I quantified transduced cells by flow cytometry on the basis of gfp expression. In addition, dead cells were omitted by forward/side scatter gating and a viability staining through propidium iodide (*PI, **Figure 8A***) as described in chapter V, 3.7.1. Representative histograms in **Figure 8B** show various cell lines at transduction levels of ≥ 80 % with HAdV-5 CMV-gfp indicated by similar proportions of green fluorescing cells. However, as summarized in **Table 2**, the initial adenovirus dose required to achieve this high level of transduction varied in a cell type-

dependent manner. For example, both melanoma cell lines were readily transduced using lower virus inoculums (≥ *80 % at 300-400 TCID$_{50}$/cell*) than any cell line of lung origin (≥ *80 % at 700-1500 TCID$_{50}$/cell*). Notably, the relatively high virus titers did not result in significantly increased cytotoxicity as shown by constant, or only slightly increased, numbers of dead cells between 2-10 % (*data not shown*). Similar experiments were conducted for PHKs and HFFs using 800 and 1500 TCID$_{50}$/cell, respectively (*data not shown*).

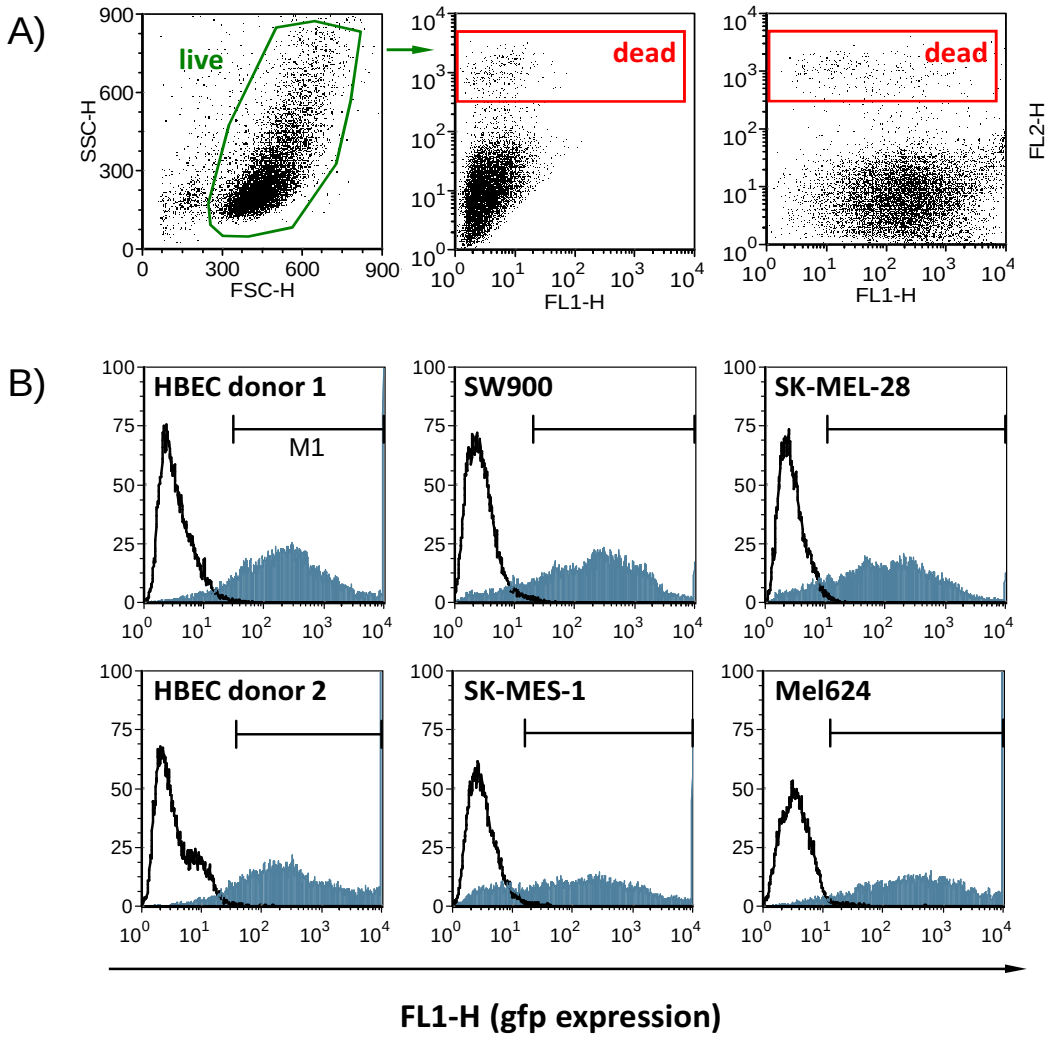

Figure 8| flow cytometry analyses of transduction rates by HAdV-5 CMV-gfp: multiple cell lines were transduced with serial dilutions of HAdV-5 CMV-gfp for 48 hours and analyzed by FACS. **A)** forward/side scatter analysis distinguished intact cells from debris (*left panel, green gate*). Propidium iodide staining excluded dead cells, determined by FL2-H intensity, in mock infected samples (*middle panel, red gate*) as well as HAdV-5 CMV-gfp transduced samples (*right panel, red gate*). **B)** Cells expressing gfp were detected in channel FL1-H. Representative histograms show distributions of mock infected controls (*black lines*) versus gfp expressing populations (*blue fills*) at titers resulting in 80-90 % transduction (*marker M1*). Exact TCID$_{50}$ titer values for ≥ 80 % average transduction rates are summarized in **Table 2**.

Table 2| titers of HAdV-5 or HAdV-5 CMV-gfp used for microarrays and related experiments

cell line	origin	$TCID_{50}$ titer/cell	average transduction rate
HBEC, both donors	lung epithelium	800	89 %
HFF	human foreskin fibroblasts	1500	84 %
Mel624	melanoma	400	80 %
PHK	primary human keratinocytes	800	85 %
SK-MEL-28	melanoma	300	85 %
SK-MES-1	lung squamous cell carcinoma	700	86 %
SW900	lung squamous cell carcinoma	1500	81 %

In conclusion, my data demonstrated the feasibility of using standardized infection conditions together with varying adenovirus inoculums in order to achieve reproducible and comparable high level adenovirus infections in several cell types. An explanation for the cell type specific susceptibility to adenovirus transduction could most likely be found in differential expression of the CAR receptor on the cell surface. Moreover, the previously observed lower cytotoxicity of HAdV-5 in melanoma cells SK-MEL-28 and Mel624 cannot be due to lower virus cell entry. Both cell lines were more susceptible to adenovirus transduction at lower titers as opposed to the primary cells or the lung carcinoma cells. Although reporter gene expression served as an indirect marker here for adenovirus infection, correlating with numbers of infectious viral genomes inside the nucleus, it should be noted again that the HAdV-5 CMV-gfp is replication-deficient. Nevertheless, the wild type HAdV-5 is identical in terms of capsid structure and function to HAdV-5 CMV-gfp. Thus, the conditions established here can be used analogous for the study of wild type HAdV-5 infections in different cell types, including virus gene expression and DNA replication.

1.4 Insights into the HAdV-5 life cycle

After the adenovirus has entered the cell and reached the outer nuclear rim via microtubule-dependent transport, the viral genome gets imported through the nuclear core complex thereby establishing infection of the host cell (*see I, 3.2*). One of the first adenoviral genes to be transcribed and expressed is the early gene E1A which acts as a master regulator in adenovirus

infection. As pointed out in the INTRODUCTION, a key feature of E1A is its ability to force the infected cell to enter the cell cycle. With beginning viral genome amplification, the major late promoter becomes active and leads to the transcription of several structural proteins such as the hexon, the fiber, the penton and others. These hallmarks are obligatory in permissive cells. However, the time to start and complete the different stages has been reported to be strongly cell type-dependent [203]. Thus my aim here was to measure the kinetics of adenovirus replication in native host cells versus tumor cells as determined by three hallmarks of adenovirus infection, namely early E1A gene expression, viral genome replication, and late fiber gene expression.

To this end, HBEC along with different primary cells (*PHK, HFF*), lung carcinoma cell lines (*SK-MES-1, SW900*), and two melanoma cells lines (*SK-MEL-28, Mel624*) were infected with individual MOI of HAdV-5 resulting in 80-89 % infection of living cells (*indicated in **Table 2***). After one hour, I removed the virus inoculums and harvested cells for isolation of total RNA and genomic DNA every four hours. Following sample purification, levels of E1A and fiber mRNA as well as copy numbers of viral genomes were determined by quantitative real time polymerase chain reaction (*qPCR*). Signals were normalized as stated in the METHODS section V, 1.9.2 to the cellular RNA or DNA input measured by the house keeping genes glyceraldehyde-3-phosphate dehydrogenase (*GAPDH, for RNA*) and β-actin (*ACTB, for viral genomes*). The HBEC from two different donors, as well as the primary keratinocytes, showed a very markedly increase of E1A mRNA at the earliest time point after infection and reached a maximum between eight to twelve hours post infection (***Figure 9A***). However, with the exception of the lung squamous cell carcinoma cell line SW900, neither other cancer cell lines nor the human fibroblasts displayed a comparable phenotype. In these cells, the E1A mRNA levels were lower and kept gradually rising even after sixteen to twenty hours post infection. This differential kinetics was also reflected in the onset of adenoviral genome replication. As shown in **Figure 9B**, the HBEC, PHKs, and SW900 began to replicate the HAdV-5 genome very early on between twelve to sixteen hours post infection. Moreover, in the second HBEC donor genome replication set in early at eight to twelve hours. This was unparalleled in any of the tested cell lines. On the contrary, the melanoma cells SK-MEL-28 and Mel624 eventually allowed HAdV-5 genome replication around sixteen to twenty and twenty to 24 hours after infection, respectively. My findings were further

supported by expression kinetics of the late fiber gene which mirrored the kinetics of viral DNA replication (***Figure 9C***).

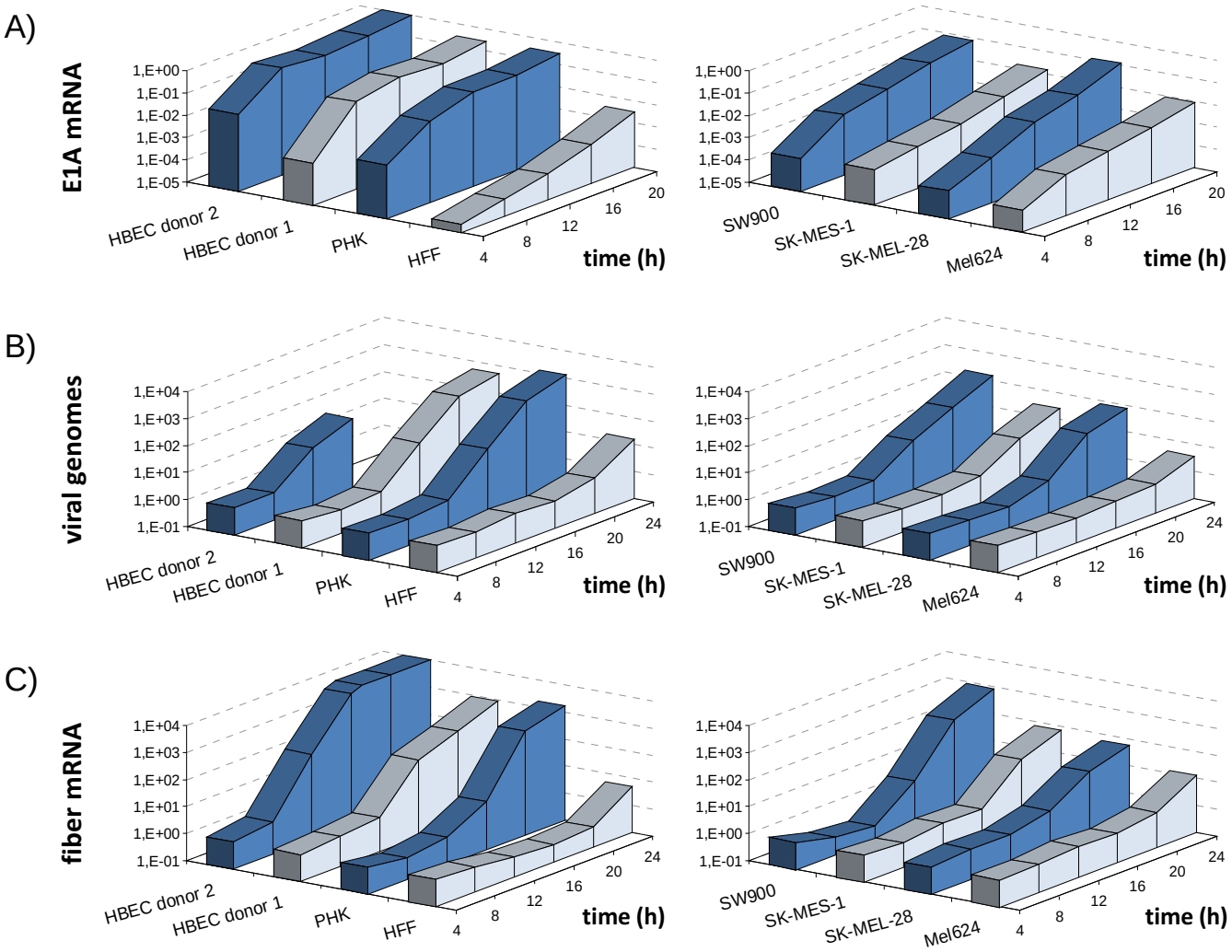

Figure 9| viral gene expression and genome replication in different cell types: human primary cells (*left panels*) and tumor cell lines (*right panels*) were infected with individual titer of HAdV-5 resulting in an infection level of 80-89 %. Total RNA and DNA was harvested for every indicated time point post infection and analyzed for relative copy numbers of E1A and fiber mRNA as well as viral genomes by qPCR. Normalization of **A)** E1A mRNA, **B)** viral genomes, and **C)** fiber mRNA was done according to METHODS section V, 1.9.2.

This was the first time that different tumor cells have been compared alongside with the primary lung epithelial cells HBEC in terms of HAdV-5 gene expression and replication. Surprisingly, HBEC allowed much faster early E1A gene expression and viral DNA synthesis than

most other cell types. Out of six cell lines tested, including other primary cells, only the lung squamous carcinoma cell line SW900 and primary human keratinocytes PHK displayed similar kinetics. Thus, cell lines that allowed rapid E1A gene expression also replicated the viral DNA early on. In strong contrast to this, both melanoma cell lines and the human foreskin fibroblasts HFF, the latter known to be only weakly permissive for HAdV-5, displayed only a gradual E1A mRNA expression which resulted in a delay of viral DNA synthesis. Hence, the onset of viral genome replication correlated very well with the E1A mRNA phenotype and was matched in expression of the late fiber gene that is controlled by the replication-dependent major late promoter. Importantly, the different kinetic profiles corresponded to those seen in the cytotoxicity assays of **Figure 7**. Therefore, my data is in line with previous publications that show varying permissivity of epithelial cells, such as HeLa or A549, and mesenchymal cell types, like fibroblasts, for infection with HAdV-5 and the closely related HAdV-2 [203]. This might indicate that less permissive tumor cells, including malignant melanoma, required a certain threshold of E1A mRNA or other downstream targets to sustain an efficient adenovirus infection. Hence, the immediate question arose if this reduced susceptibility could be explained by lower E1A promoter activity in these cells.

1.5 E1A promoter assay

The adenoviral master regulator E1A, the first gene to be expressed during infection, acts on a plethora of viral and cellular promoters. Additionally, E1A binds and disrupts the pRB/E2F regulatory pathway. As a consequence cells are prompted to enter the S-phase of the cell cycle where DNA synthesis occurs [37]. As previously shown, primary HBEC immediately expressed E1A mRNA to very high levels. In contrast, other infected tumor cells including melanoma cells SK-MEL-28 and Mel624 displayed a lower but gradually rising E1A mRNA amount. One explanation for this could be differences in the E1A promoter activity. In the same line, it would also provide a lever to potentially accelerate S-phase entry and hence DNA replication in melanoma cells by replacing the intrinsic viral promoter with a stronger recombinant promoter. Thus, this strategy might yield therapeutic HAdVs with increased oncolytic efficacy.

In order to investigate the activity of the adenoviral E1A promoter in different cell types, I cloned the left end of the wild type HAdV-5 genome encompassing the inverted terminal repeat and E1A promoter sequences (*nucleotides 37935 to 557*) into a promoterless luciferase reporter gene construct (*pGL3-E1A, refer to MATERIALS IV, 5.4*). This construct was compared with matching control plasmids that contained either the strong immediate early promoter from the cytomegalovirus (*pGL3-CMV*) or the moderately active human thymidine kinase promoter (*hTK, pGL3-hTK*). A promoterless luciferase plasmid (*pGL3-basic*) served as negative control for intrinsic background luciferase activity. Consequently, I transfected the primary HBEC, the two lung carcinoma cell lines SW900 and SK-MES-1, as well as the two melanoma cell lines SK-MEL-28 and Mel624 with the respective reporter gene constructs. Transfection efficacy was around 30 % for all cell lines as confirmed by transfection control plasmid encoding gfp (*data not shown*). After 48 hours, luciferase activity was quantified through conversion of luciferin into a luminescent substrate which can be detected by fluorometric measurement.

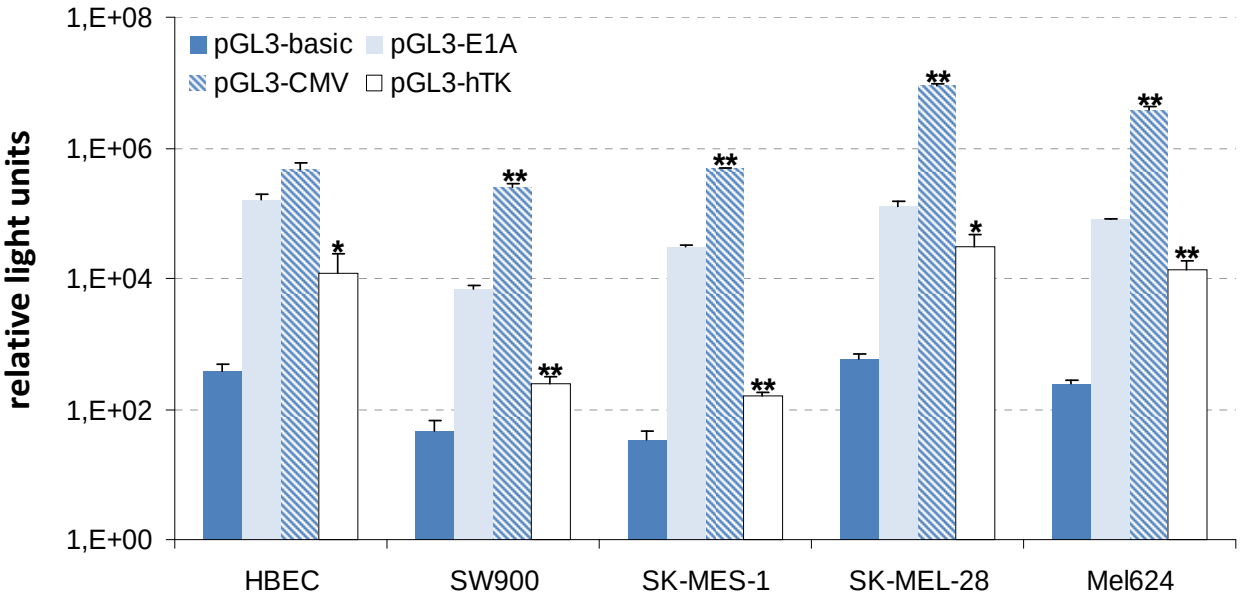

Figure 10| reporter gene assay of E1A promoter activity: various human cell lines were transfected with luciferase reporter gene plasmids. Plasmids contained either no promoter (*pGL3-basic, negative control, dark blue bars*), the E1A promoter (*pGL3-E1A, light blue bars*), the CMV promoter (*pGL3-CMV, striped bars*), or the thymidine kinase promoter (*pGL3-hTK, white bars*). Luciferase activity was quantified 48 hours post transfection and expressed as relative light units. Each bar represents mean values of triplicate transfections with standard deviation, p-values were calculated only between the E1A and CMV promoter and the E1A and hTK promoter using the Student's t-test (* $p \leq 0.05$, ** $p \leq 0.01$).

As displayed in **Figure 10**, high luciferase values were measured in all cell lines containing either the CMV or the adenoviral E1A promoter/reporter gene constructs. The hTK promoter constructs showed varying activity in a cell type-dependent manner which ranged between almost background levels, in SW900 and SK-MES-1, and moderate levels in HBEC, SK-MEL-28, and Mel624. Interestingly, in HBEC E1A and CMV promoter activities reached almost similar levels whereas in the tumor cell lines the CMV promoter was generally between one (*SW900, SK-MES-1*) or two (*SK-MEL-28, Mel624*) orders of magnitude stronger. Nevertheless, all cell types allowed similar luciferase expression and activity after transfection of the E1A promoter constructs. Background signals of cells transfected with the negative control were comparable among all cell types.

Analyzing promoter activities in several cell types revealed that the adenoviral E1A promoter was strongly active in all tested tumor cell lines as well as in primary HBEC, where it was equally active than the CMV promoter. If considering the CMV reporter gene levels as maximum, this might indicate that the E1A promoter has adopted to efficiently function in cells of the respiratory epithelium. On the other hand, the moderately strong hTK promoter control is active to a comparable level in HBEC, SK-MEL-28, and Mel624 and weaker in both lung squamous cancer cell lines allowing no conclusive readout. In my previous experiment the HBEC displayed a rapid and strong increase of E1A mRNA after HAdV-5 infection, mirrored by the SW900 lung squamous carcinoma cell line. However, in both entities the E1A promoter activity was comparable to the other tumor cell lines SK-MES-1, SK-MEL-28, and Mel624 which allowed only gradual E1A mRNA expression. Therefore, I could not find a correlation between the promoter activity and the two E1A expression kinetic profiles. Intriguingly, my data implies that other mechanisms like posttranscriptional regulation or mRNA export might be responsible for the differences in E1A expression between infected tumor cell types. Yet another possibility could be that the E1A promoter activity is dependent on the DNA context which is far more complex in the whole adenoviral genome than in expression plasmids. Next, I wanted to assess if reduced E1A gene expression and delay of DNA synthesis in melanoma cells results in reduced production of virus particles.

1.6 Production of virus progeny

A key determinant of adenoviral oncolysis is infectious viral particle production which is ultimately results from viral DNA replication, expression of structural genes, virus assembly, and cell lysis. Thus, they provide another critical parameter that can be assessed *in-vitro* by a so-called burst assay. This approach further allows me to determine if slower E1A expression and adenoviral genome replication in melanoma cells can be linked to reduced HAdV-5 particle production or release from infected cells which would explain reduced cytotoxicity.

Therefore, the melanoma cells SK-MEL-28 alongside the primary lung epithelial cells HBEC were inoculated with 1 $TCID_{50}$/cell wild type HAdV-5 for one hour. The low titer resulted in an equal transduction efficacy of virus particles in both cell lines as determined by HAdV-5 CMV-gfp (*data not shown*). A low titer was favored since it allowed a more precise quantification of newly synthesized progeny virions versus the initial virus input. Afterwards, I carefully washed the cells to remove any residual unbound virus and immediately collected separate samples from cell culture supernatants and cell pellets for background normalization. Over a period of three days, further samples were harvested and subsequently analyzed for infectious particle content by a limiting dilution assay (*see **Figure 11***). As early as 36 hours post infection, pellets from HBEC contained significantly (*over two orders of magnitude*) more infectious virus particles as SK-MEL-28 cells. In the latter, amounts of progeny virions kept gradually rising and reached levels comparable to HBEC as late as 72 hours post infection. For both cell lines there were no or only statistical insignificant small amounts of virus detectable in culture supernatants until 72 hours post infection. Final virus titers in the supernatants and pellets were similar for both cell lines.

Taken together, the results from the crystal violet assay as well as the burst assay demonstrated that HAdV-5 infection is more efficient in primary lung epithelial cells than in melanoma cells. Indeed, the premature DNA replication in HBEC reflected in considerable higher intracellular virus titers early during infection. However, this effect was diminishing over time and no further difference could be distinguished between HBEC and melanoma cells. Interestingly, I did not observe noticeable amounts of released viruses in the supernatants until 72 hours post infection for both cell types. A possible explanation might be that the virus progeny was not released earlier or that the viruses were spreading directly from cell to cell and

therefore could not be detected in smaller quantities in the supernatants. Regardless of this, the observed differences in viral DNA replication, generation of progeny virions, and cytotoxicity between melanoma cells and primary HBEC provide a point of attack to unravel limiting cellular factors for HAdV-5 based virotherapy of malignant melanoma. This topic will be addressed in the following part of my study.

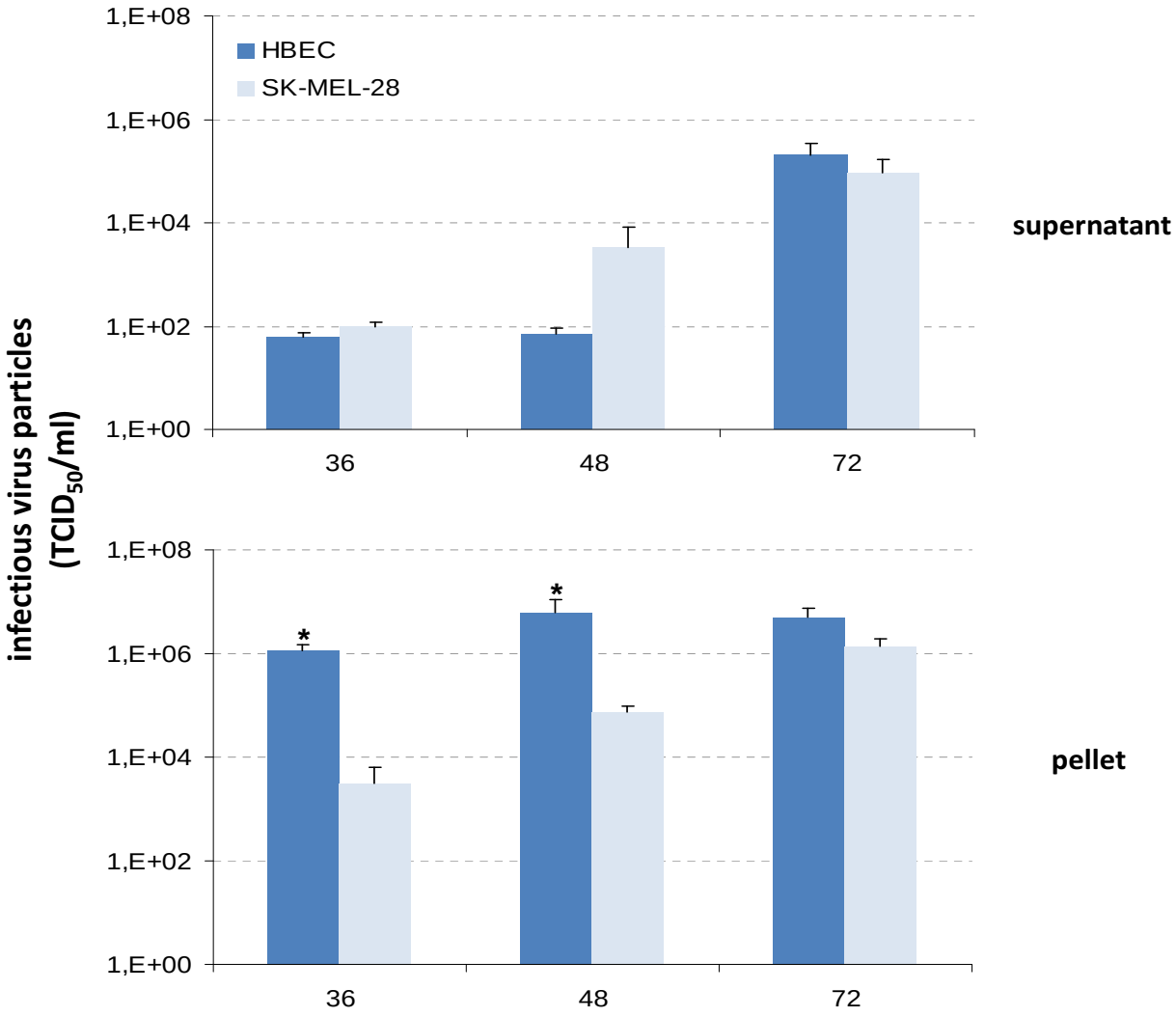

Figure 11| quantification of HAdV-5 progeny virions: primary lung epithelial cells HBEC (*dark blue bars*) or melanoma cells SK-MEL-28 (*light blue bars*) were infected with 1 $TCID_{50}$/cell HAdV-5. After one hour incubation, inoculums were removed and cells washed three times. Supernatants (*upper panel*) and cell pellets (*lower panel*) were harvested at indicated time points and analyzed for infectious particle content in $TCID_{50}$/ml. Bars represent mean values of triplicate infections with standard deviation, p-values were calculated between both cell types using the Student's t-test (* $p \leq 0.05$).

2 Analysis of host cell gene expression after HAdV-5 infection

2.1 Microarray hybridization and analysis

Viruses in general are obligate intracellular parasites since they depend on the cellular replication machinery and an environment that allows creation of infectious progeny virions. Thus, a common feature of viruses is reprogramming of the host cell by induction and repression of cellular genes and proteins in order to efficiently replicate. As shown in part one of my results, HAdV-5 displayed varying cell type-dependent replication abilities which may be indicative for differences in virus-induced cellular gene expression profiles. Therefore, I wanted to study adenovirus mediated changes in the host cell gene expression during infection by a microarray approach to identify genes and regulatory pathways that play an important role herein. A major focus of my work was put on differentially regulated genes between the native host cells HBEC and melanoma.

Towards this goal, a set of five cell types including primary HBEC, the lung carcinoma cell lines SW900 and SK-MES-1 and two melanoma cell lines SK-MEL-28 and Mel624 were chosen and infected with established titers of HAdV-5 to achieve a level of approximately 80-90 % infection (*see* **Table 2**). Uninfected controls of each cell line were equivalently treated with medium only. As genome replication is the major aspect in viral oncolysis and potentially requires the most changes in host cell gene expression, I harvested and purified total RNA after viral DNA replication became apparent as determined by qPCR in **Figure 9**. This was the case at twelve hours for the HBEC donor 2, at sixteen hours for HBEC donor 1 and SW900, at twenty hours for SK-MEL-28, and 24 hours for Mel624. Consequently, three samples from HBEC (donor 1 n =2, donor 2 n = 1) and SW900, four samples of SK-MES-1 and SK-MEL-28, and two samples of Mel624 were hybridized to human Illumina Sentrix-8 V2 microarrays. Efficiency of sample labeling and hybridization to the microarray, independent from the actual sample quality and preparation, was controlled by several positive and negative Illumina control oligonucleotides. Data derived from a typical experiment is depicted in **Figure 12A-E** on the next page.

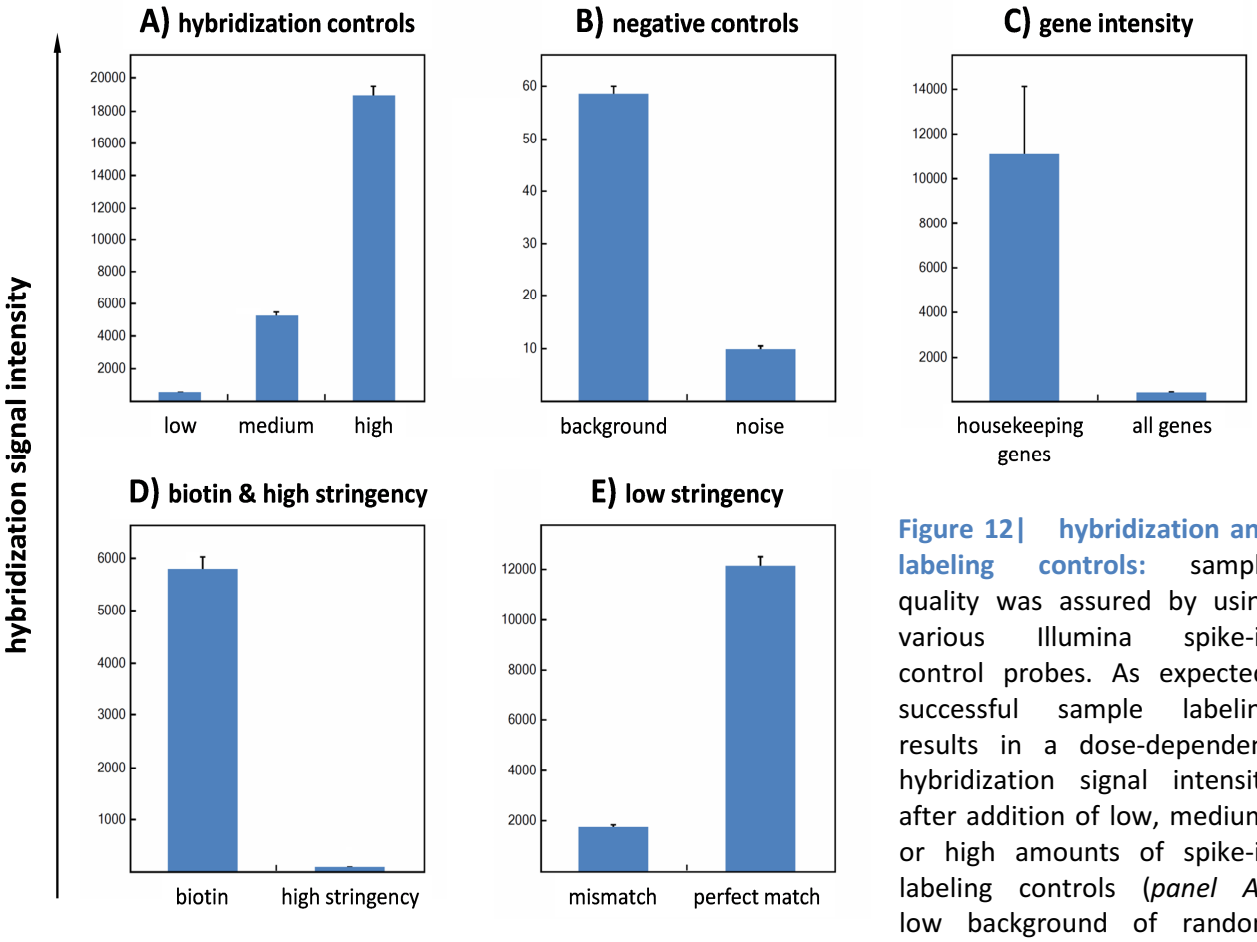

Figure 12| hybridization and labeling controls: sample quality was assured by using various Illumina spike-in control probes. As expected, successful sample labeling results in a dose-dependent hybridization signal intensity after addition of low, medium, or high amounts of spike-in labeling controls (*panel A*), low background of random non-target oligonucleotides, and noise levels (*panel B*). Hybridization of the housekeeping controls yielded higher signal intensities than expression of all genes as expected since they are ubiquitously expressed in all tissues (*panel C*). Hybridization conditions were checked by positive control biotin probes with average guanine/cytosine content versus probes containing high guanine/cytosine content which would only bind under highly stringent conditions (*panel D*). In addition, mismatched probes do not bind to their targets under optimal conditions as they require low stringency in contrast to perfectly matched probes (*panel E*). Shown data is representative for one microarray experiment including eight hybridizations.

The sample signal intensity correlated in a dose-dependent way with the concentration (*low, medium, and high*) of spiked-in labeling control probes indicating high labeling efficiency (***Figure* 12*A***). Whereas the negative controls, 800-1600 random sequence probes without corresponding targets in the human genome, resulted in extremely low background signals that were only marginally above the overall noise signals (***Figure* 12*B***). The signals from housekeeping control probes corresponding to a set of ubiquitously expressed cellular genes were found to be higher than the signal intensity of all genes, which was to be expected

according to the manufacturer (***Figure* 12*C***). The hybridization stringency was controlled using a set of different probe/target sequences. One, the high stringency control has very high guanine/cytosine content and should bind to its target sequence if the hybridization temperature is too high, independently from the success of sample RNA purification and labeling. However, the high stringency controls should be lower than the positive biotin control oligonucleotides with average guanine/cytosine content if hybridization conditions are adequate (***Figure* 12*D***). The other, four low stringency controls yielding two mismatch bases in their sequence bind very weakly to the related target sequence if the conditions are adequate but would give high signals if the stringency is too low (**Figure 12E**). Under optimal hybridization conditions, I observed that only perfectly matched probes gave higher signal values than their respective controls.

After hybridization and array readout, data was processed as described in chapter V, 1.8 together with Frank Holtrup and Kurt Fellenberg from the division of Functional Genome Analysis, DKFZ. Using the Multi-Conditional Hybridization Intensity Processing System (*M-CHiPS; http://www.mchips.org*), data was filtered according to signal intensity (*minimum 100*), p-value (*maximum 0.05*) and fold change (*minimum 1.4*) in at least one cell type. Initially, the variations between all cell types in context of their genetic background were found to be greater than the induced changes in gene expression after HAdV-5 infection of individual cell types. Therefore, the data of single hybridizations was uploaded into M-CHiPS as two-channel data, with the first channel containing expression data of uninfected and the second channel of infected samples of one cell line, respectively. Then gene expression in uninfected samples was defined as steady state and subsequently compared to gene expression levels in infected samples allowing identification of infection-specific expression changes within each cell type individually without creating a bias through inter-cell line variations by different genetic backgrounds. As a result, a list of approximately 950 genes that were significantly regulated after infection in at least one cell type, namely HBEC, was created (*refer to Dorer, Holtrup et al. in preparation*). Interestingly, HAdV-5 had the most dramatic impact on cellular gene expression in primary HBEC followed by both lung squamous carcinoma cell lines SW900 and SK-MES-1. However, this effect was drastically reduced in both melanoma cell lines SK-MEL-28 and Mel624 (*overview in* ***Table 3***).

Table 3| summary of gene regulation after infection of different cell lines

cell line	number of regulated genes	upregulated	downregulated
HBEC	943	424	519
SW900	772	326	446
SK-MES-1	709	310	399
SK-MEL-28	314	112	202
Mel624	212	90	112

A list of individual candidate genes showing the strongest and/or a reversed regulation in cells of lung origin, especially HBEC, versus melanoma cells was created (***Table 4***, *see below*). Next, I verified the microarray data by quantifying individual mRNA levels of seven representative genes by qPCR in unlabeled samples from the same experiment and associated the values with those obtained from the array. As shown in **Figure 13** below, the linear relationship for both was usually over 80 to 90 % in infected and uninfected samples from different cell lines as determined by the coefficient of determination expressed as R^2. Yet, the results gained from independent measurements of this gene panel in Mel624 samples showed a very poor correlation.

To summarize this, sample hybridization to the microarray worked under optimal conditions as demonstrated by diverse control probes. This allowed reliable detection of signals, as demonstrated by the low background as well as dose-dependent linear correlation of sample input with obtained signal output. Further, I independently confirmed the gene expression microarray data by qPCR as demonstrated by linear relationship with significant coefficients of determination, with exception for Mel624 cells. The reasons for this could be found in the underlying weak and statistically insignificant changes in gene expression after HAdV-5 infection of Mel624 cells, including the selected panel of genes herein. Accordingly, a greater variance between qPCR and microarray values from Mel624 samples accounts for the lack of linear relationship. This could be overcome by either hybridizing more replicates or selecting another panel of significantly regulated genes in Mel624 for validation. Most importantly, an algorithm has been implemented to successfully filter the data from various cell lines with different genetic background using the virtual two-color gene expression approach. This enabled me to

identify genes that were regulated in a HAdV-5 infection specific manner. Surprisingly, virus infection had the most pronounced effect on a number of cellular genes in primary HBEC. This effect was severely diminished in melanoma cells. To gain a better overview, sophisticated computational tools were applied and will be discussed in the following paragraphs.

Table 4| list of candidate genes

gene symbol	regulation in fold change expression after infection*			Entrez Gene description
	HBEC	SW900 / SK-MES-1	SK-MEL-28 / Mel624	
E2F2	11,5	1.9 / 1.7	-1.5 / (*1.1*)	transcription factor
HERC5	10,4	1.4 / 1.6	(*-1.1*) / (*1.1*)	ubiquitin ligase
H2BFS	9,3	-1.2 / -1.3	(*-1.0*) / (*1.0*)	histone
CD83	7,9	2.2 / 2.0	1.3 / (*1.6*)	unknown
HES4	5,2	2.2 / 2.5	2.3 / 4.0	transcription factor
UNG	5,1	2.8 / 1.9	(*-1.1*) / (*1.0*)	uracil-DNA glycosylase
MGC13057	4,4	5.0 / 3.8	(*1.1*) / (*-1.1*)	unknown
CHAF1B	3,9	1.9 / 1.4	(*-1.2*) / (*-1.1*)	chromatin assembly factor
CDT1	3,7	1.4 / 1.4	(*1.1*) / (*1.0*)	DNA replication factor
CDC25A	3,5	1.5 / 1.7	1.3 / (*1.3*)	phosphatase
CCNE	3,2	2.6 / 1.8	-1.8 / (*-1.1*)	cyclin
CDC45L	3,2	1.3 / (*1.0*)	-1.7 / -1.6	DNA replication factor
MCM2	3	1.4 / (*1.2*)	-1.5 / (*-1.1*)	DNA replication factor
PFS2	2,9	1.5 / (*1.2*)	(*1.4*) / -1.2	DNA replication factor
RFC3	2,8	(*1.2*) / 1.2	-1.3 / (*-1.2*)	DNA replication factor
BLM	2,7	(*1.2*) / 1.2	-1.6 / (*-1.5*)	DNA helicase
MCM7	2,6	1.4 / (*1.1*)	(*-1.4*) / -1.1	DNA replication factor
PKMYT1	2,2	1.6 / (*-1.0*)	-1.5 /(*-1.1*)	protein kinase
TIPIN	2,2	1.3 / 1.6	(*-1.1*) / (*-1.0*)	DNA damage signaling
E2F5	2	1.4 / 1.6	1.3 / (*1.0*)	transcription factor
IRS2	-2	-1.5 / -1.6	1.7 / (*1.0*)	signaling molecule
EGR1	-3,1	(*1.0*) / 2.5	1.8 / 3.3	transcription factor
FOS	-4,7	(*1.0*) / 1.3	1.7 / 2.0	transcription factor

* fold changes in brackets are statistically insignificant

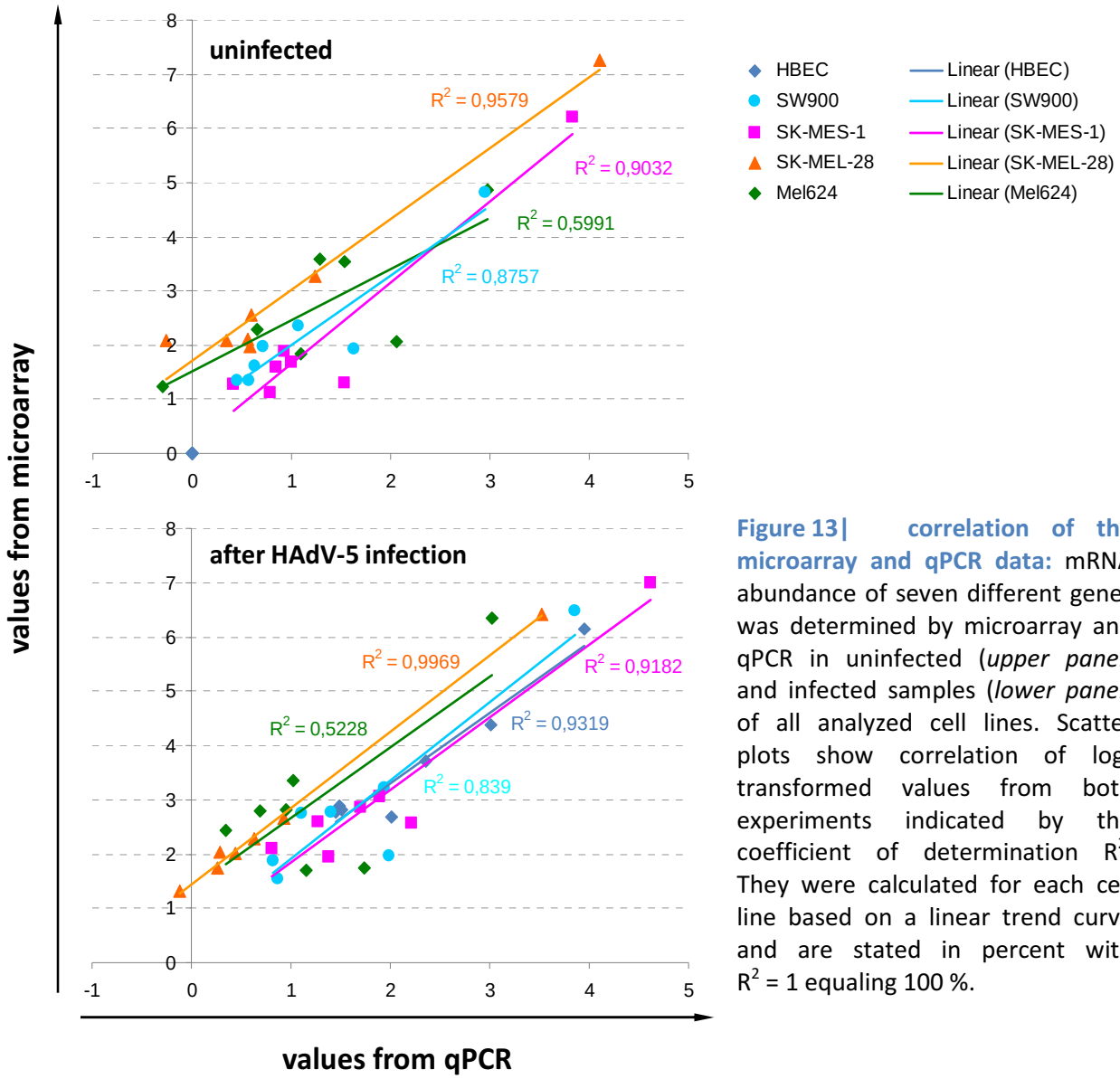

Figure 13| correlation of the microarray and qPCR data: mRNA abundance of seven different genes was determined by microarray and qPCR in uninfected (*upper panel*) and infected samples (*lower panel*) of all analyzed cell lines. Scatter plots show correlation of $\log_2$ transformed values from both experiments indicated by the coefficient of determination R^2. They were calculated for each cell line based on a linear trend curve and are stated in percent with $R^2 = 1$ equaling 100 %.

2.2 Data interpretation by diverse computational tools

As adenovirus infection affects the expression level of several hundred genes simultaneously, functional data interpretation of microarrays based on single gene analysis would be tedious and time consuming. Hence, sophisticated mathematical tools are required to elucidate cellular signaling pathways that are influenced during infection by upregulation or downregulation of single genes with critical functions for the virus. Therefore, the data was first pictured in a more comprehensive way and then analyzed by statistical approaches. As my previous data suggested

more efficient HAdV-5 replication in cells of lung origin than in melanoma cells, I particularly focused on opposing cellular gene regulation in these two moieties.

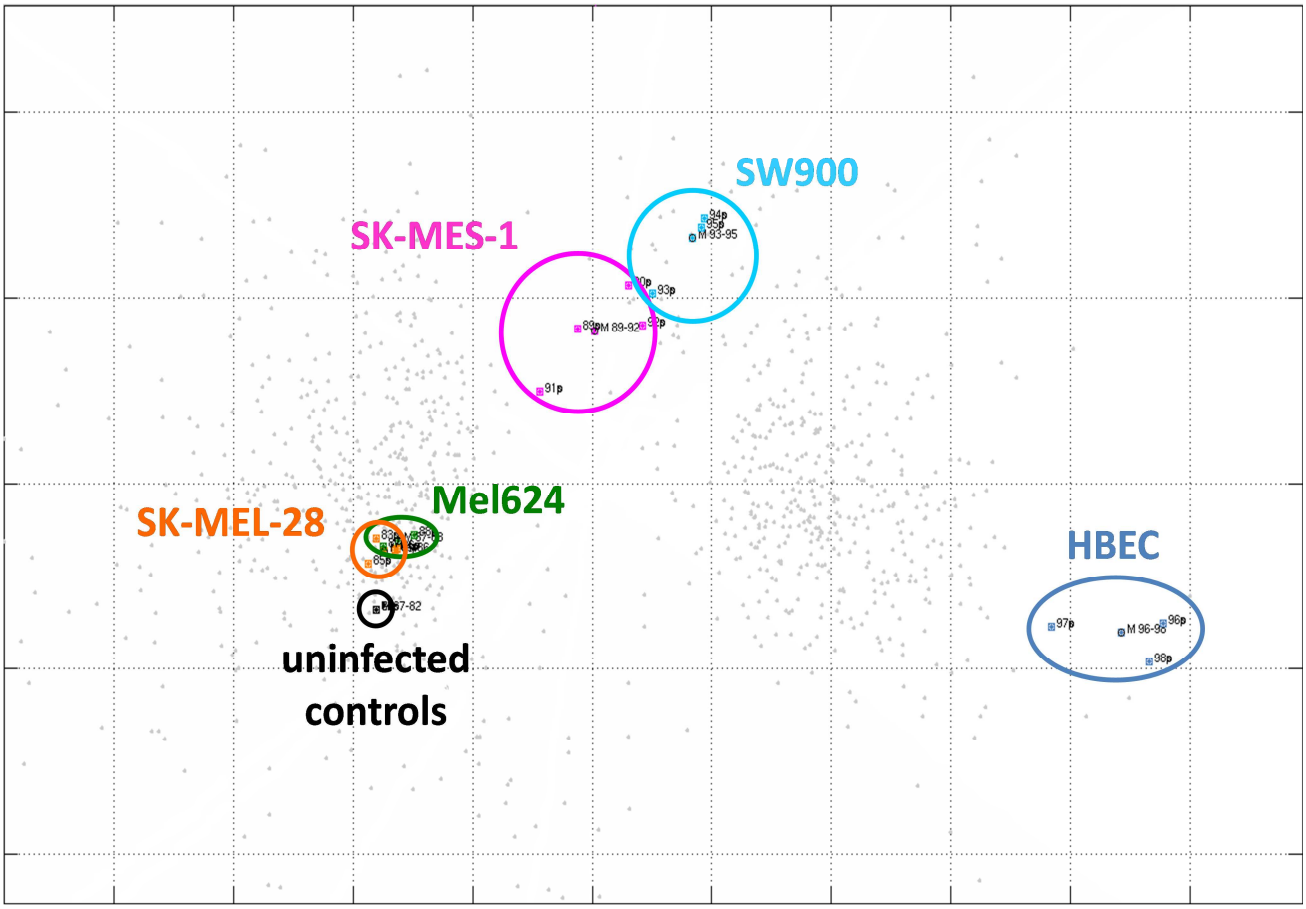

Figure 14| correspondence analysis of microarray data: multidimensional diagram shows expression of the 950 most significantly regulated genes (*grey dots*) and their regulation. Hybridized samples are represented by a colored box indicative for the cell type (*black = steady state gene expression in uninfected cells from each cell type, orange = infected SK-MEL-28, green = infected Mel624, pink = infected SK-MES-1, light blue = infected SW900, and dark blue = infected HBEC*). All boxes from one cell type surrounded by an equally colored circle are referred to as "condition". The position of single conditions relative to the uninfected controls correlates with the number and strength of regulated genes after infection with HAdV-5; that means a greater distance reflects more changes in gene expression after adenovirus infection. Data generated by the Multi-Conditional Hybridization Intensity Processing System, and filtered according to signal intensity ≥ 100, p-value ≤ 0.05, and fold change ≥ 1.4 in HBEC. Number of hybridized samples: HBEC, two donors n = 2/1, SW900 n = 3, SK-MES-1 n = 4, SK-MEL-28 n = 4, Mel624 n = 2.

The correspondence analysis plot in **Figure 14** was created by M-CHiPS using the list of approximately 950 significantly regulated genes in HBEC (*generated as described in the previous paragraph*) and visualizes all cell line samples and genes simultaneously in one multi-dimensional diagram [204]. Each hybridized sample is represented by a colored box indicative for the cell type (*see figure legend*). All boxes from one cell type are surrounded within an equally colored circle and referred herein as "condition". Thus, five conditions can be distinguished here: the steady state gene expression in uninfected controls and the infected condition from each cell type (*HBEC, SW900, SK-MES-1, and SK-MEL-28*). The position of single conditions relative to the uninfected controls correlates with the number and strength of regulated genes after infection with HAdV-5; that means a greater distance reflects more changes in gene expression after adenovirus infection. Individual genes are shown as grey dots in the diagram and their location within the correspondence analysis plot gives a rough overview of their regulation. For example, genes with high expression values in one or more conditions are located in the direction of the relevant condition(*s*). Hence, genes that are downregulated in the same condition are located in the opposite way. The majority of genes were upregulated in cells of lung origin, mostly HBEC and SW900 (*see summary in **Table 3***). An almost equal number was downregulated in all these cell types. On the other hand, infection of both melanoma cells SK-MEL-28 and Mel624 did not result in dramatic changes of cellular gene expression, including the number as well as the strength of regulated genes, which is indicated by the close proximity of each condition to the uninfected controls.

Another approach for interpretation of my microarray data is a so-called hierarchical clustering analysis of differentially expressed genes which was performed using the Multi-Experiment Viewer (*MeV 4.5.1; http://www.tm4.org*). Clustering is a mathematical way to associate different genes, and their expression values in single cell types, into sub-groups with higher similarity. In other words, clustering identifies groups of genes in a bigger data set that share similar functions. As a result, I obtained a color coded list of all regulated genes for my five analyzed cell types, also called "heat map" (***Figure 15***). In this heat map the respective color encodes how a single gene is expressed while the intensity reflects the strength of regulation, which means the brighter the color the stronger a gene is up- or downregulated.

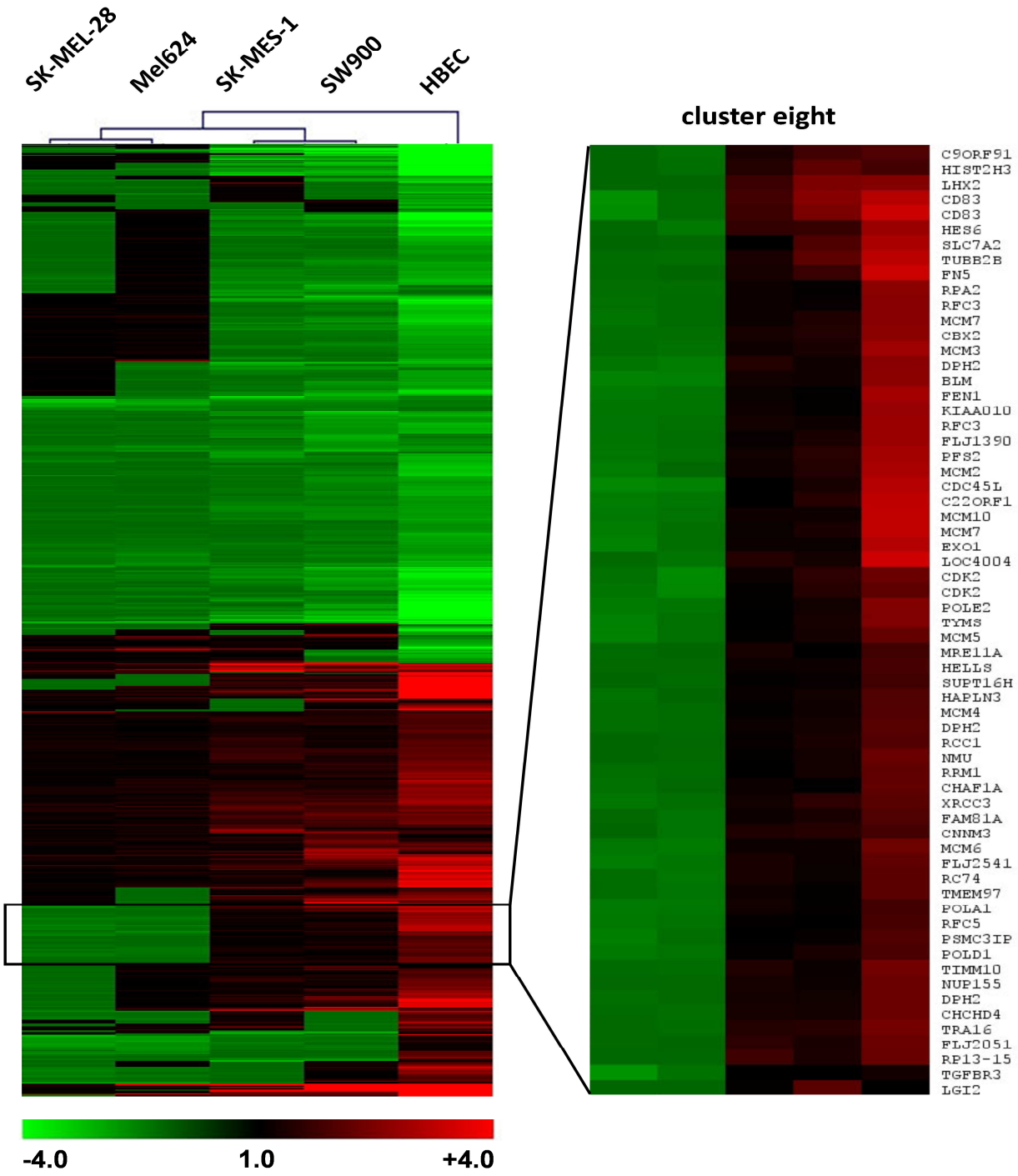

Figure 15| heat map and gene ontology analysis: Hierarchical clustering of microarray data with Multi-Experiment Viewer 4.5.1 based on the 950 most significantly regulated genes in HBEC. Color code resembles gene regulation with green for downregulation, black for no change in expression, or red for upregulation and the intensity correlates with fold change expression. Cluster borders were individually defined according to color patterns in lung versus melanoma cells. As a result, lists of genes for each cluster are obtained as demonstrated for the cluster eight containing the most conversely regulated genes between HBEC and melanoma cells (*zoom-in*). These were subjected to gene ontology analysis using the Database for Annotation, Visualization and Integrated Discovery to identify genes with similar functions (*refer to **Table 5***). P-values of GO terms were corrected for multiple testing using the Benjamini-Hochberg algorithm.

Afterwards, I determined nine individual groups, also termed clusters, of genes that show either similar (*genes in each cell type have the same color*) or gradually contrasting regulation (*colors are different in at least one cell type*). Consequently, a smaller subset of genes within each cluster was defined and subjected to a gene ontology (*GO*) analysis using the Database for Annotation, Visualization and Integrated Discovery (*DAVID; http://www.david.abcc.ncifcrf.gov*) which is an expert-curated database assigning genes to various functions or functional categories (*GO terms*).

Since my previous results demonstrated more efficient HAdV-5 replication in HBEC, I focused especially on a cluster containing genes that were strongly activated in HBEC and at the same time downregulated in melanoma cells as it was the case for cluster eight (*zoom-in of **Figure 15**).* Analysis of cluster eight revealed a number of genes involved in the GO terms cell cycle, DNA replication, nucleotide metabolism as well as the cellular DNA repair response (*summarized in **Table 5***). The GO terms were statistically analyzed and p-values corrected for multiple testing using the Benjamini-Hochberg algorithm, which determines the false discovery rate in multiple comparisons [205]. Accumulation of single genes in cluster eight with these GO terms was highly significant according to the extremely low p-values of at least $p \leq 10^{-7}$ which rules out random accumulation. Intriguingly, relevant genes within each GO term were induced in HBEC after wild type HAdV-5 infection but downregulated in both melanoma cell lines SK-MEL-28 and Mel624 (*overview in **Table 4***). For the lung squamous carcinoma an intermediary phenotype was observed, however, most gene expression levels were either unchanged or slightly upregulated but not downregulated as in the melanoma cells.

Table 5| summary of gene ontology analysis of cluster eight

GO term	number of regulated genes	p-value
DNA replication	25	2.7×10^{-28}
DNA metabolic process	30	8.3×10^{-23}
response to DNA damage stimulus	15	1.8×10^{-10}
DNA repair	13	5.7×10^{-9}
cell cycle	17	7.9×10^{-7}

As single genes and therefrom translated proteins interact in complex cellular signaling pathways, I uploaded the list of significantly regulated genes of HBEC and SK-MEL-28 to the Ingenuity Pathway Analysis software (*IPA; http://www.ingenuity.com/*). This allowed me, as opposed to the clustering analysis, an allocation of individual genes in regulatory networks. For most genes no direct connection within a common pathway could be found with exception of the canonical G1/S transition regulatory network of the cell cycle (*see **Figure 16***). Again, it was striking to see that the adenovirus infected HBEC strongly expressed several important genes for S-phase entry including E2F2, CCNE, and the CDC25A homologue while other inhibitory genes like $p21^{WAF/CIP}$ or typical G1-phase genes including CDK4/6 and CCND were downregulated. On the other hand HAdV-5 infection in SK-MEL-28 resulted in no detectable induction but rather downregulation of stimulatory genes and/or absent downregulation of inhibitors in this pathway.

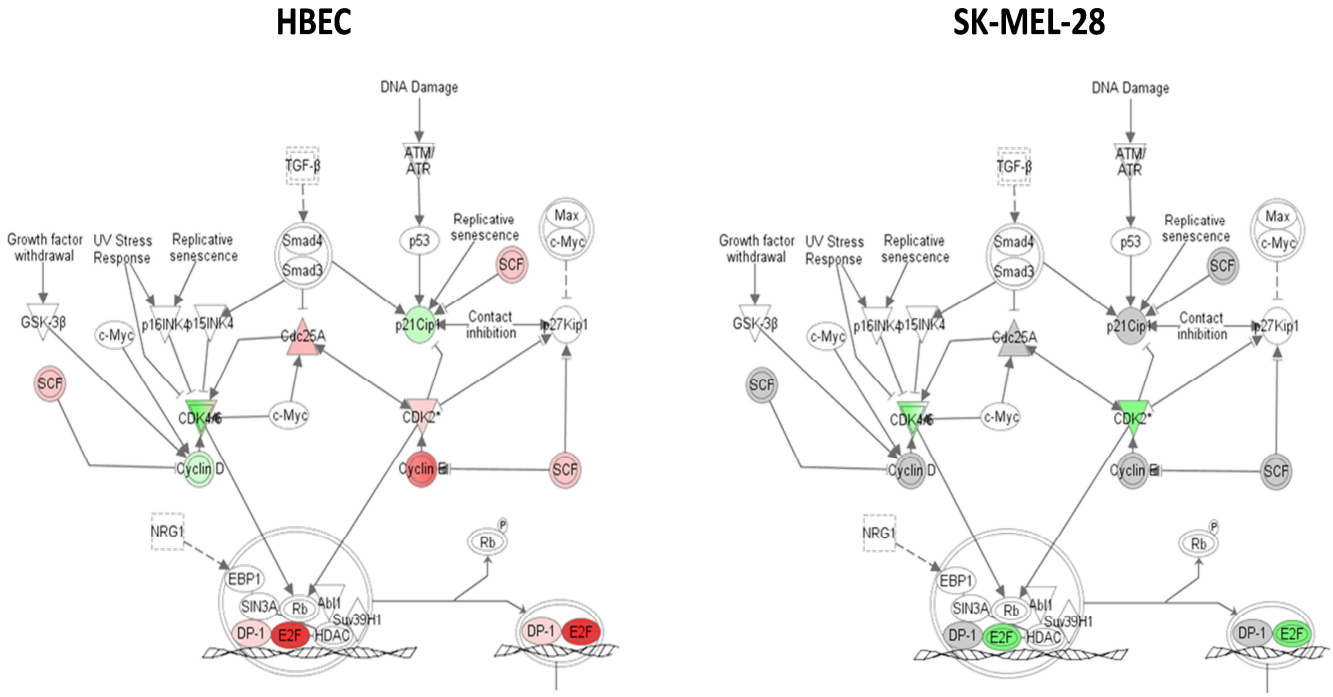

Figure 16| activation of the G1/S-phase transition pathway: expression values of the 950 most significantly regulated genes in HBEC were uploaded to the Ingenuity Pathway Analysis software and mapped onto diverse cellular pathways. This revealed a strong upregulation of several pro S-phase genes involved in the canonical G1/S-phase transition regulatory network of the cell cycle in HBEC (*left diagram*) but not melanoma, represented by SK-MEL-28 (*right diagram*). Green and red nodes equal down- and upregulated genes, respectively. Grey nodes indicate no change in gene expression. The color intensity correlates with strength of fold change expression.

Concluding all computational results, different analysis tools showed a significantly stronger gene regulation in HBEC after HAdV-5 infection than in the other tumor cell lines. Moreover, in SK-MEL-28 and Mel624 melanoma cells only a few genes were induced after adenovirus infection and surprisingly often in an opposing manner as compared to infected HBEC, SW900, and SK-MES-1 cells. In cells of lung origin, wild type HAdV-5 induced several genes with important functions in cell cycle regulation, DNA replication, and nucleotide metabolism. A similar gene expression pattern could not be observed in either melanoma cell line. Quite the contrary, in SK-MEL-28 and Mel624 many of these genes were either not or only weakly induced or often also downregulated. Furthermore, the linear ends of adenoviral genomes are expected to trigger a cellular DNA damage response, supported by the induction of relevant DNA repair genes in cells of lung origin [95,96]. Although this circumstance is normally considered a cellular defense mechanism, it was again absent in melanoma cells. Above all, I found that the signaling pathway responsible for G1/S-phase transition, a key pathway for adenoviral DNA synthesis, was strongly activated through upregulation of stimulatory genes in HBEC upon infection with HAdV-5, while inhibitory genes were downregulated at the same time. Among the activating genes in infected HBEC, the E2F2 gene presumably plays an outstanding role as E2F transcription factors induce the expression of several S-phase genes as mentioned in the INTRODUCTION. Strikingly, E2F2 and other activating S-phase genes were again not induced or downregulated in SK-MEL28 and Mel624 melanoma cells. Hence the gene expression signature identified in infected melanoma cell lines, involving the key pathway for S-phase entry, might provide a molecular basis for the previously observed inefficient adenovirus DNA replication compared to cells of lung origin. Subsequently, I investigated S-phase entry by an independent biological assay using a modified luciferase reporter gene approach.

2.3 S-phase reporter gene assay

Induction of S-phase is a key feature of human adenoviruses enabled by the E1A master regulator proteins. This is achieved through disruption of pRB/E2F regulatory network and release of E2F transcription factors. Eventually, they will bind and activate a plethora of cellular and adenoviral promoters bearing E2F responsive elements.

These are usually found in genes involved in cell cycle regulation and DNA replication like those previously identified by my microarray approach. The computer assisted cluster gene ontology and ingenuity pathway analysis of the microarray data showed a significant induction of a panel of genes involved in the G1/S transition regulatory network after HAdV-5 infection in lung cells but no melanoma. To study this effect in infected cells more closely, I developed an independent biological assay for S-phase induction. The design capitalizes on a shortened E2F promoter element which can be activated in a positive feedback loop by transcription factors of the E2F family in order to drive luciferase expression and thus served as "sensor" for S-phase entry.

First, I transfected this construct along with a similar construct containing the simian virus 40 (*SV40*) promoter into different tumor cell lines and in primary HBEC. The SV40 promoter does not contain an E2F responsive element and served as constitutively active control. Second, I inoculated the cells with relevant $TCID_{50}$ titers for 80 % transduction with wild type HAdV-5 or a replication-deficient HAdV-5 CMV-gfp variant on the next day. The latter encodes all adenoviral genes except the ones in the E1 and E3 region and provided a control for E1A/viral DNA replication-independent effects on the promoter activity. Luciferase expression was measured at or shortly before the estimated time of virus DNA replication. Thus, I chose a twenty hour time point post infection for every cell line which should be sufficient for prior or coinciding activation of the S-phase reporter construct even in the case of Mel624 where adenovirus DNA replication became apparent around 24 hours. In all cells of lung origin (*upper panels,* ***Figure 17A*** *see next page*) HAdV-5 was able to activate the E2F promoter constructs resulting in significant higher luciferase activity compared to the E1 region deleted HAdV-5 CMV-gfp negative control. A similar activation but to a severely reduced amount was observed in SK-MEL-28 after infection with HAdV-5 but not in Mel624. The stimulatory effect of wild type HAdV-5 was specific for the E2F promoter since there was no or only a minor luciferase increase from the SV40 promoter after infection with HAdV-5 or HAdV-5 CMV-gfp. Moreover, transduction with the HAdV-5 CMV-gfp did not significantly increase E2F or SV40 promoter activity in any of the cell types. For better comparison, I calculated the fold change increase of luciferase activity from both promoter constructs after infection with HAdV-5 and set the values from transduction with HAdV-5 CMV-gfp as one (***Figure 17B****, see next page*). Again, the lung cells showed the highest fold induction of

the E2F promoter compared to the relevant SV40 control. The melanoma cells showed the lowest or no fold change increase. Nevertheless, both were considerably below the primary HBEC, A549, and SW900.

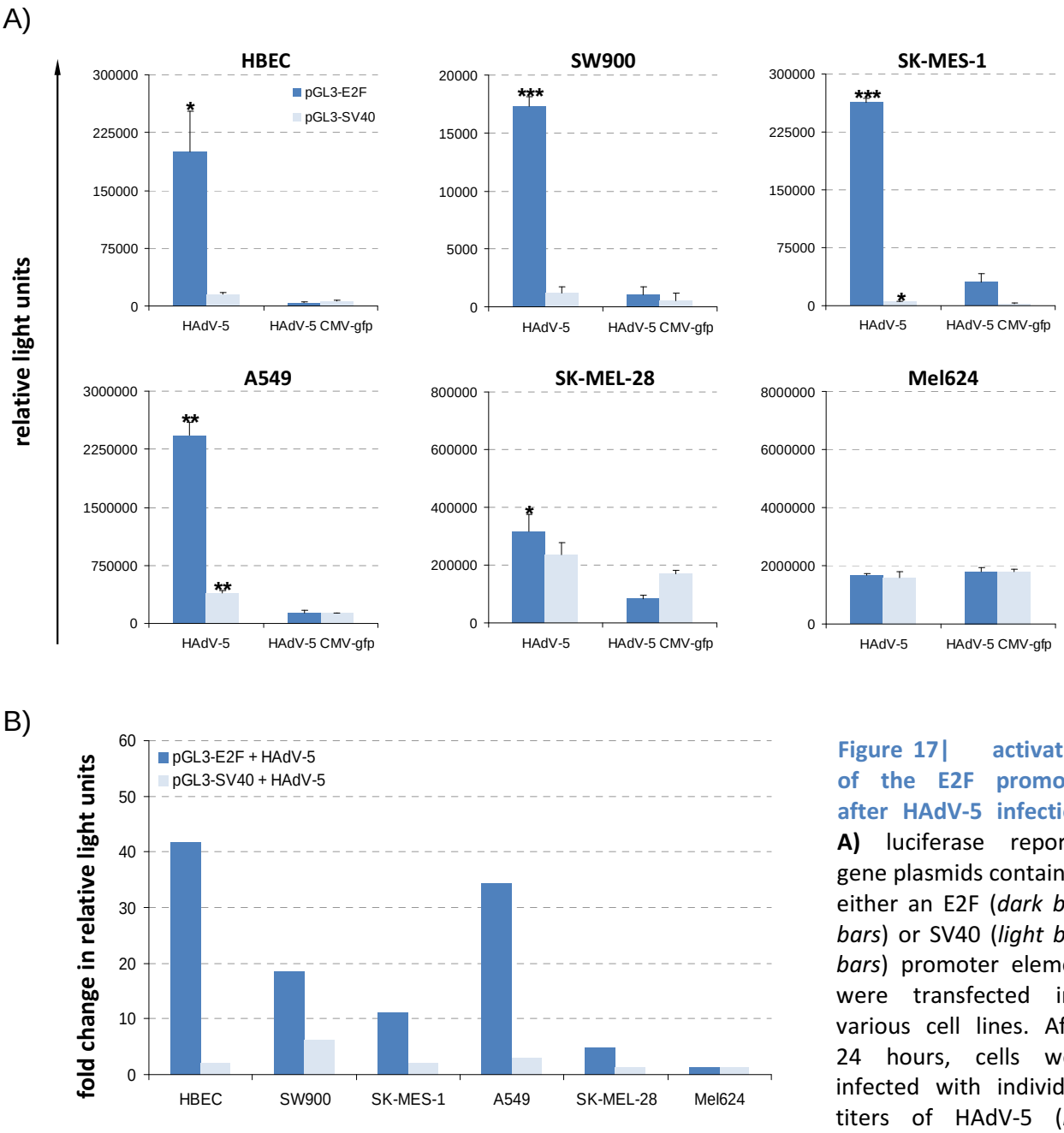

Figure 17| activation of the E2F promoter after HAdV-5 infection: **A)** luciferase reporter gene plasmids containing either an E2F (*dark blue bars*) or SV40 (*light blue bars*) promoter element were transfected into various cell lines. After 24 hours, cells were infected with individual titers of HAdV-5 (*left columns*) or the E1 region deleted HAdV-5 CMV-gfp (*negative control, right columns*) resulting in 80-90 % infection. Luciferase activity was quantified twenty hours post infection. Each bar with standard deviation represents mean values of triplicate transfections and infections. P-values were calculated between HAdV-5 and HAdV-5 CMV-gfp of the same promoter construct using the Student's t-test (** $p \leq 0.05$, ** $p \leq 0.01$, *** $p \leq 0.001$*). **B)** Fold change induction of the E2F promoter compared to SV40 promoter after HAdV-5 infection.

Therefore, the S-phase reporter gene data related to the computational microarray analysis. Activation of the G1/S-phase transition pathway, involving the release of E2F transcription factors from pRB by adenovirus E1A proteins, could be determined through induction of an E2F responsive promoter/reporter gene construct after infection with HAdV-5 but not an E1 region deleted control virus. As before, HBEC followed by several lung carcinoma cells showed potent activation of this pathway after infection with HAdV-5 while melanoma cells were mostly refractory to the same stimulus. In conclusion, my microarray data together with the described assay might provide a rationale and tool to study the limited ability of HAdV-5 to efficiently replicate in malignant melanoma cells. Eventually, I wanted to analyze expression of single candidate genes in a wider melanoma cell panel.

2.4 Candidate gene expression in a wider melanoma cell panel

The adenovirus specific gene expression signatures identified in infected SK-MEL-28 and Mel624 cells revealed that several genes with functions in cell cycle regulation and S-phase entry, nucleotide metabolism, and DNA replication were not or only weakly induced and sometimes even downregulated. My goal therefore was to look at mRNA expression levels of individual genes in a wider melanoma cell panel and investigate whether the inability of HAdV-5 to activate these genes in SK-MEL-28 or Mel624 is a more common phenomenon in other melanoma cells. In the end, certain gene expression signatures might be useful to predict adenovirus replication efficacy in other cell types.

For this experiment I evaluated candidate mRNA abundance in a panel of infected established cell lines and low passage melanoma cells. This set included cells originally derived from pigmented (*SK-MEL-28, Mel624, Mel888, Colo-829, pMel A, pMel A2, and pMel L*) as well as amelanotic malignant melanomas (*C8161 and A375M*) to determine the impact of pigmentation on adenovirus replication. As reference, they were compared to relevant uninfected controls as well as primary HBEC, the lung squamous carcinoma cell lines SW900 and SK-MES-1, and the lung adenocarcinoma cell A549. Most of which showed good susceptibility for HAdV-5 infection and cell lysis demonstrated in earlier cytotoxicity assays (*refer to II, 1.2*).

Table 6| HAdV-5, HAdV-5 CMV-gfp, or HAdV-5/3 titers for 80-90 % infection of other cancer cell lines

cell line	origin	CAR expression	virus type	$TCID_{50}$ titer/cell
A375M	amelanotic melanoma	no	HAdV-5/3	1000
A549	lung adenocarcinoma	yes	HAdV-5	400
C8161	amelanotic melanoma	no	HAdV-5/3	700
Colo-829	melanoma	yes	HAdV-5	300
Mel888	melanoma	yes	HAdV-5	400
pMel A	low passage melanoma	no	HAdV-5/3	500
pMel A2	low passage melanoma	no	HAdV-5/3	1000
pMel L	low passage melanoma	no	HAdV-5/3	500

Subsequently, cells were incubated with individual MOIs of wild type HAdV-5 or HAdV-5/3 (*depending on CAR expression, see **Table 6***) leading to 80-90 % infection rates. Total RNA was harvested at twenty hours post infection from infected and equivalently treated uninfected samples. After purification, I quantified mRNA expression of selected candidate genes involved in cell cycle regulation and DNA replication by qPCR and normalized the signals to the cellular RNA input determined by ACTB. These genes were previously found to be induced in infected HBEC but not or only weakly in SK-MEL-28 and Mel624 (*also refer to **Table 4***). Relative mRNA levels were correlated to the level measured in uninfected HBEC cells and are depicted in **Figure 18**. For all genes, I did see a strong virus dependent increase of mRNA abundance in infected HBEC cells as expected. Disappointingly, there was no obvious general adenovirus mediated pattern of gene expression in any of the other cell lines. This observation was independent of the evaluated cell type and pigmentation status as discussed for the example of the E2F2 gene, the most strongly induced gene after HAdV-5 infection in HBEC. Whereas, E2F2 mRNA expression was stimulated during infection in HBEC, SW900, and several other cell lines including most melanomas, it was downregulated in SK-MEL-28 and A549. Regarding SK-MEL-28 this turned out to be as expected. However A549 cells, like HBEC and SW900, are known to optimally support HAdV-5 infection. Thus, downregulation of E2F2 in A549 was astonishing. Moreover, the steady state levels of mRNA in uninfected cell samples were commonly higher than in HBEC. This however did not limit the ability of HAdV-5 to further increase the mRNA abundance during infection as in case of SK-MES-1 or Mel888 cells.

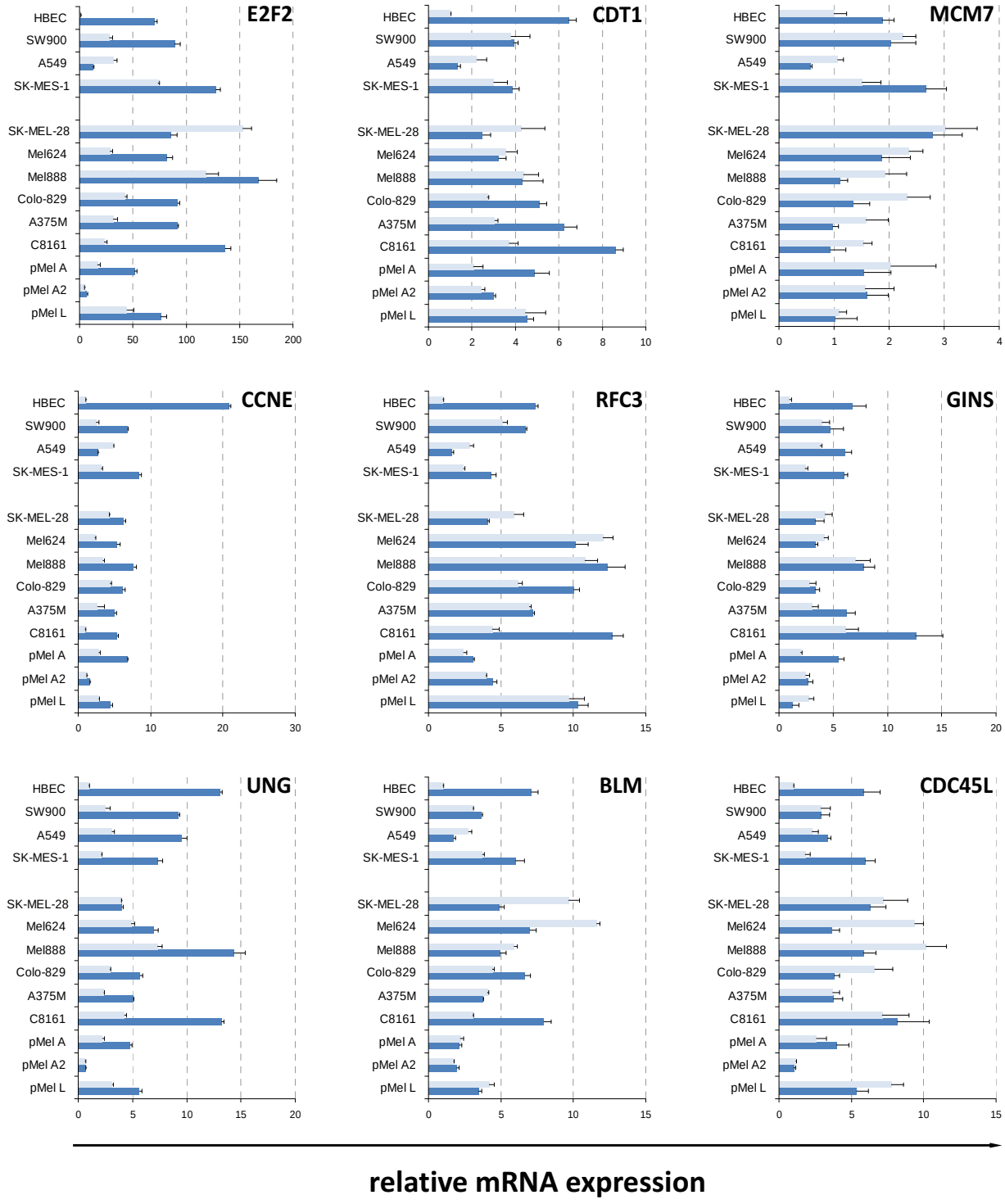

Figure 18| expression of selected cell cycle related genes in infected melanoma cells: various cells of lung origin (*upper group in each diagram*) and different pigmented and amelanotic melanomas (*lower group in each diagram*) were infected with relevant titers of HAdV-5 or HAdV-5/3 (*as indicated in* ***Table 6***). Relative mRNA expression levels of single genes were normalized to ACTB signals using Q-Gene software (*see paragraph V, 1.9.2*). As a reference, mRNA abundance from uninfected primary HBEC was set as one. Respective diagrams show gene expression after infection (*dark blue bars*) compared to the relevant uninfected control sample (*light blue bars*). Bars and standard deviation represent triple measurements from the same sample.

As a general bottom line, a phenotype similar to infected SK-MEL-28 and Mel624 cells with unchanged gene expression or even downregulation of single genes could not be observed in a wider panel of melanoma cells. Indeed, almost all of the assessed candidate genes were induced in infected melanoma cells, which have been characterized by me and others and are usually modestly permissive for HAdV-5. At the same time they were differentially expressed in infected cells with high permissivity including HBEC (*upregulated*) and A549 (*downregulated*). Thus, a direct relationship of single gene expression and replication efficiency or cytotoxicity was only feasible for the set of cells investigated in our microarray study, but not in a wider panel of melanoma cells. Also, it might be possible that S-phase entry in the latter is affected by regulatory mechanisms other than upregulation of gene expression. One has to keep in mind that my experiments based on quantification of mRNA and therefore cannot account for changes in posttranscriptional regulation, *de novo* protein translation, protein-protein interactions, and interplay in regulatory networks. Hence, several aspects might explain why cell type-dependent replication efficacy could be linked to individual marker genes in a few cell lines as in case of SK-MEL-28 and Mel624 but not in others. This reasoning strengthens the importance of comprehensive analyses of complex cellular signal pathways rather than single factors in order to predict replication efficacy of HAdV-5 in other cell types. Nonetheless, the knowledge gained from my microarray data might help to engineer oncolytic adenoviruses with enhanced replication potential, at least for a subset of melanoma represented by SK-MEL-28 or Mel624 that were investigated here. In the following chapter different strategies are employed utilizing overexpression of regulatory transgenes, small inhibitory RNAs, or drugs that might lead to activation of relevant host genes or signaling pathways.

3 Identification of strategies to enhance HAdV-5 replication in cancer cells

3.1 Overexpression of regulatory genes

During the last two chapters of my study it became evident that viral DNA replication in infected melanoma cell lines SK-MEL-28 and Mel624 is lower compared to primary lung cells that resemble the natural host cell type of HAdV-5. This is accompanied by lacking or reduced S-phase induction and subsequent expression of cellular host genes involved in cell cycle regulation, nucleotide metabolism, and DNA metabolism. Both aspects could potentially limit the clinical benefit of HAdV-5 based virotherapeutics for malignant melanoma as virus amplification is the most important mechanism of action. Hence, one approach to overcome this utilizes mutation or engineering of adenoviruses to express additional genes that increase their lytic potency. For example, deletion of the E1B-19k gene, a cellular homologue of the anti-apoptosis gene BCL2 resulted in increased cytotoxicity in several but not all cancer cells [172-174]. Thus, the concept to enhance a naturally evolved virus for cancer therapy is in general feasible.

In my case, I wanted to apply this concept by transfecting various genes characterized for their stimulatory effects on the cell cycle (*summary and function given in **Table 7***) in adenovirus infected melanoma cells and thereby complement possible defects in S-phase activation of HAdV-5. Among them were human genes found in the microarray analysis comprising the E2F transcription factors but also different viral oncogenes from human papilloma viruses (*HPV*), the SV40; and the human herpes virus type 8 (*HHV-8*) that served as proof of principle controls. To determine their impact on adenovirus replication, I transfected the respective constructs along with an empty vector control in SK-MEL-28 melanoma cells. The transfection efficiency was controlled by a gfp tagged version of the CDC25A phosphatase to rule out that absent activation by any of the selected genes was due to insufficient transfection (*data not shown*). Following a short incubation time of sixteen to twenty hours, cells were infected with an MOI of 1 $TCID_{50}$/cell HAdV-5. Thereby, I tried to mimic a situation where the oncolytic adenovirus is used as vector for *de-novo* expression of a relevant transgene synchronized with infection. As a read-out viral genome copy numbers were determined 24 hours post infection by qPCR since viral DNA replication is a direct consequence of S-phase induction.

Table 7| genes with stimulatory effects on the cell cycle

gene	host	function
CCNE	human	cyclin associated with G1/S-phase transition
CDC25A	human	phosphatase involved in G1/S-phase transition, gets degraded in response to DNA damage
E2F1	human	transcription factor of genes whose products are involved in S-phase entry or in DNA replication
E2F2	human	transcription factor of genes whose products are involved in S-phase entry or in DNA replication
E2F5	human	transcription factor of genes whose products are involved in S-phase entry or in DNA replication
E7	human papilloma virus 16	disrupts pRB/E2F complexes, interferes with histone deacetylation and activates transcription
E7	human papilloma virus 18	disrupts pRB/E2F complexes, interferes with histone deacetylation and activates transcription
E7	human papilloma virus 31	disrupts pRB/E2F complexes, interferes with histone deacetylation and activates transcription
large T antigen	simian virus 40	disrupts pRB/E2F complexes, possesses helicase activity
small T antigen	simian virus 40	accelerates both G1- and S-phase progression, may inhibit cap dependent mRNA translation
v-cyc	human herpes virus type 8	forms a complex with CDK6 that inactivates pRB, resistant to actions of $p16^{INK4a}$ and $p21^{WAF/CIP}$
YB1	human	transcription factor, interferes with TP53 induced apoptosis but not $p21^{WAF/CIP}$ dependent cell cycle arrest

As can be seen in Figure 19, the virus replicated to high amounts of around 4.5×10^6 viral genome copies in cells containing the empty vector control. This was seen to a similar extend in presence of CCNE, the cellular phosphatase CDC25A, the Y-box binding protein 1 (YB1), and the viral SV40 large T antigen as well as the E7 genes from HPV-16 or HPV-31. Only after transfection of HPV-18 E7, I observed a strong and significant increase of adenoviral genomes. However, this effect could not be reproduced with statistical significance in further assays (*data not shown*). Interestingly, the SV40 small T antigen and the HHV-8 viral-cyclin (*v-cyc*) had reproducible inhibitory effects on adenovirus replication. Further, this was dominant for the small T antigen as implied by double transfections of both small and large T antigens. Similar experiments with the E2F transcription factors, based on double

infections with a replication-deficient HAdV-5 E2F1, HAdV-5 E2F2, or HAdV-5 E2F5 together with wild type HAdV-5, also yielded no enhancing effect (*data not shown*).

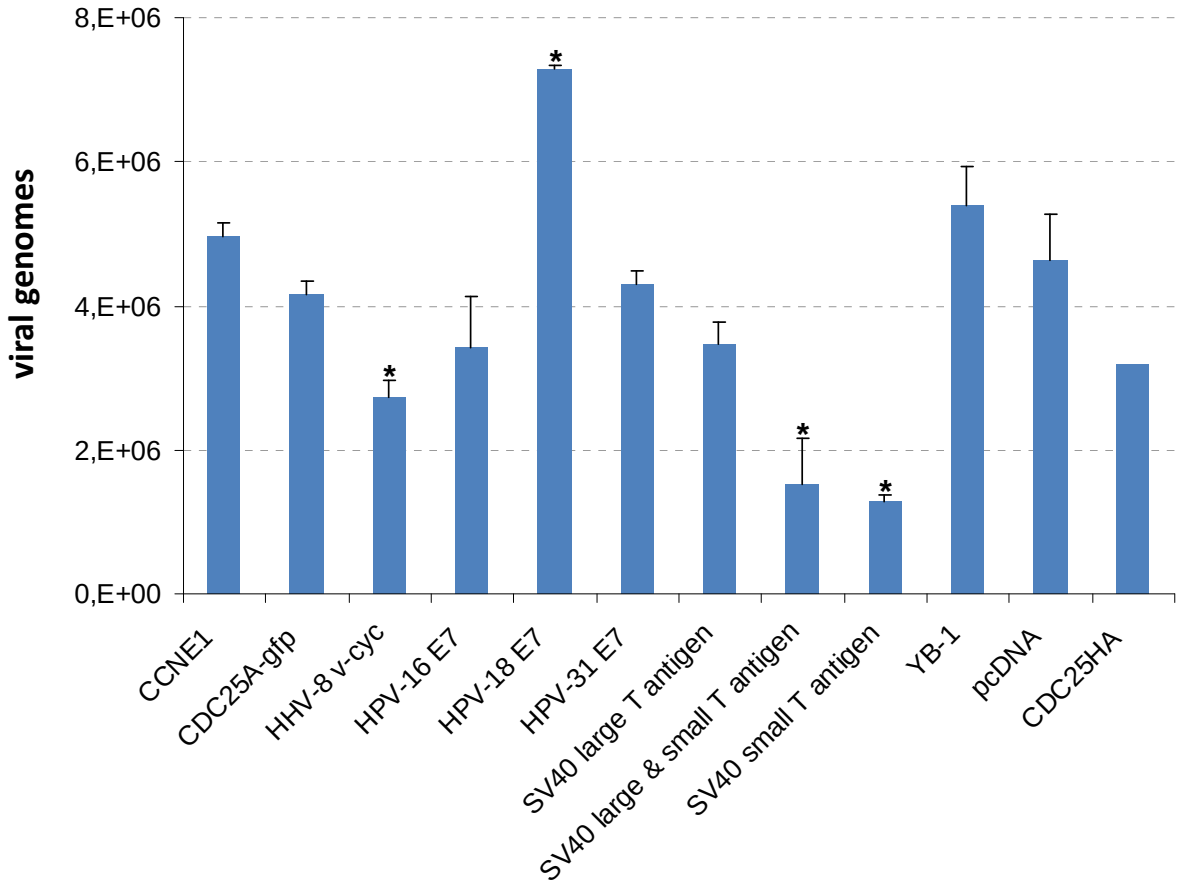

Figure 19| transfection of cell cycle related genes and their impact on adenovirus replication: SK-MEL-28 cells were transfected with relevant cellular and viral genes (***Table 7***). In addition, a negative control comprising an empty expression plasmid (*pcDNA3.1*) was included. Shortly afterwards, cells were inoculated with 1 $TCID_{50}$/cell of HAdV-5. After 24 hours post infection, pellets were harvested for purification of total DNA. Means of viral genomes per ACTB were determined by qPCR and are shown as dark blue bars with standard deviation, resembling mean values of triplicate transfections/infections. Significance was calculated according to the Student's t-test versus pcDNA (** $p \leq 0.05$*).

To sum up, transfections of diverse genes with known inducing effects on S-phase entry of the cell cycle did not augment adenovirus replication in SK-MEL-28 cells. In some assays, a weak enhancing effect of HPV-18 E7 could be observed. However, statistical significance could not be reproduced. Besides, inhibition of adenovirus DNA replication by some transgenes was more pronounced than any potential benefits. Identical results were obtained when I repeated

these experiments using the HAdV-5/3 Δ24 T2A-luc which expresses the luciferase reporter gene in a DNA replication-dependent manner under control of the major late promoter. Despite several efforts to optimize my assay, major drawbacks remained as transgene expression was transient, inhomogeneous, and not in context of a replication-competent virus bearing the transgene. Nevertheless, even similar assays using double infections of wild type HAdV-5 together with replication-deficient adenoviral vectors bearing E2F transcription factors did not show any promise. In the end, I did not succeed to enhance adenovirus replication by overexpression of single genes and therefore tried a knockdown approach of two cell cycle inhibitors.

3.2 Knockdown of cell cycle inhibitors

With the discovery of small interfering RNA (*siRNA*) it became possible to selectively knockdown particular target genes with limiting side effects on the residual cellular gene expression. This system has been frequently used to study regulation of signal transduction pathways for example by screening for unknown genes or by knocking down key players [206-208]. In theory, it can be used likewise to induce a certain cellular state, in my case transition into S-phase, by eliminating relevant inhibitors. Prominent examples for negative regulators of the cell cycle are the $p16^{INK4a}$ and $p21^{WAF/CIP}$ proteins. Normally $p16^{INK4a}$ inhibits the proliferation of normal cells by interacting strongly with the CDK4/6 which in turn inhibits their ability to destabilize pRB/E2F complexes (*summarized in **Figure 4***). On the other hand, $p21^{WAF/CIP}$ binds and inactivates complexes of CDK2 and cyclin E or A which usually stimulate cell cycle progression through phosphorylation of diverse substrates. Hence, inhibition of CDK/cyclin complexes leads to a cell cycle arrest in G1-phase. In addition, a recent publication illustrated the viability of this approach by increased wild type adenovirus replication and formation of progeny virions in a $p21^{WAF/CIP}$ deficient colorectal carcinoma cell line [209].

Therefore, I purchased verified and tested siRNAs against each inhibitor and utilized them for transfection of SK-MEL-28 and Mel624 cells accordingly. A randomized pool of four nonsense siRNAs without known cellular targets served as a negative control. The knockdown efficacy was determined by qPCR and generally ranged between 60-90 % compared to the control (*refer to **Figure 20A***).

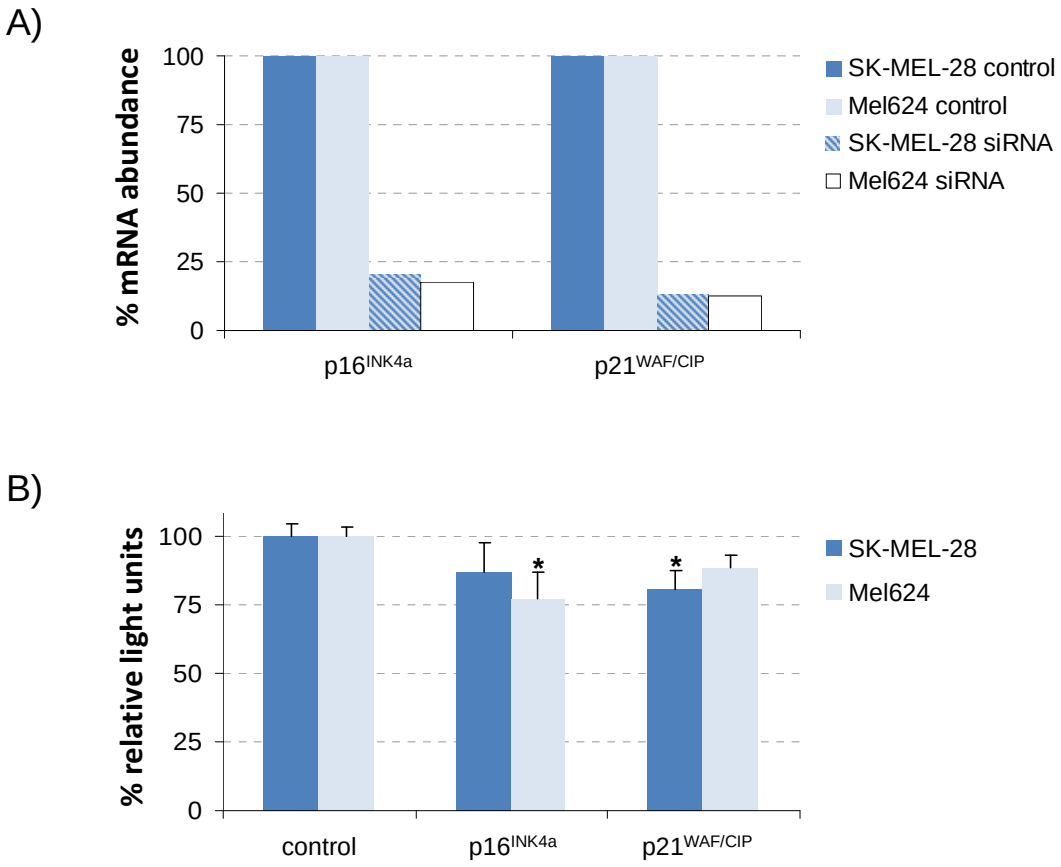

Figure 20| impact of $p16^{INK4a}$ and $p21^{WAF/CIP}$ mRNA knockdown on adenovirus replication: **A)** after siRNA transfection GAPDH normalized mRNA levels of both inhibitors were determined by qPCR. Values from SK-MEL-28 and Mel624 cells containing a pool of nonsense control siRNAs (*dark and light blue bars, respectively*) were set as 100 % and compared to cells after transfection of gene specific siRNAs (*striped and white bars, respectively*). **B)** luciferase reporter gene assay of SK-MEL-28 (*dark blue bars*) as well as Mel624 (*light blue bars*) cells after transfection with indicated siRNAs and infection with 1 $TCID_{50}$/cell HAdV-5/3 Δ24 T2A-luc for 48 hours. Bars and standard deviation represent triplicate experiments normalized to the control siRNA, p-values were calculated according to the Student's t-test compared to the control (** $p \leq 0.05$*). **C)** shown on the next page, relative mRNA expression of individual host cell candidate genes after nonsense siRNA (*light blue bars*) or $p21^{WAF/CIP}$ specific siRNA transfection (*dark blue bars*). Bars and standard deviation are based on three measurements of the same sample; normalization was done using Q-Gene software.

Following transfection, I incubated the cells with 1 $TCID_{50}$ HAdV-5/3 Δ24 T2A-luc for 48 hours and harvested samples for subsequent luciferase assays and qPCR. Unfortunately, neither $p16^{INK4a}$ nor $p21^{WAF/CIP}$ knockdown resulted in an elevated luciferase activity after infection which is a direct consequence of virus genome amplification (***Figure 20B***). Quite the contrary, downregulation of each cell cycle inhibitor acted in a negative way on luciferase expression. In

addition, I investigated the relative mRNA expression levels of my candidate genes from **Table 4** in order to find evidence for an altered host cell environment after knockdown of both $p16^{INK4a}$ (*data not shown*) and $p21^{WAF/CIP}$ (***Figure 20C***). However, I did not find dramatic changes in mRNA abundance for most genes although CCNE or CDC25A seemed to be weakly upregulated whereas EGR1 and FOS were slightly downregulated in uninfected SK-MEL-28 48 hours after siRNA transfection.

C)

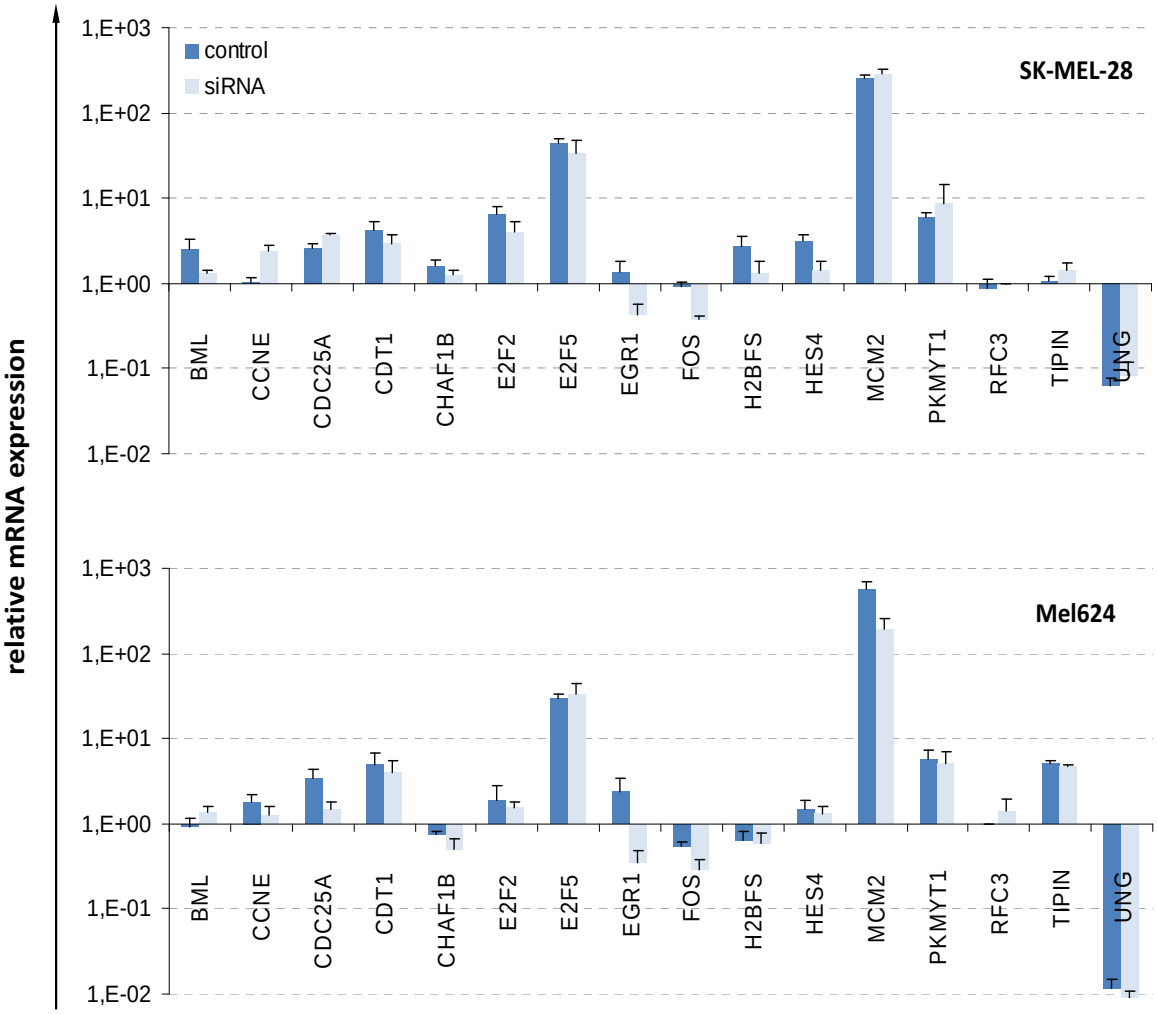

In conclusion, knockdown of two different cell cycle inhibitors could not enhance adenovirus replication in melanoma cells. Although, the knockdown did weakly enhance expression for individual cell cycle related genes in one cell line. The greater majority of my

candidate gene expression, however, remained unaffected. Here, knockdown of $p16^{INK4a}$ or $p21^{WAF/CIP}$ seemed to moderately inhibit adenovirus replication as determined by indirect reporter gene assays. Although this approach has been published for a human colon carcinoma cell lines, it did not work in my hands for melanoma cells despite efforts to optimize the system. Especially detection of $p16^{INK4a}$ and $p21^{WAF/CIP}$ proteins proved to be impossible by Western Blot which could be due to their low abundance in these cells. However, the knockdown efficiency was high on mRNA level which should have depleted relevant protein levels, especially as they possess only a short half-time. Thus, from a technical point of view my approach worked but did not yield the desired increase in HAdV-5 replication. Combined with previous experiment, my data again strongly suggested that expression/inhibition of individual genes, rather than activation of a whole regulatory network, was insufficient to enhance adenoviral lysis. To address this point, a combinatorial treatment of chemotherapeutic drugs with HAdV-5 was applied.

3.3 Impact of chemotherapeutics on adenovirus replication

Combination therapies are a major focus in treatment of cancer as single based treatments often cannot achieve complete eradication of the tumor. So far, most studies involving therapeutic viruses showed no reciprocal interference or even a superior effect of chemo- and virotherapy regarding tumor destruction [210,211]. This aspect might be supported by the individual drug toxicity or by direct and indirect synergism, which has often been postulated to be dependent on a cell cycle arrest and activation of apoptosis which might help the virus to amplify and spread. Cell cycle arrest in S-phase might indeed support better virus growth as it sustains the S-phase environment over longer times. Hence, several stimulatory factors for DNA replication would become available in greater amounts. To investigate and potentially exploit that mechanism, I tested the impact of several chemotherapeutics on adenovirus replication.

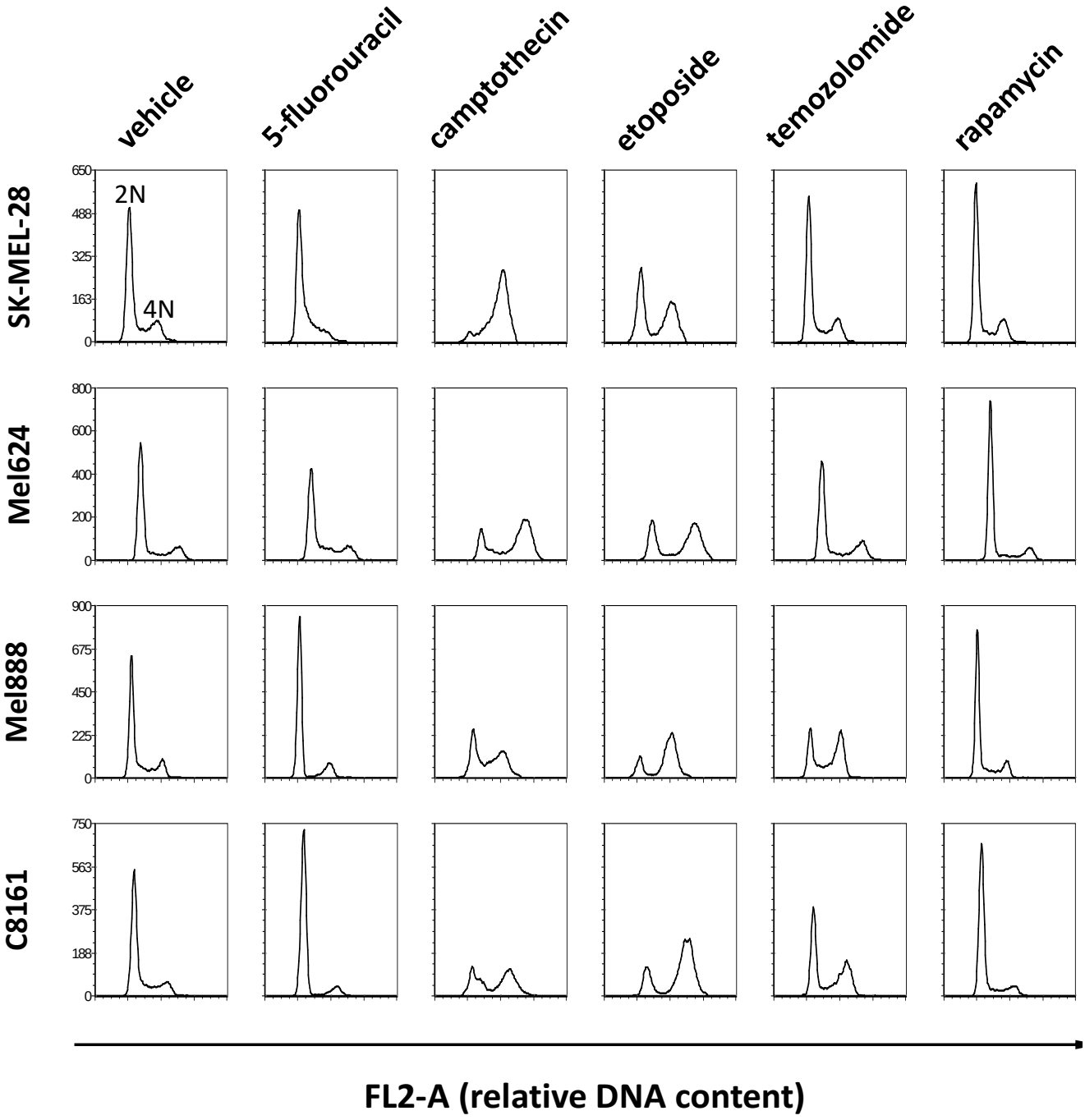

Figure 21| impact of chemotherapeutic drugs on the cell cycle of melanoma cells: cell lines were treated with either 25 nM camptothecin, 1.5 µM etoposide, 650 µM temozolomide, 10 nM rapamycin, or 4 µM 5-fluorouracil for 48 hours (*concentrations according to* [210,211]). Samples receiving medium containing only the relevant solvent served as mock control. Afterwards, cells were fixed and stained with propidium iodide for flow cytometry. Single cells were discriminated from doublets, clumps, and debris by fluorescence pulse area FL2-A versus fluorescence pulse width FL2-W gating to avoid false positive signals. Histograms show the relative DNA content measured in FL2-A (*black lines*).

Table 8| chemotherapeutic drugs and their mechanism of action

name	cell cycle block	mechanism
5-fluorouracil	G1/S-phase	affects pyrimidine synthesis by inhibiting thymidylate synthetase; induces TP53 dependent apoptosis.
camptothecin	S-phase	inhibitor of DNA-topoisomerase I; induces apoptosis by cell cycle-dependent and cell cycle-independent processes.
etoposide	S-phase and G2/M-phase	inhibitor of DNA topoisomerase II; induces apoptosis by cell cycle-dependent and cell cycle-independent processes
rapamycin	G1-phase	inhibits the molecular target of rapamycin that enhances cellular proliferation via the phosphoinositol 3-kinase/AKT pathway.
temozolomide	G2/M-phase	DNA methylating agent; induces apoptosis through inactivation of the DNA repair base excision pathway.

Towards this goal, various established drugs for cancer treatment featuring different mechanisms of action and impact on the cell cycle were evaluated (*summarized in **Table 8***). First, I analyzed the cell cycle distribution of four melanoma cell lines in presence of particular chemotherapeutics (*shown in **Figure 21***). SK-MEL-28, Mel624, Mel888, and C8161 cells treated with a vehicle control showed a normal unsynchronized DNA content reflecting cells in the different phases of the cell cycle. Here, quiescent cells contain a diploid set of chromosomes (*2N*) represented by a characteristic high G1-phase peak, a low proportion of cells have entered the S-phase (*chromosome content > 2N but < 4N*), and a moderate number of cells reached the G2/M-phase (*end of DNA replication, chromosome amount doubled to 4N*). After incubation with camptothecin or etoposide the proportion of cells in S-phase and G2/M-phase drastically increased. This effect albeit comparably weaker could also be seen after temozolomide treatment for all tested melanoma cell lines. Here, Mel888 cells showed the highest impact on the cell cycle arrest by temozolomide as previously shown by our lab [212]. In contrast, rapamycin led to a potent G1-phase arrest evident through a strong signal increase of the G1-phase peak. Incubation with 5-fluorouracil had a similar outcome although in Mel624 and SK-MEL-28 an incomplete block was observed resembled by an increased proportion of cells in S-phase while the G2/M peak vanished compared to the vehicle control.

Second, I incubated freshly infected SK-MEL-28 melanoma cells with serial dilutions of each drug. The cells had been previously inoculated with 1 $TCID_{50}$/cell of the replication-competent HAdV-5/3 Δ24 T2A-luc expressing luciferase dependent on viral DNA replication. Following 48 hours incubation, I determined the luciferase activity in each sample. As depicted in **Figure 22**, the drugs mostly had no enhancing effect or even lowered luciferase levels in case of 5-fluorouracil and rapamycin.

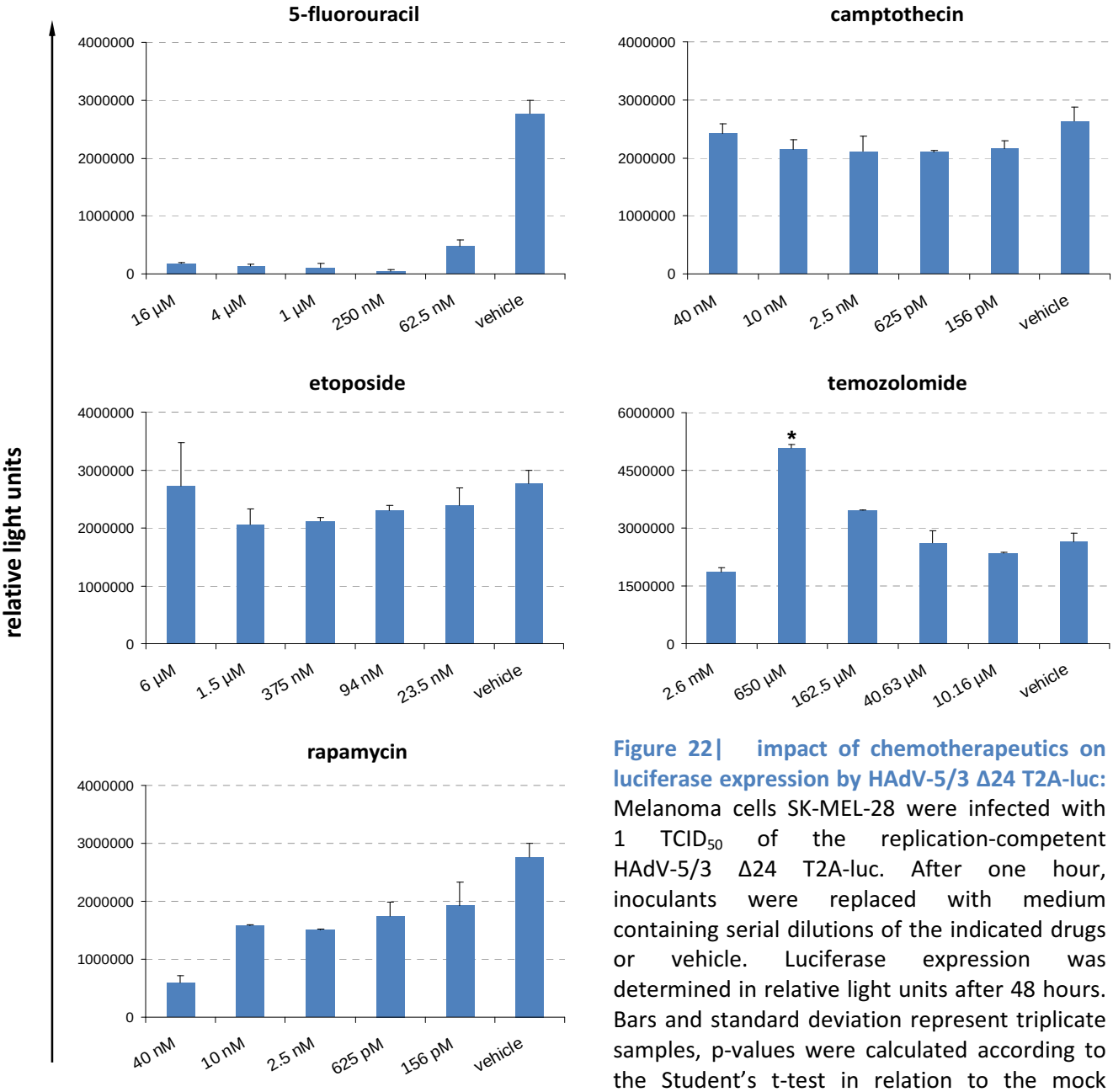

Figure 22| impact of chemotherapeutics on luciferase expression by HAdV-5/3 Δ24 T2A-luc: Melanoma cells SK-MEL-28 were infected with 1 $TCID_{50}$ of the replication-competent HAdV-5/3 Δ24 T2A-luc. After one hour, inoculants were replaced with medium containing serial dilutions of the indicated drugs or vehicle. Luciferase expression was determined in relative light units after 48 hours. Bars and standard deviation represent triplicate samples, p-values were calculated according to the Student's t-test in relation to the mock control (* $p \leq 0.05$).

However, this was not true for temozolomide which significantly increased luciferase activity of infected SK-MEL-28 cells in a dose-dependent way. Here, a temozolomide concentration of 650 µM yielded the strongest increase. A similar but less prominent tendency could be seen in identical experiments using 312 µM temozolomide for Mel624 cells (*data not shown*). Further, I pre-treated the cells for 24 hours with TMZ prior to infection which also resulted in significantly enhanced luciferase expression for SK-MEL-28 cells but not Mel624 (*data not shown*). These experiments were repeated using wild type HAdV-5 and determination of genome copies or late structural mRNA content by qPCR and yielded identical results, that is a strong increase of genome copy numbers and fiber mRNA after treatment with TMZ (*data not shown*).

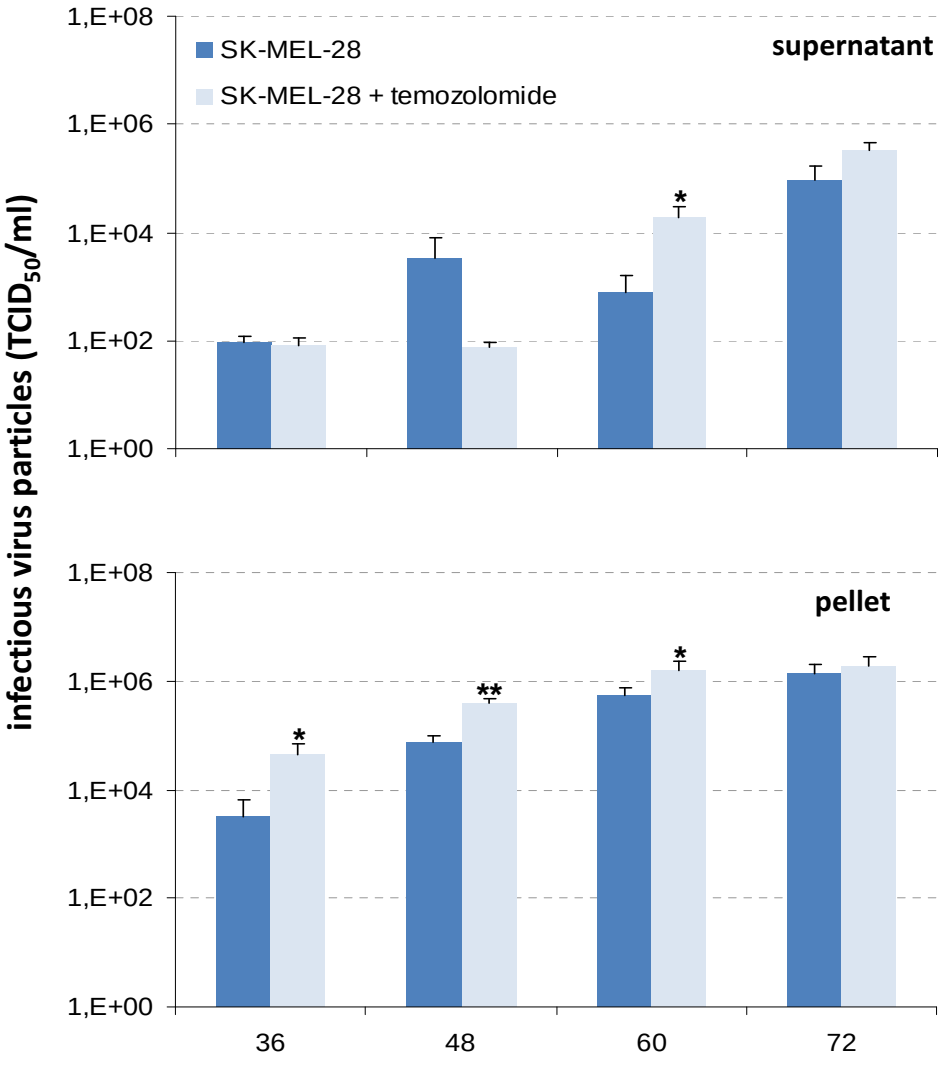

Figure 23| effect of temozolomide on virus particle production: SK-MEL-28 melanoma cells were infected with 1 $TCID_{50}$/cell of HAdV-5 (*dark blue bars*). After one hour incubation, virus inoculums were removed and cells washed three times. Additionally, samples were incubated in 650 µM temozolomide (*light blue bars*). Then, samples of supernatants (*upper panel*) and cell pellets (*lower panel*) were harvested at indicated time points and analyzed for infectious particle content stated in $TCID_{50}$/ml. Bars and standard deviation were calculated from mean values of triplicate infections, p-values were calculated using the Student's t-test (** $p \leq 0.05$, ** $p \leq 0.01$*).

Next, I evaluated the impact of temozolomide on virus progeny formation as a more direct means to determine the benefit for adenovirus replication. Therefore, SK-MEL-28 cells were infected with 1 $TCID_{50}$/cell HAdV-5 and incubated in 650 µM temozolomide over 72 hours. Separate samples of cell culture supernatants and cell pellets were harvested every twelve hours. Afterwards, I quantified infectious progeny virions by a $TCID_{50}$ assay. The results shown in **Figure 23**, demonstrate an up to fivefold enhancing effect on virus production as more particles can be found early on inside the cells between 36 to 60 hours post infection and also in the supernatant at 60 hours post infection compared to vehicle treated control cells. At 72 hours post infection, the titers of progeny viruses were similar in untreated and TMZ treated SK-MEL-28 cells.

Taken together, various established anticancer drugs resulted in different cell cycle blocks in four tested melanoma cell lines. At the same time, most chemotherapeutics had no stimulatory effect on virus replication. On the other hand, 5-fluorouracil and rapamycin seemed to inhibit adenovirus replication either due to direct effects of the drug on the adenovirus genome or indirectly as a result of the G1-phase block. However, cell cycle arrest later then G1-phase was not deleterious for adenovirus replication. This is in line with most publications demonstrating the feasibility of combined chemo- and virotherapy. Here, temozolomide increased adenovirus replication and production of progeny virions in SK-MEL-28 cells at early time points. The prodrug is converted at physiological pH to the toxic form 5-(3-methyltriazen-1-yl)imidazole-4-carboxamide which is an established front line therapeutic against gliomas and malignant melanomas. Interestingly, temozolomide enhanced adenovirus infection in some melanoma cell lines suggested by the replication-dependent increase in luciferase expression, viral DNA copy numbers, and virus progeny formation. Moreover, this drug had a considerably weaker impact on S-phase arrest than camptothecin or etoposide which were ineffective to achieve similar results even at lower concentrations. However, the enhancing effect on amplification of adenoviruses was temporary and could not be observed at 72 hours post infection in SK-MEL-28. A possible explanation is that at late time points the active temozolomide concentration diminished and therefore could not sustain the enhancing effect on generation of infectious adenoviruses. Hence, a combination therapy seems to be advantageous but needs further investigation in animal studies or in cancer patients with focus on the drug's direct and indirect mechanism of action. The last part of my work dealt with an alternative strategy to increase the cytotoxicity of single agents like an oncolytic virus, namely arming.

4 Arming of oncolytic adenoviruses with therapeutic antibodies

4.1 Virus design

A further facet of my work addressed the concept of arming oncolytic adenoviruses with therapeutic transgenes. This is a commonly used feature of virotherapy to increase the antitumoral efficacy by exerting a toxic effect on non-infected cancer cells, the so-called "bystander effect" (*also see I, 3.4*). Indeed, proof of principle studies with several different oncolytic viruses and diverse transgenes showed encouraging results. A prominent example is the first oncolytic human herpes virus expressing a rat cytochrome P450 enzyme responsible for bioactivation of cyclophosphamide or ifosfamide into toxic compounds [177]. The advent of the hybridoma technology together with identification of tumor-specific surface molecules resulted in use of monoclonal antibodies for clinical applications such as Trastuzumab against HER2/neu positive cancers or Rituximab for CD20 positive Non-Hodgkin lymphoma [6,190]. Consequently, I wanted to combine virotherapy with therapeutic antibody expression which has been successful for an oncolytic Newcastle disease virus, but so far has not been investigated for oncolytic adenoviruses [184]. In theory, this approach provides a flexible tool regarding different tumor antigens and effector domains that can be combined within recombinant antibodies. Moreover, the oncolytic virus delivered antibodies can be produced locally to high concentrations and thus synergize with the virus mediated tumor cell killing. This mode of delivery is potentially superior to systemic antibody injections.

To this end, the fiber-chimeric oncolytic HAdV-5/3 Δ24 served as platform since it generally results in greater transduction rates of tumor cells due to the chimeric 5/3 fiber bearing the HAdV-3 knob domain. The latter has recently been shown to bind desmoglein-2 which is expressed in epithelial cell types and therefrom derived tumors [59]. In addition, the 24 bp deletion in the E1A gene renders the virus conditionally replication-competent as it requires a deregulated pRB/E2F pathway, a hallmark of several malignancies. Regarding the therapeutic antibody, the carcinoembryonic antigen (*CEA*) was chosen as a model target because it is well characterized and frequently found in pancreatic, gastric, and lung cancers. In collaboration with Roland Kontermann from the University of Stuttgart, I received the coding sequence for a modified CEA single-chain antibody fused to the mouse heavy chain gamma 2 constant region (*scFv$_{CEA}$-Fc, **Figure 24A***). The Fc domain is recognized by serum

complement and various immune cells such as natural killer cells where it plays an important role in antibody-dependent cellular cytotoxicity [187]. Besides, the coding sequence is in frame with a secretion signal from mouse immunoglobulin κ that allows translation into and secretion from the endoplasmatic reticulum, the natural compartment of antibody production in B cells. Another key aspect is that the antibody can form dimers due to the constant regions. As a result, longer circulation times in blood and hence greater tumor uptake can be achieved [189].

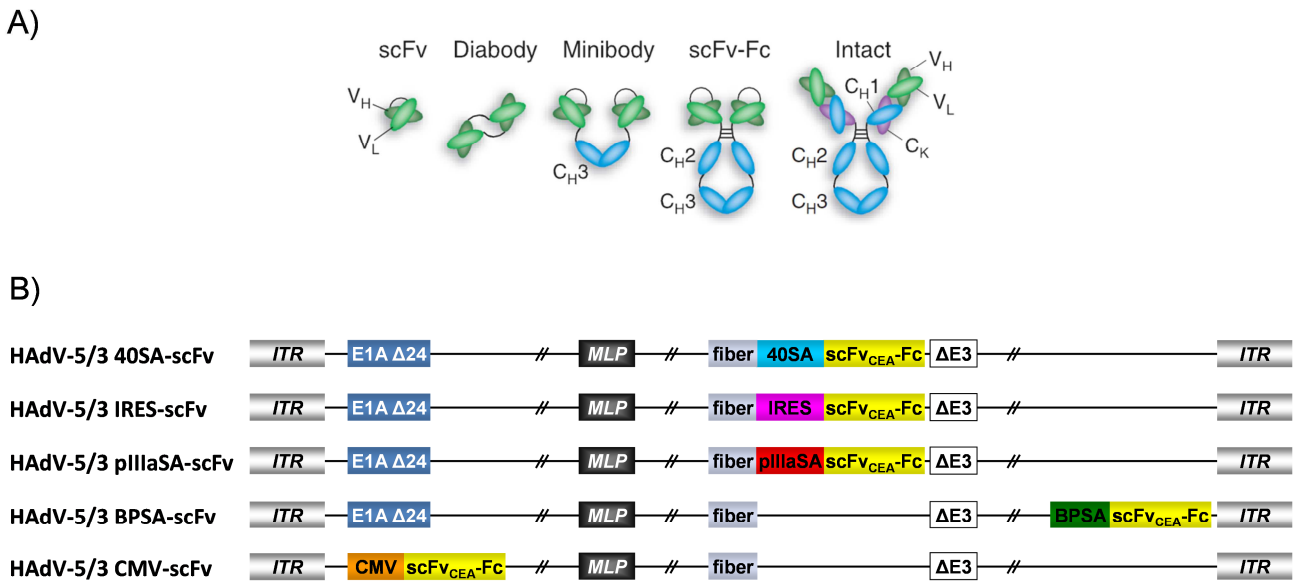

Figure 24| antibody and armed oncolytic virus design: A) schematic structures of different routinely used antibody formats including scFv (*~25 kDa*), diabody (*~55 kDa*), minibody (*~80 kDa*), scFv-Fc used herein (*~105 kDa*), and intact antibodies (*~150 kDa*). *Modified according to Wu & Senter, Nature Biotechnology, 2005* [189]. **B)** overview of genetically engineered HAdV-5/3 virus variants. Linear genomes carry inverted terminal repeats (*grey boxes*) at each end. For cancer selective replication, the E1A gene bears a 24 bp deletion (*dark blue box*). The major late promoter (*black box*) transcribes late gene expression in dependency of virus DNA replication. Among them is the chimeric 5/3 fiber for enhanced infectivity (light *blue box*) but also the $scFv_{CEA}$-Fc transgene (*yellow box*) under control of either the HAdV-40 long fiber gene splice acceptor (*bright blue box*), an IRES site (*pink box*), the HAdV-2 L1 pIIIa splice acceptor (*red box*), or the human beta globin splice acceptor (*green box*). A replication-deficient control virus carries a constitutively active CMV promoter/transgene cassette replacing the E1 genes (*orange/yellow box*).

Shown in **Figure 24B**, are five HAdV-5/3 variants which I generated and utilized in the following experiments, refer to the MATERIALS section IV, 5.4 for cloning. Among them a replication-deficient control virus where the E1 genes have been replaced with a

CMV promoter/scFv$_{CEA}$-Fc transgene cassette. Furthermore, four replication-competent viruses expressed the antibody under control of the major late promoter via different splice acceptor sites or the well characterized internal ribosomal entry site (*IRES*) from the encephalomyocarditis virus [213,214]. To this end, I included the HAdV-40 long fiber gene splice acceptor (*40SA*), the HAdV-2 L1 pIIIa splice acceptor (*pIIIaSA*), and the human beta globin splice acceptor (*BPSA*) to express the antibody via alternative splicing. Last but not least, the IRES can be used for expression of two genes from one common bi-cistronic mRNA. In this virus, the scFv$_{CEA}$-Fc was expressed together with the late fiber gene. Accordingly, all recombinant adenoviruses were propagated in cell culture and analyzed for their oncolytic potential and transgene expression.

4.2 Antibody expression and cytotoxicity

A critical issue of all arming approaches is interference of a heterologous transgene with virus amplification, and hence oncolytic activity in tumor cells. This might result in genomic instability, toxic effects of the transgene on the cell, or improper timely transgene expression which disturbs expression of viral genes. Further, the produced transgene amounts may be low due to inefficient virus replication which in turn limits the “bystander effect”. To investigate these issues, I first infected two highly permissive cell lines that either expressed CEA or were devoid for it.

Therefore, serially diluted oncolytic HAdV-5/3 variants were added to the A549 cells (*CEA positive*) or HeLa cells (*CEA negative*) and incubated for eight days. Controls included uninfected cells as well as a replication-deficient HAdV-5/3 CMV-scFv or HAdV-5/3 CMV-luc variant, where the luciferase transgene replaced the antibody. A similar but replication-competent HAdV-5/3 IRES-luc served as control for optimal lysis after transgene insertion and was previously established in our laboratory [215]. After eight days, cytotoxicity visualized by crystal violet staining allowed assessment of my genetically engineered adenoviruses in terms of their ability to efficiently kill tumor cells and spread. As shown in **Figure 25A**, infection with any replication-competent HAdV-5/3 variant led to fairly similar cell killing at titers between 1 and 0.1 TCID$_{50}$/cell for HeLa cells and at even lower amounts of 0.1 to 0.01 TCID$_{50}$/cell in A549. These effects correlated, or were slightly stronger, compared to the previously generated

replication-competent HAdV-5/3 IRES-luc. On the other hand, no cytotoxicity was visible after infection with any of the replication-deficient controls demonstrating that the observed cytotoxicity is replication-dependent.

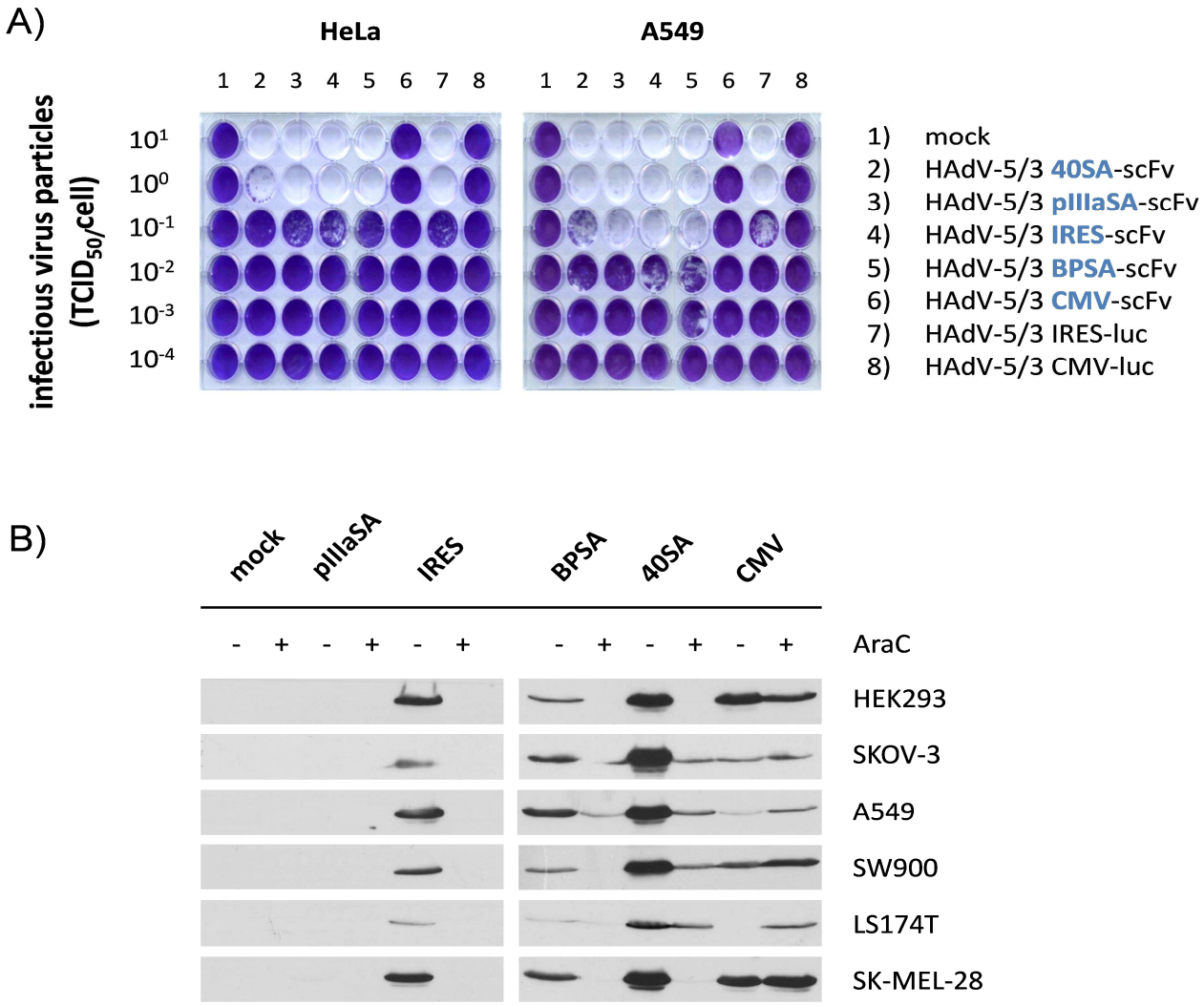

Figure 25| oncolysis and antibody expression of scFv$_{CEA}$-Fc carrying adenoviruses: A) CEA negative (*HeLa, left panel*) and positive (*A549, right panel*) cells were infected with different virus variants in serial dilutions containing 10^{1} to 10^{-4} TCID$_{50}$/cell as indicated in the legend. The cellular tool used for expression of single-chain antibodies is shown in dark blue. After eight days, surviving cells were stained with crystal violet. As negative controls for transgene toxicity, viruses encoding luciferase instead of scFv$_{CEA}$-Fc were included. Similar replication-deficient virus variants containing the CMV promoter instead of the E1 genes were used to check for replication-dependent cytotoxicity. **B)** adenovirus infection of several cell lines was carried out in presence or absence of 25 µg/ml AraC to block viral DNA replication. After 72 hours, equal volumes of cell culture supernatant were loaded on a denaturing gel for immunoblotting. Monomeric scFv$_{CEA}$-Fc was detected by anti-mouse-horseradish peroxidase antibodies and a chemoluminescent reaction. Abbreviations represent scFv$_{CEA}$-Fc expressing viruses using the stated cellular tool for transgene expression.

Next, I infected several cell lines, that again were either devoid for or expressing the CEA molecule, with my armed oncolytic HAdV-5/3 variants. A titer of 100 $TCID_{50}$ per cell was used and samples from supernatants as well as cell pellets were collected three days post infection. Additionally, I incubated one sample of each cell line with 25 µg/ml arabinosyl-cytosine (*AraC*), a nucleotide analog and known replication inhibitor of DNA viruses [216,217]. This allowed me to analyze whether antibody expression via the different insertion strategies is replication-dependent. Equal volumes of all samples were subsequently analyzed by Western blotting. Referring to **Figure 25B**, secreted antibody was readily detectable in supernatants from all tested cell lines infected with any of the recombinant HAdV-5/3 variants, except one where the $scFv_{CEA}$-Fc is under control of the L1 pIIIa splice acceptor. Supernatant from uninfected cells did not give a signal showing that the bands I observed were specific. Moreover, antibody production and secretion drastically diminished in the presence of AraC with exception of samples from HAdV-5/3 CMV-scFv infected cells. Here, even an opposing effect could be seed in some cell lines represented by stronger band intensities compared to mock treated samples. When I examined cell pellets for intracellular $scFv_{CEA}$-Fc antibodies, no or only a barely visible signal was obtained by immunoblotting regardless of AraC treatment (*data not shown*).

Taken together, I could show that insertion of a single-chain antibody gene into the adenoviral genome led to production and secretion of antibodies from tumor cells without significant loss of oncolytic potency. Also there was no obvious difference between CEA positive and negative cell lines suggesting that the $scFv_{CEA}$-Fc antibody per se was not toxic to the cells. In addition, the absence of detectable antibodies in the cell pellet indicated a highly efficient transgene secretion in adenovirus infected cells. Overall the highest transgene expression in all tested cell lines resulted from infection with HAdV-5/3 40SA-scFv and HAdV-5/3 IRES-scFv, respectively. The amount of secreted antibodies was strongly dependent on the transgene insertion strategy and on viral DNA replication, implied by the dramatic loss after incubation with AraC. This was also supported by the observation that AraC had no deleterious effect on cells harboring the constitutively active, but replication-deficient, HAdV-5/3 CMV-scFv variant. The fact that AraC treatment sometimes led to higher antibody amounts might be attributed to a cell cycle arrest in S-phase which presumably created optimal conditions for transgene expression via the CMV promoter. However, HEK293 cells stably express the adenoviral E1 genes which allow replication of the otherwise replication-deficient HAdV-5/3 CMV-scFv.

Hence, AraC treatment of infected HEK293 cells inhibited viral genome replication and antibody expression. Next, I wanted to determine the antibody amounts in supernatants from infected cells more precisely.

4.3 Kinetics of antibody expression

A routinely used method for quantification of soluble antibodies is the enzyme linked immunosorbent assay (*ELISA*) based on an antibody-antigen reaction which combines high sensitivity with high specificity. For generation of a standard curve known concentrations of antibodies, in this case purified $scFv_{CEA}$-Fc antibodies, are added to micro titer plates coated with their respective antigen, here commercially available CEA, and detected through a secondary species specific antibody/enzyme reaction. In parallel, the antibody concentration of unknown samples can be determined. This approach enabled me to rapidly and reliably measure the concentration of secreted $scFv_{CEA}$-Fc in cell culture supernatant of infected samples.

Since my previous immunoblots suggested that the highest amounts were generated through infection with HAdV-5/3 40SA-scFv and HAdV-5/3 IRES-scFv, I used these viruses for infection of CEA positive A549 lung carcinoma cells and SK-MEL-28 melanoma cells. In addition, the non-replicating HAdV-5/3 CMV-scFv virus was included as control for constitutive expression of antibodies. Here, a titer of 1 $TCID_{50}$/cell was used for each virus variant and samples were collected every day over five days until cell lysis was microscopically apparent throughout the cell monolayer (*data not shown*). In both A549 and SK-MEL-28 cells I detected an almost stable level of soluble $scFv_{CEA}$-Fc 24 hours after HAdV-5/3 CMV-scFv infection, which only gradually increased over time up to 40-fold in A549 and 10-fold in SK-MEL-28 cells (***Figure 26A***). In contrast, antibody titers after infection with the replication-competent variants HAdV-5/3 40SA-scFv or HAdV-5/3 IRES-scFv were already 30 to 60-fold higher at 24 hours post infection and peaked at day two in A549 cells with up to 750-fold higher antibody levels as compared to the replication-deficient virus. Although a marginal increase was detectable on day five, the biggest differences resulted early between day two and day three post infection. Infection of SK-MEL-28 cells reflected a similar but slightly delayed antibody expression profile for the HAdV-5/3 40SA-scFv or HAdV-5/3 IRES-scFv. Here, the 24 hour samples did not contain

any measurable antibody titer followed by a strong increase over day two and day three. However, the differences to the non-replicating CMV virus were only about 15-fold over the whole time period and therefore not as pronounced as in A549 cells. In parallel, I carried out an almost identical experiment using HAdV-5/3 variants carrying the luciferase transgene instead of the $scFv_{CEA}$-Fc antibody cassette (***Figure 26B***). Contrasting to the latter, luciferase could not be secreted from infected cells and accumulated in the cytosol. Nonetheless, I found a strikingly similar pattern for luciferase expression after infection with the non-replicating HAdV-5/3 CMV-luc variant and the replication-competent HAdV-5/3 40SA-luc or HAdV-5/3 IRES-luc. Here transgene expression via IRES was slightly better than via the 40SA tool. Moreover, the kinetics of expression was again cell type specific as noted in the antibody production profile for A549 and SK-MEL-28 cells.

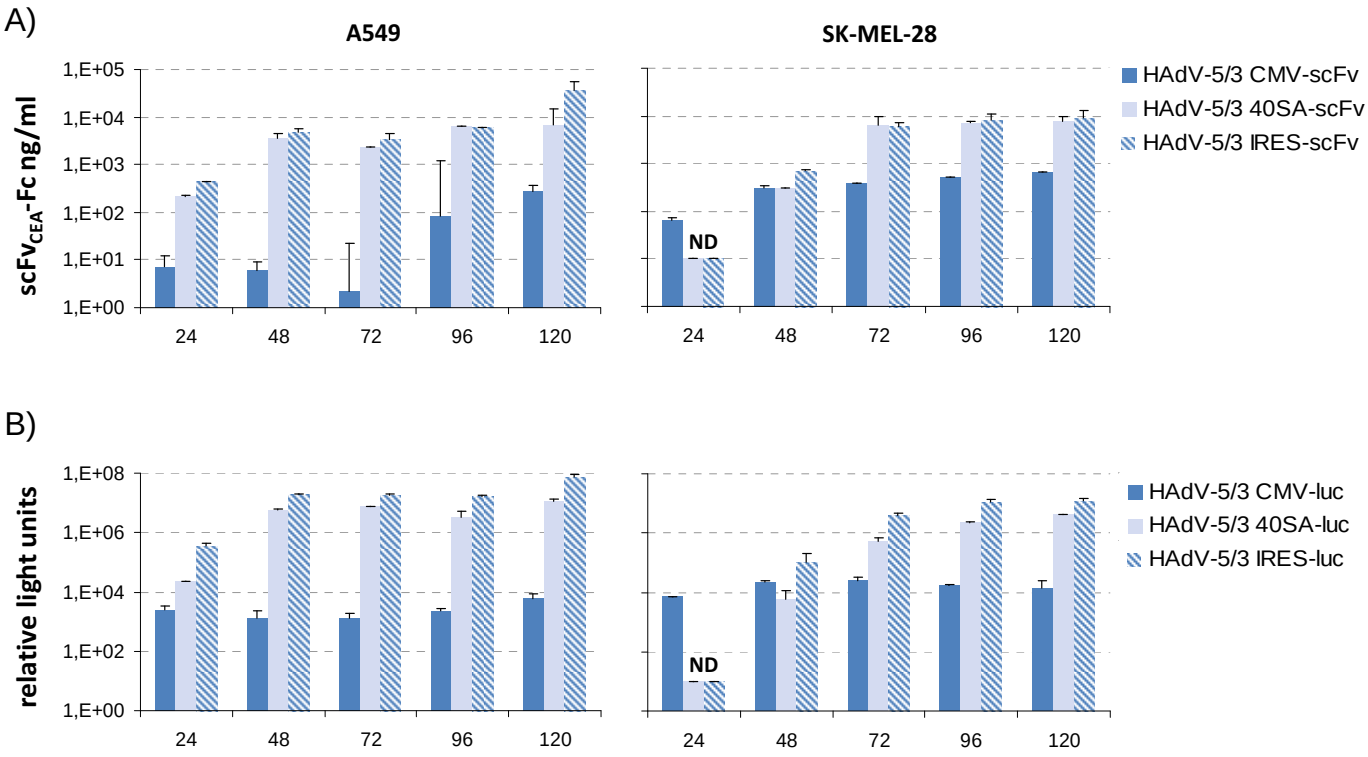

Figure 26| expression kinetics of $scFv_{CEA}$-Fc versus an intracellular transgene: A549 cells (*left panels*) and SK-MEL-28 cells (*right panels*) were infected with 1 $TCID_{50}$/cell of different $scFv_{CEA}$-Fc expressing viruses (*scFv, upper panels*) or matching luciferase controls (*luc, lower panels*). **A)** for antibody titers supernatants were collected every day and analyzed by ELISA. Bars represent means of double measurements from one sample, error bars were calculated according to the standard deviation. **B)** for luciferase expression cell pellets were harvested accordingly and assayed for luciferase activity indicated by relative light units. Bars represent means of triplicate samples, error bars were calculated according to the standard deviation, ND = not detectable.

In conclusion, as shown before, adenovirus DNA replication significantly enhanced antibody production and secretion for HAdV-5/3 40SA-scFv and HAdV-5/3 IRES-scFv. This coincided between 24-48 hours in A549 cells and 48-72 hours in SK-MEL-28 cells which most likely reflected cell type specific differences and permissivity for adenoviral replication also seen in my previous experiments of chapter II, 1.4. The cell type-dependent expression was also notable when comparing the antibody levels to the non-replicating HAdV-5/3 CMV-luc which seemed to be more active in melanoma cells than in A549 cells. These findings correlated with the immunoblot results from the previous paragraph II, 4.2. Further, the comparison to the luciferase expression profiles showed that the amounts and kinetics of a secreted transgene were comparable to an intracellularly produced one demonstrating that oncolysis does not interfere with secretion. Thus, arming of oncolytic adenoviruses with therapeutic antibodies combined with efficient transgene expression was feasible. Last but not least, the produced antibodies from infected tumor cells bound to purified antigen CEA *in-vitro*. To demonstrate their functionality in binding living cells expressing CEA, I subsequently tested the antibody-antigen reaction by flow cytometry.

4.4 Binding of secreted antibodies to CEA on the cell surface

With the advent of hybridoma technology, antibodies became popular tools in immunology to study cellular surface antigens. Similarly to ELISAs, living cells are usually exposed to a primary antibody solution which binds to the molecule of interest. Then, this antigen/antibody complex can be detected through a secondary antibody staining usually including the use of fluorescent molecules. High throughput analysis by flow cytometry allows rapid and reliable quantification of antigen expression on single cells. In contrast to ELISAs, the antigen is presented in its natural context here. Therefore, I analyzed if the antibodies produced during infection with oncolytic adenoviruses can access and bind to cellularly displayed CEA.

Accordingly, the previously generated supernatants from cells infected with the HAdV-5/3 40SA-scFv or HAdV-5/3 IRES-scFv (*experiment shown in **Figure 25***) were used as primary antibody solutions. Further, I also included the corresponding samples treated with AraC to determine its impact on transgene expression more precisely. As target cell line, I chose LS174T cells derived from a colorectal CEA positive tumor and incubated them in serially diluted

supernatants or with an irrelevant isotype matched antibody (*negative control*) as stated in **Figure 27**. Binding of primary antibodies was detected with a fluorescently labeled anti-mouse immunoglobulin G_{2a} (*IgG_{2a}*) antibody which recognizes the mouse heavy chain gamma 2 constant domain.

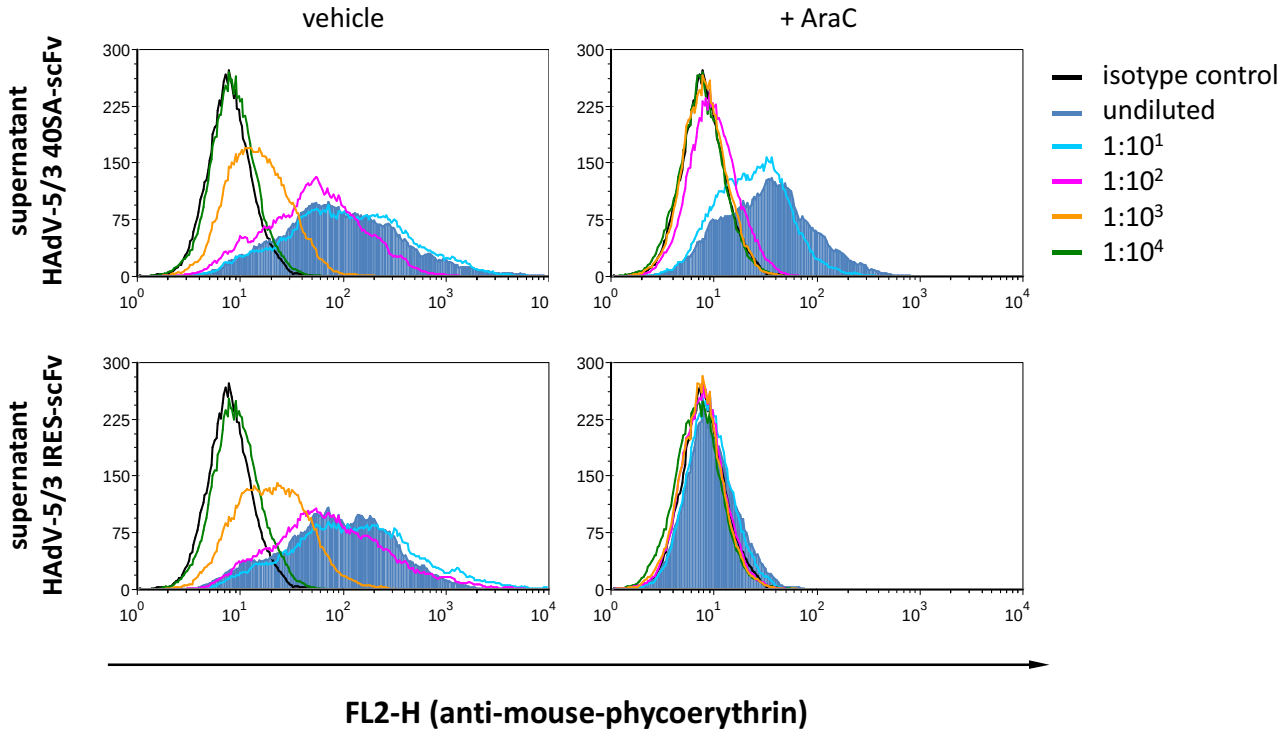

Figure 27| binding of $scFv_{CEA}$-Fc to living CEA positive cells: at day three, supernatants from the HAdV-5/3 40SA-scFv (*upper panels*) or HAdV-5/3 IRES-scFv (*lower panels*) infected HEK293 cells were harvested and used as primary antibody against CEA expressing LS174T cells in serial dilutions (le*ft panels, see figure legend*). In parallel to samples receiving only vehicle, infected cells were incubated in the presence of 25 µg/ml AraC (*right panels*). A non-specific isotype IgG_{2a} antibody served as negative control (*black lines*). Bound $scFv_{CEA}$-Fc or isotype control was performed by staining with a secondary anti-mouse-phycoerythrin antibody and detected in FL2-H.

In flow cytometry analysis, supernatants obtained from infected cells by either virus strongly bound to the surface of living LS174T cells. Whereas I did not detect any signal mediated through bound negative control antibodies. Overall, the signal intensity diminished with increasing dilutions revealing a threshold level for 1000-fold diluted supernatants from HAdV-5/3 40SA-scFV or HAdV-5/3 IRES-scFv infected cells. Further, AraC treatment of

virus infected cells drastically decreased signal intensities for both cell culture supernatants. However, the inhibitory effect of AraC was more pronounced in case of the HAdV-5/3 IRES-scFv infection than for the HAdV-5/3 40SA-scFv variant which still produced a detectable signal at a tenfold dilution. A similar staining pattern and threshold was observed for recombinant $scFv_{CEA}$-Fc purified from a stably transfected cell line and diluted accordingly for flow cytometry (*data not shown*).

In summary, $scFv_{CEA}$-Fc antibodies secreted in course of oncolytic adenovirus infection specifically interacted with surface CEA on living cells, adding another piece of evidence for the functional antigen binding domain. Binding properties of HAdV-5/3 40SA-scFv produced antibodies were similar to those diluted from supernatants of HAdV-5/3 IRES-scFv infected cells. Treatment with AraC decreased production of antibodies as previously seen by immunoblot analysis indicating the relevance of genome replication for efficient transgene production. Moreover, the inhibitory effect differed depending on the transgene insertion strategy as it was more potent against the HAdV-5/3 IRES-scFv than the HAdV-5/3 40SA-scFv variant. This difference could be due to leaky expression caused by alternative splicing of the 40SA site. The latter was most certainly circumvented through bi-cistronic expression of fiber and $scFv_{CEA}$-Fc from a common mRNA. Consequently, I checked if the effector domain, represented by the recombinant mouse heavy chain gamma 2 constant region, was able to mediate Fc receptor engagement on immune cells.

4.5 Influence of $scFv_{CEA}$-Fc on phagocytosis of CEA positive tumor cells by macrophages

Several immune cells, including natural killer cells, neutrophils, macrophages, and mast cells, display Fc receptors on their cell surface that are able to bind various constant domains of immunoglobulins. Normally antibodies react with pathogen associated antigens, a process called opsonization, and if engaged by Fc receptors trigger antibody-dependent cellular cytotoxicity or antibody-dependent cellular phagocytosis [187]. As shown in the previous two paragraphs the antigen binding domain in the single-chain antibody was fully functional. Here, I assessed the effector domain in context of macrophage-dependent phagocytosis of CEA positive tumor cells in an *in-vitro* model system using my recombinant $scFv_{CEA}$-Fc.

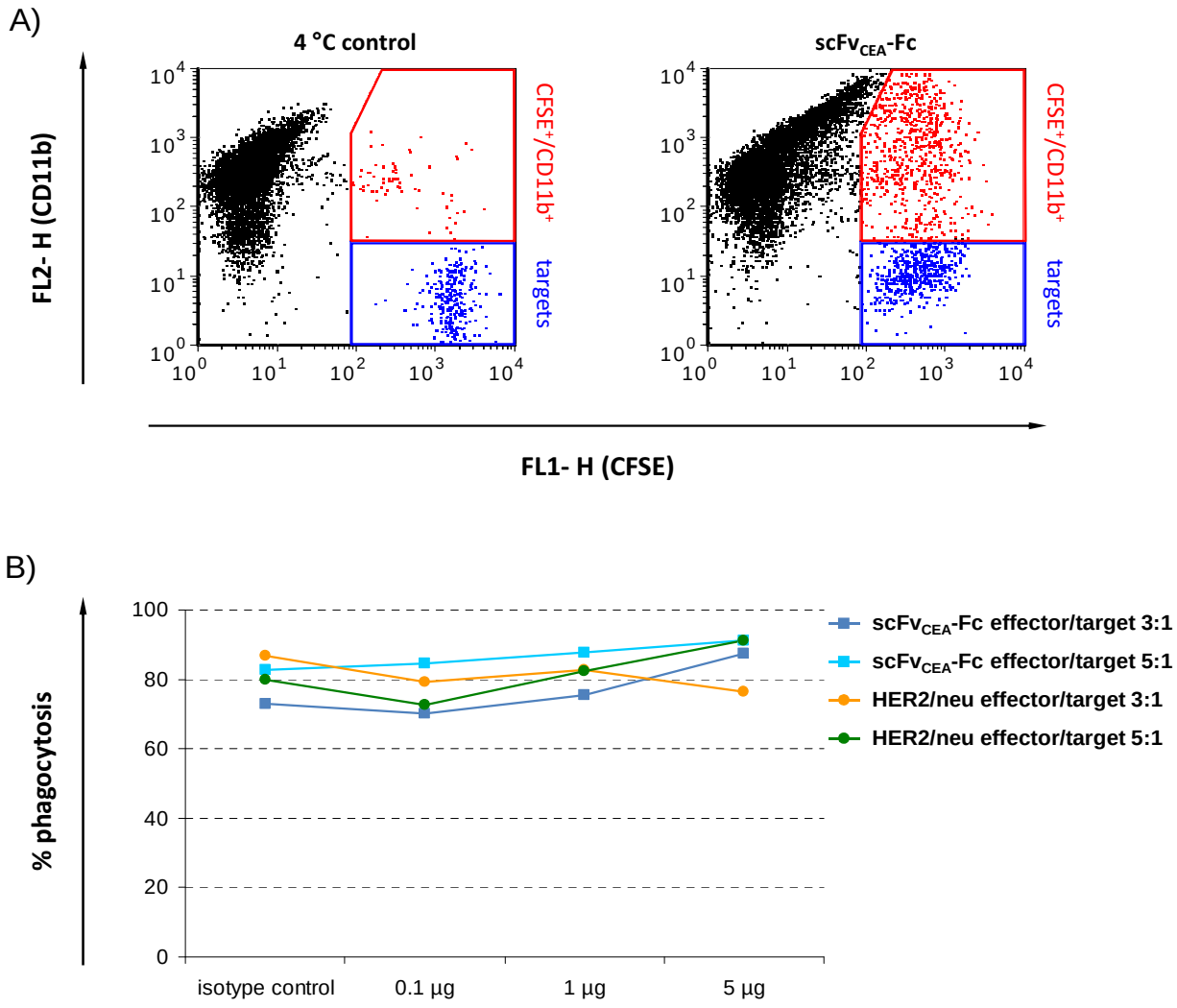

Figure 28| evaluation of scFv$_{CEA}$-Fc antibody-dependent phagocytosis: CFSE labeled tumor targets were boiled at 56 °C to induce necrosis. Afterwards, macrophages were added to the targets in a 3:1 or 5:1 ratio. Further, medium was supplemented with different antibodies. **A)** gating strategy showing macrophages labeled with anti-CD11b-phycoerytrhin antibodies (*FL2-H, black dots*) and tumor targets (*FL1-H, blue gate*). Population of CFSE$^+$/CD11b$^+$ (*red gate*) represents phagocytosis of targets by macrophages. Controls incubated at 4 °C show significantly lower uptake of tumor targets (*left panel*) than samples incubated at 37 °C (*right panels*). **B)** percentages of phagocytosis were calculated according to the formula stated in V, 3.7.4 for each effector/target ratio. Medium contained either recombinant scFv$_{CEA}$-Fc (*dark blue and light blue boxes*) or anti-HER2/neu antibodies (*orange and green circles*) at increasing concentrations. In addition, samples were incubated with relevant isotype controls at the highest concentration.

To this end, the immortalized mouse macrophage cell line RAW264.7 was incubated with different target cells and antibody concentrations. As target cells, I chose the CEA positive colorectal cancer cell line LS174T as well as the lung adenocarcinoma cell line A549. The latter

expressed also the HER2/neu antigen. Both were labeled with the green fluorescent dye carboxyfluorescein diacetate succinimidyl ester (*CFSE*) which is passively taken up by living cells and trapped in the cytosol [218]. After labeling, I boiled the targets at 56 °C to induce necrosis and degradation of cells into small green vesicles that can be easily internalized. Then, target cells were added in different effector/target ratios to macrophages with increasing amounts of recombinantly expressed and purified $scFv_{CEA}$-Fc or a relevant positive control antibody targeting the HER2/neu antigen. Additionally, I incubated some samples at 4 °C in order to allow distinction between mere binding of macrophages to targets and real phagocytosis. Following incubation for four hours, phagocytosis was analyzed by flow cytometry (***Figure 28A***). Therefore, I stained macrophages with a specific marker (*CD11b, red fluorescence FL2-H*) whereas tumor cells or particles were green (C*FSE, green fluorescence FL1-H*). Macrophages readily internalized around 80 % of CFSE labeled necrotic cells or particles marked by the increased proportion of CFSE/CD11b positive cells as compared to the 4 °C control. Disappointingly, the efficiency of phagocytosis for either target moiety could not be further augmented by my recombinant single-chain antibody or by a HER2/neu control antibody (*refer to* ***Figure 28B***). Assays were repeated using living target cells but yielded identical results independent of the used antibody (*average phagocytosis values around 30 %, data not shown*). Also, increasing the effector/target ratio or incubation with the corresponding isotype controls had no further inhibitory or stimulatory properties on phagocytosis.

Thus, although the recombinant $scFv_{CEA}$-Fc was able to bind to CEA positive cells it did not notably enhance antibody-dependent cellular phagocytosis of different tumor cells in an *in-vitro* setting. This held even true for the established anticancer antibody HER2/neu implying that my results were unlikely to be caused by a nonfunctional Fc domain in my recombinant single-chain antibody. Alternatively, my system was either not sensitive enough or other factors were required to mediate antibody-dependent phagocytosis of opsonized tumor cells. However, the average ratios of macrophages containing green tumor cells or particles were already high. This observation could indicate that the mechanism of antibody-mediated phagocytosis might be of higher relevance in an *in-vivo* system where physiological effector/target ratios and antibody concentrations exist. As an outlook, future studies comprising alternative *in-vitro* assays involving natural killer cells and *in-vivo* mouse studies will be carried out to evaluate the clinical benefit of antibody-producing oncolytic adenoviruses.

III DISCUSSION

To date most conducted clinical trials with oncolytic viruses have investigated the clinical use of HAdV-5 based oncolytic viruses. They have shown a favorable safety profile but also an insufficient overall antitumoral efficacy [103,104]. The aims of my study were to investigate wild type HAdV-5 infections and compare different aspects of the virus life cycle in the natural host cells to cancer cells, especially in malignant melanoma. This was followed by a thorough microarray analysis of infected cells to find cellular genes with critical functions for adenovirus genome amplification in order to provide a rationale for enhancing oncolytic adenovirus DNA replication in melanoma cells. Finally, an arming strategy should be developed for the expression of therapeutic antibodies via replication-competent human adenoviruses.

Although not all aspects contributing to efficient viral oncolysis are known, it is widely accepted that virus genome replication is a major aspect for virus mediated tumor cell killing [21-23]. Since adenoviruses are obligate intracellular parasites they depend on the cellular DNA synthesis machinery. Hence to exploit this, the virus has to drive infected cells into the S-phase where several factors are provided by the host. This aspect is realized through expression of the adenovirus master regulator protein E1A which disrupts the pRB/E2F regulatory network and leads to transcriptional activation of cellular and viral promoters [42,43,69,76,77]. As a model system for HAdV-5 infection, I chose primary human bronchial epithelial cells which so far have only been used as controls in cytotoxicity assays for transcriptionally targeted or mutant oncolytic adenoviruses [176,219-221]. Characterization by immunofluorescence demonstrated expression of typical epithelial markers and initial experiments including cytotoxicity assays, viral gene expression, and DNA replication showed that HBEC resemble an optimal primary lung cell model for *in-vitro* analyses of HAdV-5 infections in native host cells. In infected HBEC and closely related lung squamous carcinoma cell line, which originate from epithelial lesions in the respiratory tract, the adenovirus E1A gene was transcribed immediately after infection to very high extends. This was followed by early onset of virus DNA replication and expression of late structural genes. In striking contrast, two melanoma cell lines SK-MEL-28 and Mel624 showed a markedly reduced E1A mRNA transcription resulting in delayed virus genome amplification. A similar phenotype was described by Zhao *et al.* for human fibroblasts that normally do not serve HAdV-5 as host [195].

My investigations of the E1A promoter fragment in transient transfection assays revealed an equally strong activity profile in HBEC and melanoma cells implying that a posttranscriptional regulatory mechanism or additional regulatory elements outside the promoter region account for differences in E1A mRNA expression in both cell types. Although increased E1A expression through heterologous promoter elements in melanoma cells is possible, it did not result in enhanced oncolysis as demonstrated for a replication-competent HAdV-5 CMV-E1A [222]. However, my analysis of HAdV-5 cytotoxicity in different cell types could be closely correlated with their respective E1A expression/DNA replication phenotypes. In other words, slower expression and viral DNA replication kinetics resulted in lower cytotoxicity most probably because of delayed virus spread. A similar albeit less pronounced correlation was found in the generation of infectious virus progeny, which was delayed in SK-MEL-28 cells compared to HEBC. The overall virus yield was comparable to previous results for viral replication assays using primary bronchial epithelial cells [176,219]. Further, HAdV-5 infection of primary HBEC resulted in similar toxicity to infected A549 cells which are a major reference cell line in the oncolytic adenovirus field. Although more facets of the virus life cycle are essential for these effects, slower DNA replication and formation of infectious progeny virions ultimately impede efficient viral oncolysis. As shown here, certain cell type specific differences allowed the virus to amplify faster in HBEC than in melanoma. Therefore, I investigated genome-wide differences in the host cell gene expression of primary and several cancer cells after infection with HAdV-5 and related uninfected equivalents. Several studies have been published aiming to unravel virus host interactions during infection with HAdV-2 and HAdV-5 [194,195,197,223-225]. The gene expression data comprises different stages of adenovirus infection such as early responses to the incoming virus, modulation of inflammatory processes, events during viral DNA replication, and targeting of cellular structures at late stages of infection. Yet, the investigators used exclusively either fibroblast or cervical carcinoma cells for their experiments; both are not natural host cells for HAdV-2 or HAdV-5 unlike HBEC. Also, there is no available study that simultaneously compares gene expression in infected native host cells versus tumor cells.

For the present microarray study, cells and infection conditions were first adapted to optimal *in-vitro* conditions for all cell types including similar medium formulations (*especially low serum content*), cell number passage, normalized titers for a high level infection, as well as

determining appropriate time points for RNA extraction. As viral DNA replication was my main focus I chose cell type specific time points where adenovirus genome replication became apparent. Subsequently, the microarrays could be successfully hybridized and measured with great reproducibility as well as sensitivity but they nevertheless revealed only minor changes in gene expression after adenovirus infection. In addition, the overall differences between individual cell types and their transcriptomes prevailed. To solve this problem, my data was analyzed together with Frank Holtrup, Kurt Fellenberg, and Jörg Hoheisel (*division of Functional Genome Analysis, DKFZ*) which led to the development of a procedure to filter the data according to infection dependent changes in cellular gene expression regardless of the analyzed cell type or genetic background. Astonishingly, I found that HAdV-5 had the most pronounced impact on host cell gene regulation in HBEC (*950 regulated genes*) and the lung squamous carcinoma cell lines SW900 (*772 regulated genes*) and SK-MES-1 (709 *regulated genes*). Both melanoma cell lines SK-MEL-28 (*314 regulated genes*) or Mel624 (*212 regulated genes*) were mostly refractory to adenovirus induced changes in gene regulation. Besides, I found the number of downregulated genes was generally equal or higher to the number of upregulated genes. Although the overall number of regulated genes appears to be small compared to the size of a cell's transcriptome, my findings are supported by other microarray studies showing that usually only a small set of genes is altered during adenovirus infection [194,195,197,223,224]. However, Miller and colleagues found that adenovirus infection of quiescent fibroblasts had a dramatic impact on the cellular gene expression leading to the regulation of at least 2000 genes with a two-fold change in mRNA amount or more [225]. These observed discrepancies most likely reflect different experimental setups, including the cell type and proliferation state, and the methods used to collect and analyze the hybridization data. An alternative explanation could be that in primary cells, especially if they are quiescent, the virus has to reprogram the cell in a more dramatic way as compared to infection of a cycling transformed tumor cell. Nonetheless, the differential gene expression patterns observed between HBEC and the melanoma cells could provide a possible explanation for the delayed expression of viral genes, DNA replication, and reduced cytotoxicity.

For further in-depth analysis, sophisticated computational tools including hierarchical clustering, gene ontology search, and Ingenuity Pathway Software were used. This allowed me to identify striking differences in gene activation patters linked to the G1/S-phase transition

pathway. Whereas, HAdV-5 stimulated expression of several key player genes comprising E2F2, CCNE, or CDC25A in infected HBEC and also in some closely related lung squamous cell carcinomas, the two melanoma cell lines again responded by indolence or even suppression of these genes. Besides cell cycle regulation, several downstream targets of the pRB/E2F pathway including genes known to be important for DNA nucleotide metabolism, DNA replication factors, or DNA repair were similarly inert in melanoma cells but not in cells of lung origin. Regarding the primary bronchial epithelial cells, my findings exactly mirror the results from Miller *et al.* who analyzed HAdV-5 infection of quiescent fibroblasts [225]. In addition several genes, like the E2F family members, CCNE, and the cellular phosphatase CDC25A, have also been identified by others as primary targets in context of S-phase induction by adenoviruses during infection of fibroblasts, lung adenocarcinoma cells A549, and cervical carcinoma cells HeLa [74,75,194,197,225]. Especially, CDC25A is a major target of E1A which leads to a rapid increase in expression and phosphatase activity in quiescent cells. Alternatively, the E1B-55k protein might have redundant functions in increasing CDC25A levels in infected cells as shown by microarray experiments from Rao *et al.* [226]. Together with CCNE, a potential co-stimulatory molecule for CDC25A, these two proteins are sufficient to induce S-phase through activation of CDK2/CCNE complexes [74,75]. This important point for adenovirus infection was further addressed as I developed a modified reporter gene assay to measure S-phase entry in various cells. HBEC as well as all lung carcinoma cell lines analyzed showed an E1A dependent, specific, and strong increase in E2F promoter activity upon HAdV-5 infection. This was most likely a result of the auto-feedback loop activation by released E2F transcription factors from E1A inactivated pRB/E2F complexes [227,228]. Even though likewise events are supposed to occur in infected melanoma cells, this effect was drastically diminished or absent in SK-MEL-28 or Mel624. Therefore, my data might elucidate why S-phase related genes became less activated in these cells but certainly not why most of these genes were strongly downregulated.

Unfortunately, all my attempts to link expression of single candidate genes, identified in the previous comparison of infected HBEC versus SK-MEL-28 and Mel624, to the susceptibility for HAdV-5 infections in a wider melanoma cell panel failed. Indeed, wild type adenovirus infection sometimes resulted in quite opposing gene regulation patters for this set of analyzed genes. For example, whereas most genes were likewise downregulated in the highly permissive A549 cell line, they were often upregulated in less permissive pigmented and amelanotic

melanoma cells other than SK-MEL-28 and Mel624. This finding emphasized that it is vital in the future to investigate cell type specific changes in genome wide expression patterns, *de-novo* protein synthesis, and protein-protein interactions besides single gene expression in order to correlate susceptibility for oncolytic adenoviruses in various melanomas. Nonetheless, this was the first study which investigated adenovirus related alterations in host cell gene expression of various cancer cells and primary human bronchial epithelial cells that resemble a natural environment for HAdV-5. The presented data confirms previous publications investigating changes in cellular gene expression after infection with HAdV-2 and the closely related HAdV-5 [194,195,197,223,225]. Since gene expression was analyzed shortly before the onset of viral DNA replication, I could not see a pronounced regulation of genes or pathways involved in immune responses, growth arrest, or cell architecture as previously described. This, however, was expected as suppression of the immune system is an immediate action of the incoming virus while growth arrest and destruction of the cell cytoskeleton are features of later infection stages prior to cell lysis. Therefore, my work adds to the current understanding of adenovirus mediated cell cycle regulation to induce an optimal S-phase environment for DNA synthesis and further outlines major differences in gene regulation between native host cells versus cancer cells which ultimately determine the efficacy of viral replication and oncolysis.

To date, mainly two strategies are applied to create novel oncolytic adenoviruses with improved replication and/or spread in tumor cells. In so-called bioselection approaches, a virus stock is randomly mutagenized through chemical compounds, such as nitrous acid, and passaged in cancer cells several times [229-231]. Afterwards, mutants with enhanced oncolytic activity are isolated and characterized for the underlying mutation. Examples for successful bioselection are the tumor-selective ONYX-201 and -203 viruses expressing a truncated i-leader protein, which presumably is involved in initiation of viral DNA replication or switch to the late phase of the viral life cycle [229]. As a consequence, viral oncolysis is increased in various tumor cells as compared to the parental viruses. Alternatively, oncolytic activity can be increased by targeted mutations, such as deletion of the anti-apoptotic E1B-19k gene, resulting in more efficient viral release and enhanced cell-to-cell viral in some cancer entities while in others oncolysis was not enhanced [172-174]. In contrast to bioselection and targeted mutation, the here presented microarray approach is a more systematic way to identify certain virus host

interactions directly influencing efficient viral DNA replication. My data comprising the striking abundance of genes associated with regulation of the G1/S-phase transition raises the question why S-phase induction seems to be so essential for infection of rapidly dividing tumor cells. In contrast to HBEC, most tumor cells bear several mutations that lead to continuous initiation and progression of the cell cycle which is thought to provide an optimal environment for the replication of oncolytic viruses per se. However, there seems to be a major difference in the quality of cell cycle regulation in tumor cells versus S-phase induction in normally growing primary cells regarding adenovirus infection. The underlying mechanisms to this might hold the answer to the paradigm of cell type specific differences in adenovirus genome replication and lysis. In successive transient transfection assays, I tried to enhance viral DNA synthesis or generation of progeny virions. First, several cellular regulators of the G1/S transition pathway including the activating transcription factors E2F1, E2F2, E2F5 as well as CCNE or CDC25A were evaluated for their ability to stimulate adenovirus DNA replication but showed no promise. Simultaneously, multiple viral oncogenes from human papilloma viruses, herpes viruses, and the simian virus 40 known to trigger cell cycle progression of infected host cells in a similar fashion to adenoviruses were assessed but again found to be ineffective for this approach [37,232,233]. Thus, the regulation of G1/S-phase transition or modulation of the S-phase environment in infected melanoma cells appeared to be far more complex or robust towards overexpression of single activator genes. Alternatively, the applied transient transfection system might be inappropriate to achieve stimulating effects on adenovirus replication using the assessed transgenes and/or these transgenes failed to induce S-phase in SK-MEL-28 melanoma cells.

The results from the transient transfection assays were also supported by small interfering RNA knockdown assays that aimed to deprive melanoma cells of the cell cycle inhibitory $p16^{INK4a}$ and $p21^{WAF/CIP}$ proteins. The latter competes with CDC25A for CDK2/CCNE complexes and thus inhibits cell cycle progression [234]. Similar experiments using $p21^{WAF/CIP}$ knockdowns for HAdV-5 infected colorectal cancer cells have been successful and yielded increased numbers of infectious virus particles [209]. However, in my hands knockdown of $p16^{INK4a}$ or $p21^{WAF/CIP}$ in infected melanoma cells did not increase adenovirus replication or virus particle formation. A possible explanation for this discrepancy might be found in the different cell types meaning that knockdown of $p21^{WAF/CIP}$ affects colorectal cancer cells in another way than melanoma cells and thus viral replication. Last but not least, the necessity to

combine different treatments for effective cancer therapy inspired me to analyze how chemotherapeutic drugs affect adenovirus replication and hence virotherapy. A common mechanism of most drugs is induction of DNA damage and consequently initiation of a cell cycle arrest and eventually apoptosis [235,236]. At first glance a cell cycle arrest seemed counterintuitive to forcing S-phase entry in melanoma cells. However, there is evidence that prolonging an S-phase environment comprising high nucleotide levels and other DNA replication factors can synergize with oncolytic virus amplification and spread [210,211,237,238]. For that reason, I tested the impact of different chemotherapeutic drugs on the cell cycle of melanoma, preferably those which block in or after S-phase. Whereas etoposide or camptothecin caused a prominent cell cycle block in the G2/M-phase, they had no enhancing effect on adenovirus DNA amplification. Treatment with two other drugs, rapamycin and 5-fluorouracil, resulted in G1-phase arrest and inhibited viral replication. Nonetheless, a similar study from André Lieber's lab showed an enormous increase in virus DNA replication after treatment with any of these drugs at the herein applied concentrations [210]. As in my experiments, DNA replication was deduced from expression of a replication-dependent transgene but I was not able to reproduce these results with exception for the drug temozolomide. Intriguingly, temozolomide is a frontline therapeutic prodrug against malignant melanoma which is converted at physiological pH to the toxic form 5-(3-methyltriazen-1-yl)imidazole-4-carboxamide [239]. The latter is an alkylating agent leading to DNA damage induction and subsequent S-phase arrest. In the present study, temozolomide treatment of infected melanoma cells enhanced adenovirus genome replication in some but not all cell lines, which is in line with previous observations from our lab [212,240]. In addition, I could show for infected SK-MEL-28 cells that temozolomide altered the host cell environment in a way that adenovirus genome replication was not only more efficient but also led to the generation of up to fivefold more infectious virus progeny. Although this increase seems to be minor, one has to keep in mind that in an optimal patient's setting the virus will amplify over several days thereby multiplying this increase which potentially favors a better therapeutic outcome.

Finally, I developed various transgene insertion strategies to produce antibodies from oncolytic adenoviruses in order to combine viro- and antibody therapy for the treatment of cancer. The latter is a widely accepted approach to fight cancer and other diseases [185]. So far, almost all concepts of arming oncolytic adenoviruses with therapeutic transgenes encompass

either prodrug-activating enzymes, apoptosis inducing factors, immunomodulatory molecules, or molecules that affect the tumor microenvironment [241]. Examples are numerous and include recombinant viruses expressing yeast cytosine deaminase which is able to convert a systemically applied non-hazardous drug precursor into its toxic form [242,243], tumor necrosis factor related apoptosis-inducing ligand [182], granulocyte macrophage stimulating factor or interleukin-12/B-Lymphocyte Activation Antigen B7-1 [180,181], or extracellular matrix degrading proteins such as relaxin [183]. The bottom line of all these arming approaches is to achieve better tumor cell killing and/or enhanced virus spread either directly through the bystander effect on uninfected surrounding tumor cells or indirectly by redirecting the immune system to the tumor site. Similarly, arming with therapeutic antibodies aims at more efficient tumor destruction in order to increase the clinical benefit of virotherapy. This approach, in contrast to well-established arming concepts, features mainly two vital advantages beyond the local production of high antibody titers in the tumor. First, the format and function of therapeutic antibodies is extremely flexible allowing for several modifications of single domains. In other words, the antigen binding domain can be exchanged to target different available cancer surface markers and thus different tumor entities. Additionally, the effector domain can be altered to either induce direct tumor cell killing by fusing the antibody to toxic molecules such as the subunit A of the bacterial diphtheria toxin or indirectly by recruiting immune cells, such as natural killer cells, via the Fc domain to the tumor site [187,244]. Alternatively, the antibody format can be changed to incorporate bi-specific antibodies that bind to the tumor cell on the one hand and to cytotoxic T cells on the other [245,246]. Second, locally produced therapeutic antibodies have the potential to spread systemically and are therefore capable to target distant metastases, which were not and/or cannot be efficiently destroyed by the oncolytic virus or by untargeted therapeutic genes such as prodrug-activating enzymes. At the same time, toxicity for the patient is expected to remain low since systemic application of therapeutic antibodies has been well tolerated in clinical setting [185].

Towards the goal of combined oncolytic adenovirus and antibody therapy, I created four different replication-competent viruses in order to express antibodies at late stages of adenovirus infection. Therefore, different tools comprising the internal ribosomal entry site, the HAdV-40 long fiber gene splice acceptor, the HAdV-2 L1 pIIIa splice acceptor, and the human beta globin splice acceptor were evaluated for their ability to control expression of recombinant

antibodies via the adenovirus major late promoter. This strategy is commonly used for arming of replication-competent adenoviruses in order to minimize detrimental effects of the transgene on the infected host cell potentially resulting in reduced viral replication and virus progeny formation [129,241]. As a control, a replication-deficient virus bearing the constitutively active CMV promoter for transgene expression was also created. For proof of principle, I successfully introduced a CEA specific single-chain antibody in each virus format. The antibody binding domain is fused to the mouse heavy chain IgG_{2a} constant region which, similar to other G type immunoglobulins has the intrinsic ability to activate the classical complement cascade resulting in formation of a membrane attack complex and cell killing as well as activation of antibody-dependent cellular cytotoxicity by natural killer cells after Fc receptor engagement [187]. Alternatively, antibody/Fc receptor interactions trigger phagocytosis of opsonized pathogens and tumor cells by macrophages.

All recombinant virus variants showed unaltered oncolytic capacity in CEA positive and negative cells as well as highly efficient secretion of soluble antibodies into the supernatant. Nonetheless, the produced antibody amounts were clearly distinguishable on the basis of the genetic insertion strategy/tool ranging between undetectable amounts when expressed from the pIIIa splice acceptor up to several micrograms per milliliter when expressed via IRES or the HAdV-40 long fiber gene splice acceptor. The antibody concentrations were similar to a replication-competent oncolytic Newcastle disease virus expressing a complete immunoglobulin antibody targeted against a vascular tumor marker [184]. In different experimental settings including an ad hoc established ELISA system, the highest titers resulted from infection of various CEA positive or negative cancer cell lines with the HAdV-5/3 40SA-scFv or HAdV-5/3 IRES-scFv. The titers were several orders of magnitude higher compared to my replication-deficient control HAdV-5/3 CMV-scFv and could be drastically diminished by inhibition of adenovirus replication using the nucleotide analog arabinosyl-cytosine. Furthermore, the time points of peaking antibody amounts, produced from viruses with replication-dependent transgene expression cassettes, coincided with the time of virus genome replication in a cell type specific manner. Hence, infected lung adenocarcinoma cells A549 reached this point faster than infected melanoma cells SK-MEL-28. My findings, together with previous publications, highlight the enormous potential of adenovirus DNA replication to produce high transgene levels for therapeutic applications [241,247]. In addition, the secreted

antibodies were fully functional to bind their antigen in flow cytometry analysis of CEA displaying target cells or using recombinant CEA antigen in ELISA demonstrating proof of principle for oncolytic adenoviruses expressing antibodies for the first time. The effector domain was studied in an *in-vitro* assay for antibody-mediated phagocytosis involving mouse macrophages. Therefore, tumor targets were incubated in presence of recombinantly produced CEA specific single-chain antibodies or relevant controls in different ratios with macrophages. However, phagocytosis of living or necrotic tumor target cells was already very efficient so that opsonizing antibodies had no further stimulatory effect. Usually these assays are performed with erythrocytes or latex beads rather than tumor cells which could account for the difficulties I observed with my assays [248]. Besides, the relevance of antibody-dependent cellular phagocytosis of tumor cells by macrophages might play a more important role *in-vivo*. Future experiments will address the functionality of the effector domain in terms of tumor cell killing by immune cells in alternative *in-vitro* assays involving natural killer cells or more importantly in xenograft mouse model studies.

In summary, this is the first study investigated HAdV-5 infections and genome-wide changes in cellular gene expression in human primary bronchial epithelial cells, resembling the natural host environment, versus various cancer cells. Major differences between these cell moieties were reduced viral gene expression, genome replication, and cytotoxicity in the melanoma cells SK-MEL-28 and Mel624 as compared to HBEC, accompanied by absent activation of cellular genes involved in the G1/S-phase transition pathway. Despite several efforts, adenovirus replication and lysis could not be enhanced in SK-MEL-28 and Mel624 melanoma cells, neither by overexpression or knockdown of key regulator genes nor by addition of various chemotherapeutic drugs. Yet there was one exception, the combination of viro- with chemotherapy involving the front line melanoma drug temozolomide resulted in enhanced viral DNA replication and progeny virus generation, but only in the SK-MEL-28 cell line. The underlying mechanism certainly deserves further attention in the future and might improve combined cancer treatment modalities for malignant melanoma. Additionally, I established novel strategies for efficient expression of therapeutic antibodies from oncolytic adenoviruses for wide applications. This approach capitalizes on the already established concept of antibody therapy and combines it with the prospects of oncolytic viruses in order to facilitate high expression of therapeutic antibodies at the tumor site.

IV MATERIALS

1 Chemicals

name	supplier	name	supplier
2-mercaptoethanol 50 mM for cell culture	Invitrogen, Karlsruhe	**lithium chloride**	CARL ROTH, Karlsruhe
5-fluorouracil	Sigma-Aldrich, Taufkirchen	**Luria Bertani medium "Lennox" (*LB*)**	CARL ROTH, Karlsruhe
2-mercaptoethanol 8.3 M for *in-vitro* use	Sigma-Aldrich, Taufkirchen	**magnesium chloride ($MgCl_2$)**	CARL ROTH, Karlsruhe
agarose	Invitrogen, Karlsruhe	**magnesium sulfate ($MgSO_4$)**	CARL ROTH, Karlsruhe
Airway Epithelial Cell Growth Medium	Promocell, Heidelberg	**Melanocyte Growth Medium**	Promocell, Heidelberg
ammonium persulfate (*APS*)	Sigma-Aldrich, Taufkirchen	**Minimal Essential Medium (*MEM*)**	Invitrogen, Karlsruhe
ampicillin	CARL ROTH, Karlsruhe	**penicillin**	Invitrogen, Karlsruhe
bacto-trypton	CARL ROTH, Karlsruhe	**phenylmethylsulfonyl fluoride (*PMSF*)**	AppliChem, Darmstadt
bromphenole blue	AppliChem, Darmstadt	**potassium chloride (*KCl*)**	Sigma-Aldrich, Taufkirchen
calcium chloride ($CaCl_2$)	CARL ROTH, Karlsruhe	**potassium dihydrogen phosphate (KH_2PO_4)**	Sigma-Aldrich, Taufkirchen
camptothecin	Sigma-Aldrich, Taufkirchen	**propidium iodide**	Sigma-Aldrich, Taufkirchen
cesium chloride	AppliChem, Darmstadt	**rapamycin**	Sigma-Aldrich, Taufkirchen
crystal violet	CARL ROTH, Karlsruhe	**RNase A**	Invitrogen, Karlsruhe
dimethyl sulfoxide	CARL ROTH, Karlsruhe	**Roswell Park Memorial Institute 1640 (*RPMI*)**	Invitrogen, Karlsruhe
dithiothreitol	AppliChem, Darmstadt	**Rotiphorese Gel 30**	CARL ROTH, Karlsruhe
Dulbecco's Modified Eagle Medium (*DMEM*)	Invitrogen, Karlsruhe	**skim milk powder**	CARL ROTH, Karlsruhe
Dulbecco's phosphate buffered saline (*DPBS*)	Invitrogen, Karlsruhe	**sodium acetate**	Sigma-Aldrich, Taufkirchen
ethidium bromide	AppliChem, Darmstadt	**sodium azide (NaN_3)**	AppliChem, Darmstadt

ethylenediaminetetra-acetic acid (*EDTA*)	Sigma-Aldrich, Taufkirchen	**sodium chloride (*NaCl*)**	CARL ROTH, Karlsruhe
etoposide	Sigma-Aldrich, Taufkirchen	**sodium deoxycholate**	BD Biosciences, Heidelberg
fetal calf serum	PAA, Pasching	**sodium dihydrogen phosphate (Na_2HPO_4)**	CARL ROTH, Karlsruhe
gentamicin	Invitrogen, Karlsruhe	**sodium dodecyl sulfate (*SDS*)**	Sigma-Aldrich, Taufkirchen
glucose	AppliChem, Darmstadt	**sodium fluoride**	Sigma-Aldrich, Taufkirchen
glycerol	CARL ROTH, Karlsruhe	**sodium orthovanadate**	Sigma-Aldrich, Taufkirchen
glycine	CARL ROTH, Karlsruhe	**sodium pyruvate**	Invitrogen, Karlsruhe
HEPES	CARL ROTH, Karlsruhe	**streptomycin**	Invitrogen, Karlsruhe
IGEPAL NP-40	Sigma-Aldrich, Taufkirchen	**sucrose**	Sigma-Aldrich, Taufkirchen
imidazole	Sigma-Aldrich, Taufkirchen	**TEMED (*N,N,N',N'-tetramethylethylenediamine*)**	Sigma-Aldrich, Taufkirchen
kanamycin	CARL ROTH, Karlsruhe	**temozolomide**	Sigma-Aldrich, Taufkirchen
Keratinocyte Growth Medium 2	Promocell, Heidelberg	**Trizma®**	Sigma-Aldrich, Taufkirchen
LB-agar "Luria/Miller"	CARL ROTH, Karlsruhe	**Tween 20**	Sigma-Aldrich, Taufkirchen
L-glutamine	Invitrogen, Karlsruhe	**yeast extract**	CARL ROTH, Karlsruhe
L-lysine, poly	Sigma-Aldrich, Taufkirchen	**Zeocin™**	Invitrogen, Karlsruhe

2 Prokaryotic cells, eukaryotic cells, and viruses

2.1 Bacterial strains

Escherichia coli Maximum Efficiency DH5α: genotype: F-Φ80ΔlacZΔM15, recA1, endA1, hsdR17 PhoA, supE44, gyrA96, relA1 (*Invitrogen, Karlsruhe*)

Escherichia coli Electro Maximum DH5α: genotype: F-Φ80ΔlacZΔM15, recA1, endA1, hsdR17 mcrA, mcrB, mcrC, mrr (*Invitrogen, Karlsruhe*)

Escherichia coli BJ5183: genotype: endA1, sbcBC, recBC, galK, met, thi-1, bioT, hsdR (*Stratagene, Amsterdam*)

2.2 Human primary cells and established cell lines

designation	origin	source
A375M	amelanotic melanoma cell line	Isaiah Fidler, Houston, USA
A549	lung adenocarcinoma epithelial cell line from alveolar basal epithelial cells, CEA positive	ATCC, Manassas, USA
C8161	amelanotic, CAR negative melanoma cell line	Danny Welch, Birmingham, USA
Colo-829	melanoma cell line, pigmented	Jacques Banchereau, Dallas, USA
HBEC	primary epithelial cells isolated from human bronchi of healthy donors. Lot 5092901.17 was derived from a 55 year old Caucasian male; Lot 7110910.11 originates from a 67 year old Caucasian male.	Promocell, Heidelberg
HEK293	human embryonic kidney cell, contains integrated wild type HAdV-5 DNA resulting in E1 gene expression	Quantum, Quebec, Canada
HEK293T	human embryonic kidney cell, expressing SV40 T-antigen and HAdV-5 E1 genes	Georg Fey, Erlangen
HEK293T-scFv$_{CEA}$	stably expresses recombinant single-chain antibodies against the carcinoembryonic antigen fused to the constant domain of mouse IgG$_{2a}$	established in this dissertation
HeLa	cervix adenocarcinoma, CEA negative	ATCC, Manassas, USA
HFF	primary normal foreskin fibroblasts	Manfred Marschall, Erlangen
LS174T	human colon adenocarcinoma, CEA positive	Roland Kontermann, Stuttgart
Mel624	melanoma cell line, pigmented	Jeffrey Schlom, Bethesda, USA
Mel888	melanoma cell line, pigmented	Jeffrey Schlom, Bethesda, USA
PHK	primary human keratinocytes	Frank Rösl, Heidelberg
pMel A	low passage melanoma cell line, pigmented	Detlef Dieckmann, Matthias Lüftl, Erlangen

pMel A2	low passage melanoma cell line, pigmented	Detlef Dieckmann, Matthias Lüftl, Erlangen
pMel L	low passage melanoma cell line, pigmented	Detlef Dieckmann, Matthias Lüftl, Erlangen
RAW264.7	murine macrophage cell line established from a tumor induced by the Abelson murine leukemia virus.	Philipp Beckhove, Heidelberg
SK-MEL-28	melanoma cell line, pigmented	ATCC, Manassas USA
SK-MES-1	lung squamous cell carcinoma, CEA negative	DKFZ, Heidelberg
SKOV-3	ovarian adenocarcinoma, CEA negative	Janet Price, Houston, USA
SW900	lung squamous cell carcinoma, CEA positive	ATCC, Manassas USA

2.3 Human adenoviruses

designation	features
HAdV-5	serotype 5, wild type; propagated from the pTG3602 plasmid provided by David Curiel, Birmingham, USA [249]
HAdV-5 CMV-gfp	replication-incompetent E3 deleted HAdV-5, contains the immediate early CMV promoter/enhancer and a green fluorescent protein transgene in the E1 region
HAdV-5/3	genetically similar to serotype 5 wild type, fiber gene was replaced by a chimeric 5/3 fiber for enhanced infection of CAR negative cells, provided by David Curiel, Birmingham, USA [249]
HAdV-5/3 CMV-luc	similar to HAdV-5 CMV-gfp but with a firefly luciferase transgene and a chimeric 5/3 fiber
HAdV-5/3 CMV-scFv	similar to HAdV-5 CMV-gfp but with the $scFv_{CEA}$-Fc recombinant antibody transgene a chimeric 5/3 fiber
HAdV-5/3 Δ24 40SA-luc	serotype 5, encodes a chimeric 5/3 fiber, bears a 24 bp deletion in E1A, expresses firefly luciferase from pGL3-basic under control of the HAdV-40 splice acceptor
HAdV-5/3 Δ24 40SA-scFv	similar to HAdV-5/3 Δ24 40SA-luc but with the $scFv_{CEA}$-Fc recombinant antibody transgene
HAdV-5/3 Δ24 BPSA-scFv	serotype 5, encodes a chimeric 5/3 fiber, bears a 24 bp deletion in E1A, expresses $scFv_{CEA}$-Fc under control of the human beta globin splice acceptor
HAdV-5/3 Δ24 IRES-luc	serotype 5, encodes a chimeric 5/3 fiber, bears a 24 bp deletion in E1A, expresses firefly luciferase from pGL3-basic via an IRES fused to the fiber gene
HAdV-5/3 Δ24	similar to HAdV-5/3 Δ24 IRES-luc but with the $scFv_{CEA}$-Fc recombinant antibody

IRES-scFv	transgene
HAdV-5/3 Δ24 pIIIaSA-scFv	serotype 5, encodes a chimeric 5/3 fiber, bears a 24 bp deletion in E1A, expresses $scFv_{CEA}$-Fc under control of the HAdV-2 L1 pIIIa splice acceptor
HAdV-5/3 Δ24 T2A-luc	similar to HAdV-5/3 Δ24 IRES-luc, luciferase expression via the self-cleaving motif T2A of the *Thosea asigna* insect virus [250]

3 Media

3.1 For bacteria

LB medium	25 g/l powder dissolved in bi-distilled water, sterile	**SOC Medium**	20 g/l bacto-trypton 5 g/l yeast extract 2.5 mM NaCl 10 mM $MgCl_2$ 10 mM $MgSO_4$ 20 mM glucose
LB_{AMP}	LB medium supplemented with 100 µg/ml ampicillin	**LB_{KAN}**	LB medium supplemented with 50 µg/ml kanamycin
LB_{AMP} agar	15 g/l LB-agar "Luria/Miller" dissolved in LB_{AMP}	**LB_{KAN} agar**	15 g/l LB-agar "Luria/Miller" dissolved in LB_{KAN}

3.2 For eukaryotic cells

Airway Epithelial Cell Growth Medium	4 µl/ml bovine pituitary extract 10 ng/ml epidermal growth factor 5 µg/ml insulin 0.5 µg/ml hydrocortisone 0.5 µg/ml epinephrine 6.7 ng/ml triiodo-L-thyronine 10 µg/ml transferrin, holo 0.1 ng/ml retinoic Acid 100 U/ml penicillin 100 µg/ml streptomycin	**Keratinocyte Growth Medium 2**	4 µl/ml bovine pituitary extract 125 pg/ml epidermal growth factor 5 µg/ml insulin 0.33 µg/ml hydrocortisone 0.39 µg/ml epinephrine 10 µg/ml transferrin, holo 0.06 mM $CaCl_2$ 100 U/ml penicillin 100 µg/ml streptomycin

DMEM-10 %	GlutaMAX™ 4.5 g/l glucose 10 % (*v/v*) fetal calf serum 100 U/ml penicillin 100 µg/ml streptomycin	**MEM-10 %**	Earle's salts 2 mM L-glutamine 10 % (*v/v*) fetal calf serum 100 U/ml penicillin 100 µg/ml streptomycin 100 µg/ml gentamicin
Melanocyte Growth Medium	4 µl/ml bovine pituitary extract 1 ng/ml fibroblast growth factor 5 µg/ml insulin 0.33 µg/ml hydrocortisone 10 ng/ml phorbol myristate acetate 100 U/ml penicillin 100 µg/ml streptomycin	**RPMI-10 %**	GlutaMAX™ 10 % (*v/v*) fetal calf serum 0.05 mM 2-mercaptoethanol 1 mM sodium pyruvate 100 U/ml penicillin 100 µg/ml streptomycin

4 Buffers and solutions

4.1 For common use

DPBS	137 mM NaCl 2.68 mM KCl 7.3 mM Na_2HPO_4 1.4 mM KH_2PO_4 1 mM $CaCl_2$ 2 mM $MgCl_2$ pH 7.0	**TE-buffer**	10 mM tris-HCl 1 mM EDTA pH 7.4

4.2 For gel electrophoresis of nucleic acids

10× DNA sample buffer	0.1 % (*w/v*) bromphenole blue 50 % (*v/v*) glycerol 0.1 M EDTA pH 8.0	**50× TAE buffer**	2 M tris 1 M sodium acetate 62.5 mM EDTA pH 8.5
agarose gel solutions	1× TAE buffer 0.5-2 % (*w/v*) agarose 1 µg/ml ethidium bromide	**ethidium bromide**	10 mg/ml

4.3 For gel electrophoresis for proteins

1× SDS sample buffer	200 mM tris-HCl 400 mM dithiothreitol 8 % (*w/v*) SDS 0.4 % (*w/v*) bromphenole blue 40 % (*v/v*) glycerol 10 % (*v/v*) 2-mercaptoethanol pH 6.8	**10× running buffer**	2 M glycine 250 mM tris 1 % (*w/v*) SDS
4× separating buffer	1.5 mM tris-HCl 0.04 % (*w/v*) SDS pH 8.8	**4× stacking buffer**	0.5 M tris-HCl 0.4 % (*w/v*) SDS pH 6.8
12.5 % separation gel	6 ml bi-distilled water 7.5 ml Rotiphorese Gel 30 4.5 ml 4× separating buffer 25 µl TEMED 120 µl 10 % (*w/v*) APS	**4 % stacking gel**	5.15 ml bi-distilled water 1.1 ml Rotiphorese Gel 30 2.1 ml 4× stacking buffer 17.5 µl TEMED 60 µl 10 % (*w/v*) APS
RIPA protein lysis buffer	10 mM tris-HCl 150 mM NaCl 1 % (*v/v*) IGEPAL NP-40 1 % (*w/v*) sodium deoxycholate 0.1 % (*w/v*) SDS 1 mM PMSF 20 mM sodium fluoride 2 mM sodium orthovanadate pH 7.5		

4.4 For Western Blot analysis and enzyme linked immunosorbent assays

1× transfer buffer	25 mM tris 192 mM glycine 20 % (*v/v*) methanol	**10× TBS buffer stock**	250 mM tris-HCl 1.5 M NaCl pH 7.4
blocking solution	1× TBS 5 % (*w/v*) skim milk powder 0.02 % (*v/v*) Tween 0.02 % (*v/v*) NaN_3	**washing solution (TBST)**	1× TBS 0.02 % (*v/v*) Tween
washing solution (PBST)	1× DPBS 0.05 % (*v/v*) Tween		

4.5 For protein purification

5× Na_2HPO_4 buffer stock	250 mM Na_2HPO_4 2.5 M NaCl 0.02 % (*v/v*) NaN_3 pH 7.0	**IMAC elution buffer**	1× Na_2HPO_4 buffer 250 mM imidazole 0.02 % (*v/v*) NaN_3 pH 7.0
IMAC equilibration loading buffer	1× Na_2HPO_4 buffer 20 mM imidazole 0.02 % (*v/v*) NaN_3 pH 7.0	**IMAC wash buffer**	1× Na_2HPO_4 buffer 35 mM imidazole 0.02 % (*v/v*) NaN_3 pH 7.0

4.6 For fluorescent cell activated sorting

FACS buffer	DPBS 10 % (*v/v*) fetal calf serum 0.1 % (*v/v*) NaN_3	**FACS washing buffer**	DPBS 1 % (*v/v*) fetal calf serum 0.01 % (*v/v*) NaN_3
PI staining buffer	DPBS 50 µg/ml propidium iodide 100 µg/ml RNase A		

4.7 For HAdV purification and analysis

cesium chloride solution 1.41	500 ml bi-distilled water 304.6 g cesium chloride pH 7.8, sterile	**cesium chloride solution 1.27**	500 ml bi-distilled water 227.2 g cesium chloride pH 7.8, sterile
crystal violet staining solution	70 % (*v/v*) ethanol 2 % (*w /v*) crystal violet	**VL buffer**	100 µM TE-buffer 0.5 % (*w/v*) SDS

5 Nucleic acids, oligonucleotides and plasmids

5.1 For cloning and PCR

All oligonucleotides were purchased from and synthesized by MWG-Biotech, Martinsried.

designation	sequence
3 knob forward	5'-TTAATGTAGAACTATACTTTGATGC-3'
5 knob forward	5'-AGGCAGTTTGGCTCCAATATCTGG-3'
Ad1124-1100 reverse	5'-ATTTTCACTTACTGTAGACAAACAT-3'
Ad40SALinker forward	5'-Phospho-ATCTTAATTAAGCAGGCGCAATCTTCGCATTTCTTTTTTCCAGGAAGC CACCATGGACTGACTGC-3'
Ad40SALinker reverse	5'-Phospho-CATGGTGGCTTCCTGGAAAAAAGAAATGCGAAGATTGCGCCTGCA-3'
E1A promoter forward	5'-GAGGCCCTTTCGTCTTCAAGGATCCG-3'
E1A promoter reverse	5'-TCCCATGGTCAGTCCCGGTGTCG-3'
E1AΔ24 reverse	5'-AAAGCCAGCCTCGTGGCAGGTAAG-3'
E3 forward	5'-CTGCTAGTTGAGCGGGACAGGGGAC-3'
E3 reverse	5'-GGCAAGGAGGTGCTGCTGAATAAAC-3'
E4 forward	5'-ATTGAAGCCAATATGATAATGAGGG-3'
E4 reverse	5'-CACAGCGGCAGCCTAACAGTC-3'
HPV-31 E7 forward	5'-AATTAGATCTGCCACCATGCGTGGAGAAACACCTACGTTG-3'
HPV-31 E7 reverse	5'-TTAAGGATCCTTACAGTCTAGTAGAACAGTTGGGGCAC-3'
pGL3-Seq3MCS reverse	5'-TTATGCAGTTGCTCTCCAGCGGTTC-3'
pIIIaSA forward	5'-CTTAGATCTAGTACTAAGCGGTGATGTTTCTGATCAGATGGAGACAGACACACTC CTGC-3'
scFv$_{CEA}$-Fc reverse	5'-TCGGTCGACGGATCCTTATC-3'
Seq Mfe fiber reverse	5'-TGTATAAGCTATGTGGTGGTGGGG-3'
SeqITR forward	5'-CGGGAAAACTGAATAAGAGGAAGTGA-3'
SV40 large T antigen reverse	5'-TTAAGGATCCAATTGCATTCATTTTATGTTTCAGG-3'
SV40 large/small T antigen forward	5'-AATTAGATCTGCCACCATGGATAAAGTTTTAAACAGAGAGG-3'
SV40 small T antigen reverse	5'-TTAAGGATCCTTAGAGCTTTAAATCTCTGTAGGTAGTTTGTCC-3'

5.2 For quantitative PCR

All human Quantitect™ primers were obtained from Qiagen, Hilden and reconstituted in 1.1 ml TE buffer, pH 8.0. Following primers were used: ACTB QT01680476, BLM QT00027671, CCNE1 QT00041986, CD83 QT00069923, CDC25A QT00001078, CDT1 QT00020601, CHAF1B QT00012845, E2F2 QT00045654, E2F5 QT00062965, EGR1 QT00999964, FOS QT00007070, GAPDH QT01192646, H2BFS QT00227199, HERC5 QT00007280, HES4 QT00208726, IRS2 QT00064036, MCM2 QT00070812, MGC13057 QT00221347, PKMYT1 QT00013580, RFC3 QT00019243, TIPIN QT00054334, UNG1 QT00037912;

All oligonucleotides were purchased from and synthesized by MWG-Biotech, Martinsried.

designation		sequence
ACTB	forward reverse	5'-TAAGTAGGCGCACAGTAGGTCTGA-3' 5'-AAAGTGCAAAGAACACGGCTAAG-3'
E1A	forward reverse	5'-AACCAGTTGCCGTGAGAGTTG-3' 5'-CTCGTTAAGCAAGTCCTCGATACA-3'
E4	forward reverse	5'-GGTTGATTCATCGGTCAGTGC-3' 5'-TACGCCTGCGGGTATGTATTC-3'
Fiber	forward reverse	5'-TGATGTTTGACGCTACAGCCATA-3' 5'-GATTTGTGTTTGGTGCATTAGGTG-3'
GAPDH	forward reverse	5'-GGTTTACATGTTCCAATATGATTCCA-3' 5'-ATGGGATTTCCATTGATGACAAG-3'
Hexon	forward reverse	5'-ACCTGGGCCAAAACCTTCTC-3' 5'-CGTCCATGGGATCCACCTC-3'
$p16^{INK4a}$	forward reverse	5'-ACGTGCGCGATGCCT-3' 5'-ATGGCCCAGCTCCTCAG-3'
$p21^{WAF/CIP}$	forward reverse	5'-CTGGAGACTCTCAGGGTCGAA-3' 5'-CCAGGACTGCAGGCTTCCT-3'

5.3 Small interfering RNAs

All siRNAs were obtained from Dharmacon, Braunschweig and reconstituted with 1× siRNA buffer (*Dharmacon, Braunschweig*) to give a final concentration of 20 µM for each stock.

Following siRNAs were used: $p16^{INK4a}$ J-011007-08, $p21^{WAF/CIP}$ J-003471-12, nonsense control pool D-001810-10;

5.4 Plasmids

designation	features
pcDNA3.1/hygro (+)	cloning vector for the expression of proteins in mammalian cell lines via a CMV promoter (*Invitrogen, Karlsruhe*)
pcDNA3.1-CCNE-HA/FLAG	expression plasmid for the human cyclin E protein isoform 1 fused to the hemagglutinin and FLAG tag, a kind gift from Ingrid Hoffmann
pcDNA3.1-CDC25A-gfp	expression plasmid for the human CDC25A phosphatase, fused to the enhanced greed fluorescent protein, a kind gift from Ingrid Hoffmann
pcDNA3.1-HPV-31 E7	expression plasmid for the HPV-31 E7 protein, cloned via PCR using E7 forward/reverse oligonucleotides from wild type HPV-31 DNA, a kind gift from Elizabeth Schwarz, DKFZ, inserted into pcDNA3.1/hygro(+) via BglII/BamHI sites
pcDNA3.1-SV40 LT	expression plasmid for the SV40 large T antigen, cloned from wild type DNA via PCR using the respective SV40 large T antigen forward/reverse oligonucleotides and BglII/BamHI sites
pcDNA3.1-SV40 ST	expression plasmid for the SV40 small T antigen, cloned from wild type DNA via PCR using the respective SV40 small T antigen forward/reverse oligonucleotides and BglII/BamHI sites
pcDNA4-HHV-8 ORF72	expression plasmid for the HHV-8 viral cyclin, a kind gift from Frank Neipel, Erlangen
pCMV-HPV-16 E7 HA/FLAG	expression plasmid for the HPV-16 E7 protein, contains the hemagglutinin and FLAG tags, a kind gift from Felix Hoppe-Seyler, DKFZ
pCMV-HPV-18 E7 HA/FLAG	expression plasmid for the HPV-18 E7 protein, contains the hemagglutinin and FLAG tags, a kind gift from Felix Hoppe-Seyler, DKFZ
pcDNA3-YB1	expression plasmid for the human YB1 transcription factor, a kind gift from Per Sonne Holm, Klinikum rechts der Isar, Munich
pF5/3-40SA-luc	adenovirus transfer vector containing a chimer 5/3 fiber and the firefly luciferase gene fused to the HAdV-40 long fiber gene splice acceptor site. The 40SA-luc cassette was transferred via XhoI/BamHI sites
pF5/3-40SA-scFv$_{CEA}$	similar to pF5/3-40SA-luc, created by inserting a blunted 40SA-scFv$_{CEA}$-Fc cassette, excised via XhoI/SalI digest, into XhoI/BamHI digested and blunted fiber plasmids
pF5/3-IRES-FCU1	adenovirus transfer vector containing a chimer 5/3 fiber and the yeast cytosine deaminase and uracil phosphoribosyl transferase chimera fused to it via an IRES site, provided by Michael Behr, DKFZ
pF5/3-IRES-luc	similar to pF5/3-IRES-FCU1, created by inserting the firefly luciferase gene via partial digest of NcoI/XbaI
pF5/3-IRES-scFv$_{CEA}$	similar to pF5/3-IRES-FCU1, created by partial digest of NcoI/XbaI and insertion of recombinant scFv$_{CEA}$-Fc antibody

pF5/3-pIIIaSA-scFv$_{CEA}$	adenovirus transfer vector containing a chimer 5/3 fiber and the scFv$_{CEA}$-Fc fused to the HAdV-2 L1 pIIIa splice acceptor, the transgene cassette was excised via XhoI/SalI from pGL3-pIIIaSA-scFv$_{CEA}$ and blunt end cloned into XhoI/BamHI digested and blunted fiber plasmids
pGL3-40SA-luc	pGL3-basic variant with the HAdV-40 splice acceptor site from the long fiber gene inserted through annealed Ad40SALinker sequences **via** BglII/NcoI sites
pGL3-40SA-scFv$_{CEA}$	similar to pGL3-40SA-luc, the luciferase transgene was replaced with the recombinant scFv$_{CEA}$-Fc antibody via NcoI/XbaI sites
pGL3-basic	encodes the firefly luciferase reporter gene, lacks any eukaryotic promoter sequences (*Promega, Madison USA*)
pGL3-BPSA-luc	similar pGL3-basic, additionally contains the human beta globin splice acceptor upstream of the firefly luciferase
pGL3-BPSA-scFv$_{CEA}$	similar pGL3-BPSA-luc, the luciferase transgene was replaced with the recombinant scFv$_{CEA}$-Fc antibody via NcoI/XbaI sites
pGL3-CMV	pGL3-basic containing the immediate early gene promoter and enhancer sequences from the cytomegalovirus
pGL3-E1A	pGL3-basic containing the left inverted terminal repeat and E1A promoter sequences from the HAdV-5 genomic plasmid pTG3602 (*nucleotides 37935 to 557*) cloned by PCR and transferred via BamHI/NcoI sites into BglII/NcoI digested vector
pGL3-E2F	pGL3-basic containing a shortened E2F1 promoter (*nucleotides -221 to +60*)
pGL3-hTK	pGL3-basic containing the human thymidine kinase promoter
pGL3-pIIIaSA-scFv$_{CEA}$	the recombinant scFv$_{CEA}$-Fc antibody was cloned by PCR using pIIIaSA forward and scFv$_{CEA}$-Fc reverse oligonucleotides and inserted via BglII/XbaI sites into pGL3-basic
pGL3-SV40	pGL3-basic containing the early gene promoter and enhancer sequences from the simian virus 40
pS-CMV-luc	E1 deleted adenovirus transfer vector containing the firefly luciferase gene downstream of the immediate early cytomegalovirus promoter/enhancer
pS-CMV-scFv$_{CEA}$	similar to pS-CMV-luc, the luciferase transgene was replaced with the scFv$_{CEA}$-Fc antibody, previously excised with NcoI/XbaI, using blunt end cloning into XhoI digested vector
pSecTag-HisA-scFv$_{CEA}$-Fc	plasmid contains a recombinant single-chain antibody, directed against the human carcinoembryonic antigen, fused to the constant domain of mouse IgG$_{2a}$ (*Roland Kontermann, Stuttgart*)
pSΔ24-BPSA-FCU1	adenovirus transfer vector which contains a mutant E1A gene with a 24 bp deletion to prevent binding and inactivation of pRB, carries the yeast cytosine deaminase and uracil phosphoribosyl transferase chimera fused to the human beta globin splice acceptor, provided by Michael Behr, DKFZ
pSΔ24-BPSA-scFv$_{CEA}$	similar to pSΔ24-BPSA-FCU1, the FCU1 transgene was replaced with the scFv$_{CEA}$-Fc antibody via MluI/SalI

pTG3602	plasmid containing the complete wild type HAdV-5 genome, [251]
pTriEx4-large T	expression plasmid containing the , a kind gift from Jürgen Hämmerling, DKFZ
pVK500 5/3 ΔE3	plasmid containing the HAdV-5 genome with a chimeric 5/3 fiber and a deleted E3 region
pVK500 Δ24 ΔE3	plasmid containing the HAdV-5 genome with partial deletion of the fiber gene, a 24 bp deletion in the E1A region, and deleted E3 region

6 Antibodies and recombinant proteins

description	origin	dilution	source
anti-mouse-CD11b-phycoerytrhin	Rat, monoclonal (*M1/70*), Lot 101208	1:400	BioLegend, San Diego, USA
anti-mouse-IgG-horseradish peroxidase	goat, polyclonal, Lot L21	1:5000-10000	Cell Signaling Technology, Danvers, USA
anti-mouse-IgG-phycoerythrin	goat, polyclonal, Lot 66135	1:400	BD Pharmingen, Heidelberg
anti-rabbit-IgG-horseradish peroxidase	goat, polyclonal, Lot L16	1:10000	Cell Signaling Technology, Danvers, USA
carcinoembryonic antigen	human liver metastasis of colon adenocarcinoma, Lot L25193	300 ng / well	AppliChem, Darmstadt
HAdV-5 fiber tail (*monomeric and trimeric*)	mouse, monoclonal (*4D2*), Lot 894112	1:2000	Abcam, Cambridge, UK
HAdV-5 hexon	rabbit, polyclonal, Lot 868916	1:2000	Abcam, Cambridge, UK
human ACTB	mouse, monoclonal (*AC-74*), Lot A228	1:2000	Sigma-Aldrich, Taufkirchen
isotype IgG_{2a}	mouse monoclonal (*MOPC-173*), Lot B111221	1:200	BioCat, Heidelberg
$scFv_{CEA}$-Fc	recombinant protein	1:200	Our lab

V METHODS

Standard methods of molecular biology required for this dissertation were performed according to the laboratory manual “Molecular Cloning” by Sambrook and Russel [252].

1 Recombinant DNA and RNA techniques

1.1 Gel electrophoresis of DNA fragments

Samples were supplemented with 1× DNA sample buffer and analyzed on agarose gels containing ethidium bromide. Electrophoresis done horizontally at 100 V in 1× TAE buffer led to separation of DNA fragments according to their size. Relevant fragment sizes were determined by simultaneously separating a GeneRuler™ 1 kb DNA Ladder mix (*Fermentas, St. Leon-Rot*). Afterwards, DNA was visualized with UV light at 265 nm. For cloning, respective bands were excised using a scalpel and extracted (*see below*).

1.2 Cloning of DNA fragments into plasmid vectors

Plasmids, amplified PCR products, and phosphorylated oligonucleotides were cleaved with relevant restriction endonucleases in buffers (*all Fermentas, St. Leon-Rot*) as described by the manufacturer to generate vector and insert fragments for cloning. For the conversion of DNA overhangs after a restriction digest, i.e. filling in recessed 5’-overhangs or digesting protruding 3’-overhangs, T4 DNA Polymerase (*Fermentas, St. Leon-Rot*) was utilized according to the manufacturer’s protocol. Religation of cut vector ends was prevented through dephosphorylation by subsequent treatment with shrimp alkaline phosphatase following the manufacturer’s instructions (*Fermentas, St. Leon-Rot*). If required and depending on the fragment length or desired purity, DNA fragments were directly purified using either QIAquick® PCR Purification Kit or gel electrophoresis (*see above*) for subsequent DNA extraction with QIAprep® Gel Extraction Kit (*both Qiagen, Hilden*) as described by the manufacturer. Afterwards, ligation of vector and insert was performed using the Rapid Ligation Kit

(*Roche, Mannheim*) according to the respective manual. For efficient cloning, the amount of insert was calculated according to the following formula:

$$\text{amount of insert DNA} = \left(10 \times \frac{\text{size insert}}{\text{size vector}}\right) \times \text{amount of vector DNA}$$

A tenfold molar excess of insert was mixed with 200 ng of vector DNA and the reaction mix was incubated at 22 °C overnight and used to transform bacteria (*see below*).

1.3 Production of transformation-competent bacteria

1.3.1 For heat shock

A single colony of Escherichia coli Maximum Efficiency DH5α was inoculated in 5 ml LB-medium without antibiotics and cultivated overnight at 37 °C in a shaker incubator at 180 rpm. On the next day, overnight culture was transferred to Erlenmeyer flasks containing 300 ml LB-medium. Bacteria were incubated until they reached exponential growth phase as measured by optical density at 600 nm of 0.4-0.6. Suspension was incubated on ice for 15 minutes and bacteria were collected by centrifugation at 4 °C and 3080 g for 5 minutes. Pellets were resuspended in 150 ml ice-cold, sterile 0.1 M $MgCl_2$ solution and incubated on ice for one hour. Following another round of centrifugation, bacteria were resuspended in 12 ml ice-cold, sterile 0.1 M $CaCl_2$ solution and incubated for another hour on ice. Afterwards, sterile glycerol was added reaching a final concentration of 20 % (*v/v*). Heat shock competent bacteria were stored subsequently in 200 µl aliquots at -80 °C.

1.3.2 For electroporation

A single colony of Escherichia coli Electro Maximum DH5α or Escherichia coli BJ5183 was inoculated in 10 ml LB-medium without antibiotics and incubated at 37 °C overnight in a shaker incubator at 180 rpm. Then, 4 ml of the overnight culture was added to Erlenmeyer flasks containing 500 ml LB-medium. Bacteria were cultivated until they reached an optical density of 0.8 at 600 nm wavelength before incubating the suspension for one hour on ice. Following

centrifugation at 3080 g for 10 minutes at 4 °C, bacterial pellet was resuspended in 200 ml ice-cold, sterile 10 % (*v/v*) glycerol solution. This step was repeated twice and cells were collected in 5 ml of ice-cold, sterile 10 % (*v/v*) glycerol. Aliquots of 50 µl electro-competent bacteria were stored at -80 °C.

1.4 Heat shock transformation

For transformation of small plasmids up to 15 kb, heat shock competent bacteria were thawed on ice. Then, 10-50 ng of a relevant plasmid or 5 µl of a ligation mix was added to each 50 µl aliquot of competent cells. The samples were incubated for 15 minutes on ice before exposing them to a heat shock at 42 °C for 1 minute. Afterwards, samples were immediately put on ice for 90 seconds while adding 1 ml of SOC medium. Bacteria were incubated at 37 °C, 300 rpm for at least 20 minutes before streaking them out on LB-agar dishes containing the appropriate selection antibiotic. Plates were incubated overnight at 37 °C and colonies of single clones could be picked the next day for downstream applications.

1.5 Transformation by electroporation

Plasmids larger than 15 kb required transformation in electro-competent DH5α. For each sample, 50 µl of competent cells were thawed on ice and added to 1-50 ng of a relevant plasmid or ligation mix. After incubation on ice for 1 minute, samples were transferred into pre-chilled electroporation cuvettes. Single cuvettes were placed in an electroporator and pulsed at 2.5 kV for 4.5-5.5 milliseconds. Immediately after transformation, 1 ml of SOC medium was added to the cells. Following shaking at 37 °C for one hour, bacteria were streaked out on LB-agar dishes containing a relevant selection antibiotic. Plates were incubated overnight at 37 °C before picking single clone colonies.

1.6 Generation of recombinant adenoviral genomes by homologous recombination

Alteration of adenovirus genomes was done by cloning DNA fragments into relevant shuttle plasmids and homologous recombination in electro-competent BJ5183 bacteria. Therefore, 6 µg

of shuttle plasmid was linearized through PmeI digestion at 37 °C for 5 hours or overnight. DNA was precipitated by first adding a final concentration of 800 mM lithium chloride and then 2.5× volumes of 100 % ethanol. After centrifugation at 17000 g for 30 minutes, the supernatant was aspirated and the pellet resuspended in 20 µl bi-distilled water. Electroporation was carried out as described above with 100-200 ng of a respective adenovirus backbone and 5-10 µl linearized shuttle plasmid per sample. All incubation steps were done at 30 °C rather than 37 °C. Bacteria harboring recombined adenovirus genomes were selected via a relevant antibiotic and analyzed by restriction enzyme analysis.

1.7 Preparation of DNA and RNA

1.7.1 Small scale isolation of plasmid DNA (*mini prep*)

Single clone colonies were inoculated in 5 ml LB-medium containing a relevant antibiotic and incubated overnight in a shaker incubator at 180 rpm and 37 °C. Bacteria containing adenoviral genomes the temperature was lowered to 30 °C. The next day, bacteria were harvested by centrifugation at 3080 g for 10 minutes. DNA was extracted using QIAprep® Spin Miniprep Kits (*Qiagen, Hilden*) according to the manufacturer's protocol. Briefly, bacterial pellets were resuspended in 200 µl of buffer P1 and lysed by adding 400 µl buffer P2. Lysis was stopped after 5 minutes incubation at room temperature through addition of 300 µl of buffer P3. Bacterial lysates were cleared by centrifugation at 17000 g for 10 minutes and supernatants loaded on QIAprep® columns. After another round of centrifugation again at 17000 g for one minute, purified DNA was precipitated by adding 750 µl isopropanol to each sample. After mixing, precipitated DNA was pelleted at 17000 g for 30 minutes and washed with 70 % (*v/v*) ethanol. Supernatants were aspirated and DNA resuspended in 50 µl TE-buffer for further downstream applications. Larger plasmids *(size > 15 kb*) were essentially extracted as described but leaving out the purification via columns to avoid shearing.

1.7.2 Large scale isolation of plasmid DNA (*midi lysate*)

Similarly to the small scale isolation procedure of plasmid DNA (*see above*), larger amounts of purified plasmid DNA regardless of size were obtained by using QIAGEN® Plasmid Midi Kits

(*Qiagen, Hilden*) as described by the manufacturer. Briefly, 100-250 ml of an overnight culture was harvested and bacterial pellet dissolved in 4 ml buffer P1. Cell wall lysis was enabled by adding 8 ml buffer P2 and stopped with 6 ml buffer P3, differing from standard protocol. Precipitated DNA plasmids were resuspended in 100 µl TE-buffer and stored at -20 °C.

1.7.3 DNA isolation from human cell cultures

Total DNA from human cell cultures was prepared by using QIAamp® DNA Mini and Blood Kits (*Qiagen, Hilden*). For this purpose, up to 5×10^6 cells were harvested by replacing the medium with 200 µl DPBS and usage of a cell scraper. Samples were stored at -20 °C until further purification following the manufacturer's instructions. For RNA free genomic DNA, 4 µl RNase A was added before addition of buffer AL, the remaining protocol was left unchanged. Purified DNA was stored in 200 µl TE buffer at -20 °C.

1.7.4 RNA isolation from human cell cultures

Total RNA was isolated from human cells using RNeasy® Mini Kits (*Qiagen, Hilden*) according to the manufacturer's protocol. Briefly, up to 5×10^5 cells were harvested in 350 µl RLT buffer containing 3.5 µl 2-mercaptoethanol and either processed directly or stored at -80 °C. For larger samples, QIAshredder® columns (*Qiagen, Hilden*) were utilized to ensure higher lysate homogeneity. An optional on column digest with RNase free DNase Kits (*Qiagen, Hilden*) was performed for 15 minutes at room temperature as mentioned in the manual. However, this step was left out if total RNA was extracted and to be used for gene expression analysis by microarrays (*see below*). Purified RNA was eluted with 30 µl RNase free water.

1.8 Gene expression analysis by microarray

Total RNA from uninfected and infected cells was isolated (*see above*), its concentration determined, and set to 250 ng/ml. Samples were sent to the Genomics & Proteomics Core Facility at the DKFZ, Heidelberg where further processing, labeling, and hybridization to the array platform took place using reagents from Illumina, San Diego, USA if not stated otherwise.

Briefly, sample quality was assessed by gel analysis using the total RNA Nano chip assay on an Agilent 2100 Bioanalyzer (*Agilent Technologies, Berlin*). Only samples with a RNA index value greater than 8.5 were selected for expression profiling. Biotin-labeled cRNA samples for hybridization on Illumina Human Sentrix-8 V2 BeadChip arrays were prepared according to Illumina's recommended sample labeling procedure based on the modified Eberwine protocol [253]. In brief, 250-500 ng of total RNA was used for complementary DNA (*cDNA*) synthesis, followed by an in-*vitro* transcription amplification and labeling step to synthesize biotin-labeled cRNA according to the MessageAmp™ II aRNA Amplification kit. Biotin-16-uridine-triphosphate was purchased from Roche, Mannheim. The cRNA was column purified according to the TotalPrep™ RNA Amplification Kit, and eluted in 60-80 µl of water. Quality of cRNA was again controlled using the RNA Nano chip assay quantified by a NanoDrop ND-1000 UV/VIS spectrophotometer (*Peqlab, Erlangen*). Hybridization was performed at 58 °C, in GEX-HCB buffer at a concentration of 100 ng cRNA/µl, unsealed in a wet chamber for twenty hours. Spike-in controls for low, medium and highly abundant RNA were added, as well as mismatch control, perfect match, and biotinylation control oligonucleotides. Microarrays were washed once in High Temperature Wash Buffer at 55 °C and then twice in E1BC buffer at room temperature for five minutes (*in between washed with ethanol at room temperature*). After blocking for five minutes in 4 ml of 1 % (w/v) casein Hammarsten grade in DPBS (*Pierce Biotechnology, Rockford, USA*), array signals were developed by a ten minute incubation time in 2 ml of 1 µg/ml cyanine-3-streptavidin solution (*Amersham Biosciences, Buckinghamshire, UK*) and 1 % (*w/v*) blocking solution. After a final wash in E1BC buffer, the arrays were dried and scanned. Microarray scanning was done using an Illumina BeadStation array scanner, setting adjusted to a scaling factor of one and PMT settings at 430. Data extraction was done for all beads individually, and outliers were removed if > 2.5 median absolute deviation. All remaining data points were used for the calculation of the mean average signal and standard deviation for a given probe. Data from different microarray replicates was normalized using lin-log transformation without local background subtraction. Afterwards, data was loaded into the Multi-Conditional Hybridization Intensity Processing System software as virtual two color approach. Results and raw data will be deposited in a public microarray database as stated in Dorer, Holtrup *et al. in preparation*.

1.9 Polymerase chain reaction (*PCR*)

1.9.1 For analysis and cloning

	analysis	cloning
10× PCR buffer	1×	1×
10 mM dNTP's	200 µM	250 µM
50 mM $MgCl_2$	1.5 mM	2 mM
10 µM primer, forward	500 nM	250 nM
10 µM primer, reverse	500 nM	250 nM
DNA template	500 pg – 25 ng	500 pg – 25 ng
enzyme	0.04 U Taq Polymerase	1 U PRECISOR Polymerase
final volume	25 µl	50 µl

Thermal cycler profile:

stage	description	repetitions	temperature	time
1	initial denaturation	1	96 °C	3 minutes
2	denaturation	30-40	96 °C	15 seconds
	annealing		58-62 °C	30 seconds
	extension		72 °C	15 seconds / 1 kb fragment length
3	final extension	1	72 °C	10 minutes
4	cooling	1	4 °C	~

Genomic and plasmid DNA was amplified during a polymerase chain reaction using either a Taq Polymerase Kit (*Invitrogen, Karlsruhe*) for common PCR analysis or a PRECISOR High-Fidelity DNA Polymerase Kit (*BioCat, Heidelberg*) for cloning according to the manufacturer's protocol. All primers were synthesized and purchased from Eurofins MWG, Ebersberg. Deoxyribonucleotide triphosphates (*dNTP's*) were obtained from Bioron, Ludwigshafen. Template from adenoviruses was gained by boiling 50 µl stock solution at 95 °C for 10 minutes. To remove debris, samples were centrifuged at 10000 g for 3 minutes. The PCR was run on a T3000 Thermocycler Biometra, Jena. Each sample was prepared as stated above. The annealing temperature, repetitions and extension time was individually defined for the relevant

oligonucleotide primers and expected fragment length. Ten micro liters of each PCR sample was analyzed by standard agarose gel electrophoresis (*see section V, 1.1*). PCR samples for cloning were purified using the QIAquick® PCR Purification Kit (*Qiagen, Hilden*) as suggested by the manufacturer and further processed as described in paragraph V, 1.2

1.9.2 Quantitative real time PCR

	cellular mRNA	viral mRNA	viral DNA
2× Power SYBR® Green PCR Master Mix	1×	1×	1×
50 U/µl reverse transcriptase	6.25 U	6.25 U	-
20 U/ µl RNase inhibitor	10 U	10 U	-
10 µM primer, forward	-	50 nM	50 nM
10 µM primer, reverse	-	50 nM	50 nM
10× Quantitect™ Primer Mix	1×	-	-
template	20 ng	1-100 ng	1-100 ng
final volume	25 µl	25 µl	25 µl

Thermal cycler profile:

stage	description	repetitions	temperature	time
1	reverse transcription*	1	48 °C	30 minutes
2	initial denaturation	1	95 °C	10 minutes
3	denaturation	40	95 °C	15 seconds
	annealing / extension		60 °C	1 minute
4	dissociation	1	95 °C 60 °C 95 °C 60 °C	15 seconds 1 minute 15 seconds 15 seconds

* only for mRNA templates

Adenoviral genome copies, viral mRNA as well as cellular mRNA expression levels were quantified by qPCR based on the detection of SYBR® Green. All reagents were purchased from Applied Biosystems, Darmstadt except Quantitect™ Primers which were obtained from Roche, Mannheim and used exclusively for chip candidate gene quantification. Samples were analyzed on a 7300 Real Time PCR System (*Applied Biosystems, Darmstadt*). Total RNA or genomic DNA

was isolated according to sections V, 1.7.4 and V, 1.7.3 and added to MicroAmp™ Optical 96 well plates containing the appropriate reaction mix (*see above*). Each run further included negative controls as well as appropriate standard curves if available. For quantification of adenoviral mRNA and genomes, plasmid pTG3602 containing the whole genome of HAdV-5 was diluted to 10^8, 10^6, 10^4, and 10^2 copies/well. Normalization of mRNA amounts was done accordingly with a standard of HeLa total RNA (*Stratagene, Amsterdam*), diluted to 200, 20, 2 and 0.2 ng/well. For normalization of DNA, a similar standard made from extracted total DNA of A549 cells was used. Fluorescence emitted through SYBR Green dye incorporated into double stranded PCR products was measured at the end of every cycle in stage 2. After completion of the cycling process, samples were subjected to an optional melting curve analysis from 60°C to 95°C at 0.1 °C/s with continuous fluorescence monitoring to distinguish primer dimers and unspecific amplicons from specific target gene products. Data was analyzed with the 7300 System SDS Software V1.4 (*Applied Biosystems, Darmstadt*) and presented as relative E1A or fiber mRNA, viral genomes, and relative cellular mRNA content using the formula below or Q-Gene software if no standard curve was available [254]:

$$\text{mRNA or genome content} = \left(\frac{\text{target gene copy numbers}}{\text{ng reference gene}} \right)$$

2 Biochemical and immunological protein methods

2.1 Preparation of total protein lysates

Human cells were harvested by trypsinization and pelleted at 225 g for 3 minutes. Afterwards, supernatants were removed and cells washed once in 5 ml ice-cold DPBS. Lysis was done with 100 µl per 1×10^6 cells freshly prepared RIPA buffer for 30 minutes on ice. Subsequently, cellular debris was removed by spinning samples at 17000 g for 30 minutes in a cooled centrifuge at 4 °C. Supernatants containing soluble total protein were transferred to new reaction tubes and stored at -80 °C.

2.2 Measuring sample protein concentration

The concentration of total protein lysates was determined using the Bio-Rad DC Protein Assay (*Bio-Rad, Munich*). Therefore, standard curves were generated using bovine serum albumin (*New England Biolabs, Frankfurt am Main*) diluted to 1.4 µg/µl, 1.05 µg/µl, 0.7 µg/µl, 0.35 µg/µl, and 0.175 µg/µl. Samples were diluted 1:4 in 20 µl bi-distilled water and mixed with 100 µl reagent A and 800 µl reagent B. After 20 min incubation at room temperature, absorbance at 750 nm wavelength was determined in a spectrophotometer.

2.3 Discontinuous SDS-polyacrylamide gel electrophoresis (*SDS-PAGE*)

Separation of proteins according to molecular weight and charge was performed by SDS-PAGE pursuing essentially Laemmli's method [255]. If not state otherwise, 20-100 µg lysate was mixed with 4× protein sample buffer and incubated at 95 °C for 10 minutes to obtain reduced and denatured protein. For analysis of oxidized but denatured dimerized single-chain antibodies, 4× protein sample buffer without 2-mercaptoethanol or dithiothreitol was prepared and used accordingly. Thereafter, reaction tubes were shortly put on ice and droplets collected by quick spin centrifugation. Samples were loaded on previously prepared polyacrylamide gels composed of a 12.5 % separating gel and a 4 % stacking gel. Electrophoresis was done using 1× running buffer for two to four hours at 100 V.

2.4 Analysis of proteins by Coomassie Blue staining

After separation of proteins by SDS-PAGE (*see above*), gels were boiled for two minutes in Coomassie Brilliant Blue R-250 Staining Solution (*Bio-Rad, Munich*) and incubated for 10 minutes at room temperature. Then gels were fixed and washed three times in Coomassie Brilliant Blue R-250 De-staining Solution (*Bio-Rad, Munich*) for 10 minutes and put in distilled water overnight. Gels were dried using a Model 583 Gel DRYER (*Bio-Rad, Munich*) and scanned to obtain digital images.

2.5 Western blot analysis

For immunological identification of separated proteins, electrophoretic transfer of proteins on PROTRAN® Nitrocellulose Transfer Membrane (*Schleicher & Schuell, Dassel*) with a pore size of 0.2 µm was carried out. Therefore, a sandwich of Whatman filters (*Schleicher & Schuell, Dassel*), a gel, and a nitrocellulose membrane was assembled and soaked in 1× transfer buffer. The transfer was performed in a wet blot chamber (*Bio-Rad, Munich*) at 0.8 mA/cm^2 for one hour. Afterwards, membranes were incubated in 5 ml blocking solution for 30 minutes at room temperature on a rocking platform. Membranes were extensively washed three times in 10 ml TBST washing solution for 15 minutes before incubating them in primary antibody diluted in either blocking solution or TBST containing 5 % (*w/v*) bovine serum albumin (*New England Biolabs, Frankfurt am Main*) according to the MATERIALS section IV, 6. After overnight incubation at 4 °C, membranes were washed again and following application of diluted secondary antibody conjugated to horseradish peroxidase for one hour at room temperature. Unbound antibodies were washed away and detection of bound antibody complexes was enabled by chemoluminescence. To this end, ECL Western Blotting Substrate (*Pierce Biotechnology, Rockford, USA*) was used according to the manufacturer's protocol. Exposition time of Fuji Super RX Medical X-ray films (*Kisker-Biotech, Steinfurt*) was individually determined for each blot.

2.6 Enzyme linked immunosorbent assay

PolySorb™ 96-well plates (*Nunc, Langenselbold*) were coated overnight at 4 °C with 200 µl DPBS per well containing 300 ng purified carcinoembryonic antigen. The next day, antigen solution was discarded and wells washed three times with 200 µl PBST washing solution. To reduce background signals, 200 µl DPBS containing 2 % (*v/v*) fetal calf serum was added to each well for one hour at room temperature. Wells were washed again three times before adding duplicates of 200 µl cell culture supernatant diluted in PBST washing solution containing secreted $scFv_{CEA}$-Fc. Dilutions were individually determined according to expected protein yield. Following incubation for another hour at room temperature and three washing steps, bound $scFv_{CEA}$-Fc was detected with 200 µl anti-mouse-horseradish peroxidase antibody diluted 10000-fold in PBST. Therefore, 200 µl TMB substrate (*BD Biosciences, Heidelberg*) was prepared according to

the manufacturer's manual which develops a blue color in the presence of bound peroxidase-conjugates. The reaction was stopped with 50 µl 4 M H_2SO_4 and quantified through fluorometric measurement using a FluoroskanAsentFL (*Thermo-Scientific, Braunschweig*) set to a wavelength of 450 nm.

2.7 Immunofluorescence staining

Primary HBEC and lung squamous tumor cells were grown on poly-L-lysine coated coverslips for 24 hours. Therefore, coverslips were first sterilized in 70 % (*v/v*) ethanol and air dried before coating. Then, they were incubated in 50 µg/ml of a sterile aqueous poly-L-lysine solution for 1 hour at 37 °C and washed with sterile DPBS two times afterwards. Immunofluorescence staining was done in collaboration with Werner Franke's lab and Cäcilia Kuhn. Briefly, cells were fixed in methanol or paraformaldehyde solution (*Sigma-Aldrich, Taufk*irchen) depending on the cellular antigen. If required, a permeabilization step using a Triton X-100 solution was carried out (*Sigma-Aldrich, Taufkirchen*). Detection of cellular markers was performed with respective primary antibodies and subsequent labeling using fluorescently conjugated secondary antibodies. Images and statistics were provided by Cäcilia Kuhn.

2.8 Immobilized metal affinity chromatography (*IMAC*)

Cells stably expressing and secreting recombinant $scFv_{CEA}$-Fc single-chain antibodies were expanded to twenty dishes in normal cell culture medium. Upon reaching 60-70 % confluence, growth medium was replaced by OptiMEM (*Invitrogen, Karlsruhe*) without serum. Cell culture supernatants were replaced every three days and cellular debris removed by centrifugation at 225 g for 5 minutes. After addition of 0.01 % (*v/v*) NaN_3, supernatants were stored at 4 °C up to two weeks. Then, supernatants were pooled and soluble protein precipitated by gradually adding ammonium sulfate to a final concentration of 60 % (*w/v*). Precipitates were collected by centrifugation at 3080 g for 30 minutes and 4 °C and pellets dissolved in 20 ml ice-cold DPBS. His-tagged $scFv_{CEA}$-Fc was isolated applying a modified IMAC protocol. Therefore, 2.5 ml Ni-NTA beads were equilibrated in 10 ml IMAC equilibration buffer, centrifuged at 225 g, and supernatant aspirated. The equilibrated beads were added to the protein solution and

incubated on a rotor for 30 minutes at room temperature. Afterwards, beads were recovered again by centrifugation and washed three times in 50 ml ice-cold IMAC washing buffer. Bound $scFv_{CEA}$-Fc was eluted from the beads with 10 ml IMAC elution buffer and dialyzed overnight against DPBS at 4 °C using Slide-A-Lyzer® Dialysis Cassettes (*Pierce Biotechnology, Rockford, USA*) with a 10000 molecular weight cut off (*MWCO*). The next day, protein samples were concentrated using VivaSpin columns (*Sartorius, Göttingen*) with a 10000 MWCO. Concentrated samples stored at 4 °C for immediate use or at -20 °C for long term storage. Quality and purity was checked by Coomassie Blue staining (*see chapter V, 2.4*).

2.9 Luciferase reporter gene assay

For the determination of luciferase activity, the Luciferase Assay System (*Promega, Madison USA*) was utilized as described by the manufacturer. Cells were washed once with DPBS and lysed in 200 µl Reporter Lysis buffer. After incubation for at least 30 minutes at -80 °C, lysates were thawed at room temperate. For each sample, 50 µl cell lysate was mixed with 50 µl Luciferase Assay substrate and immediately measured in a FluoroskanAsentFL (*Thermo-Scientific, Braunschweig*). Cells devoid for luciferase expression were used as negative controls to determine nonspecific background.

3 Cell culture techniques

All cells were kept in a Steri-Cult 200 incubator at 37 °C with 5 % CO_2 and a humidified atmosphere. Respective growth media were prepared as described in the MATERIALS section IV, 3.2 and stored at 4 °C. Media were pre-warmed to 37 °C in a water bath before use. Cell lines A549, C8161, HeLa, HEK293 and derivatives, LS174T, Mel624, RAW264.7, SK-MEL-28, SK-MES-1, SKOV-3, and SW900 were cultivated in DMEM-10 %. The cell lines and low passage melanoma cells A375M, Colo-829, Mel888, pMel A, pMel A2, and pMel L were maintained in RPMI-10 %. For primary melanomas medium was additionally supplemented with 10 mM HEPES, 0.1 % (v/v) amphotericin B (*Sigma-Aldrich, Taufkirchen*) and 0.2 % (v/v) gentamicin. HFFs were kept in MEM-10 % medium. Primary HBEC as well as PHK cells were cultivated in complete Airway Epithelial Cell Growth Medium and Keratinocyte Growth Medium 2, respectively. For

establishing and maintaining stable cell lines, 50-300 µg/ml Zeocin™ was used as a relevant selection antibiotic.

3.1 Sub-cultivation of adherent cell lines and primary cells

Upon reaching 60-80 % confluence, cells were washed with 15 ml DPBS and detached by trypsinization with 100 µl/cm² 0.05 % (*w/v*) trypsin-EDTA (*Invitrogen, Karlsruhe*) at room temperature. Enzyme activity was stopped by adding a corresponding amount of medium containing 10 % (*v/v*) fetal calf serum. For primary HBEC cells, Trypsin Neutralizing Solution (*Promocell, Heidelberg*) was used instead of serum. Cells were collected by centrifugation at 1500 g for 3 minutes, the supernatant discarded, and pellets resuspended in the respective growth medium. Suspension was split in a ratio of 1:3 to 1:10 depending on the individual cell line or used for further experiments

3.2 Sub-cultivation of permanent cell lines for microarray experiments

Melanoma cells SK-MEL-28 and Mel624 as well as lung squamous carcinoma cell lines SW900 and SK-MES-1 with similar, low passage numbers were slowly adapted to low serum conditions. Therefore, fetal calf serum content was gradually reduced by mixing DMEM-10 % with rising volumes of Melanocyte Growth Medium or Airway Epithelial Cell Growth Medium, respectively. Cells were passaged at least once before further reduction of serum. Finally, cells were sub-cultivated in a mixture of one volume DMEM-10 % and three volumes of Melanocyte Growth Medium or Airway Epithelial Cell Growth Medium, respectively (*referred to as "microarray growth medium" herein*). Frozen aliquots of adapted cells were made as described below.

3.3 Cryopreservation and resuscitation of frozen cells

For long term storage, cells were collected by trypsinization, counted (*see below*) and centrifuged at 225 g for 3 minutes. Pellets were resuspended in ice-cold fetal calf serum with 10 % (*v/v*) dimethyl sulfoxide at a concentration of 1×10^6/ml cells and transferred to Cryovials® (*Nunc, Langenselbold*). A special freezing medium Cryo-SFM (*Promocell, Heidelberg*) without serum was used for primary HBEC cells. Then, aliquots were put in a container allowing freezing

at constant rate of approximately -1 °C per minute and kept at -80 °C overnight before storing them at -196 °C in liquid nitrogen. To re-cultivate frozen cell line stocks, samples were quickly thawed in a water bath at 37 °C and washed once with 10 ml of the relevant growth medium before seeding cells at an appropriate density.

3.4 Cell number quantification

To determine viable cell count, an equal amount of cell suspension was mixed with trypane blue solution (*Sigma-Aldrich, Taufkirchen*) and filled into a Neubauer counting chamber. Cell number was calculated using the following formula:

$$\text{number of cells/ml} = \text{number of cells in large squares} \times \text{dilution factor} \times 10^4$$

3.5 Transfection of nucleic acids into human cells

3.5.1 Plasmid DNA

Twenty four hours prior transfection, 5-7.5×10^4 cells (*depending on the cell line*) were seeded out in 0.5 ml of their respective growth medium in 24 well plates. Cells reached approximately 60-80 % confluence on the next day and were transiently transfected in triplicates using Lipofectamine™ and PLUS™ reagent (*both Invitrogen, Karlsruhe*) as suggested by the manufacturer. Briefly, for every sample 0.5 µg DNA was mixed with 100 µl OptiMEM® containing 0.5 µl PLUS™ reagent and incubated at room temperature for 15 minutes. Then, 2.5 µl Lipofectamine™ was added and samples mixed by vortexing. Following another 30 minutes incubation time at room temperature, transfection mix was added directly to the cells. Medium was replaced after 24 hours.

3.5.2 Small interfering RNAs

In order to knock down expression of single genes, 1.6-3×10^5 cells (*depending on the cell line*) were seeded in 1 ml of their respective growth medium in 12 well plates shortly before transfection. Transfection mix was set up by diluting 225 ng of a relevant siRNA in 100 µl

OptiMEM® medium containing 3 µl HiPerFect (*Qiagen, Hilden*). Samples were mixed by vortexing and incubated for 10 minutes at room temperature before adding them to the cells in triplicates. Transfection was repeated after 14-16 hours and knockdown efficacy verified by qPCR analysis (*see section V, 1.9.2*) 72 hours post transfection. Knockdown cells were used for infection assays 24-48 hours post transfection as stated in the respective experiments.

3.6 Generation of $scFv_{CEA}$-Fc expression clones

To obtain HEK293T clones stably expressing soluble recombinant single-chain antibody, cells were transfected as described above with pSecTag-HisA-$scFv_{CEA}$-Fc encoding a resistance marker against Zeocin™. Following transfection, cells were split 24 hours later and diluted 1:10-1:80 in growth medium containing 300 µg/ml Zeocin™. Colony formation of resistant cells could be observed after 7-14 days whereas untransfected controls died within 3-5 days. Medium was frequently replaced with freshly diluted antibiotics. Stable clones were further cultivated and analyzed for protein expression by Western blot analysis (*see chapter V, 2.5*).

3.7 Fluorescence activated cell sorting (*FACS*)

All samples were analyzed on a FACScan machine (*BD Biosciences, Heidelberg*). For green fluorescence, such as CFSE or green fluorescent protein expression, the fluorescent channel FL1 was used. For red fluorescence, like propidium iodide or phycoerythrin staining, channel FL2 was applied. Appropriate compensation if required was set up for each experiment individually and data was recorded for at least 10000 events. Data was analyzed using FCS Express Version 3 software.

3.7.1 Viability staining

Up to 10^6 cells were harvested by trypsinization, washed twice in FACS washing buffer and collected by centrifugation at 225 g for 3 minutes. For staining of dead cells, pellets were resuspended in 100 µl DPBS containing a final concentration of 50 µg/ml propidium iodide. After incubation at room temperature for 10 minutes, cells were further diluted in 200 µl FACS buffer and analyzed immediately.

3.7.2 Cell cycle analysis

Cell pellets consisting of 10^6 living cells were fixed in 1 ml ice-cold 70 % (*v/v*) ethanol while vortexing to reduce cell clumping. Samples were incubated at 4 °C for at least one hour or overnight. To stain for cellular DNA content, fixed cells were washed twice in DPBS and pelleted at 225 g for 3 minutes before dissolving the pellets in 100 µl PI staining buffer. Following incubation for 30 minutes at room temperature, 200 µl FACS buffer was added to the cells which were analyzed immediately.

3.7.3 Staining of surface antigens

To stain for proteins expressed on the cell surface, cells were harvested by trypsinization and rinsed once with DBPS. After centrifugation at 225 g for 3 minutes, pellets were resuspended in 50 µl FACS buffer containing a diluted primary antibody (*see section IV, 6*). Staining was carried out for 30 minutes at room temperature and cells rinsed again in FACS washing buffer to remove unbound antibodies. Subsequently, cells were dissolved in 50 µl FACS buffer with a diluted secondary antibody conjugated to a relevant fluorochrome. Before acquisition on a FACS machine, samples were washed again in FACS washing buffer and diluted in 300 µl FACS buffer.

3.7.4 Antibody-dependent cellular phagocytosis

Shortly before incubation with mouse macrophages RAW264.7, 5×10^6/ml target cells were labeled in 1.5 nM CFSE/DPBS staining solution (*Sigma-Aldrich, Taufkirchen*) for 10 minutes in the dark at room temperature. Afterwards, an equal amount of ice-cold fetal calf serum was added. Then, cells were washed two times in ice-cold DPBS and centrifuged at 225 g for 3 minutes. Labeled targets were then either boiled at 56 °C to induce necrosis or added directly to the macrophages in triplicate wells of a flat bottom 96 well plate. The final volume was 200 µl and contained 5×10^4 targets with a number of 3 or 5 times more effector cells. In addition, medium contained serially diluted antibodies or relevant isotype controls as stated in the experiment. Samples were incubated at 37 °C or 4 °C for 24 hours, pooled, and subsequently stained for the murine macrophage specific marker CD11b. Afterwards, the double positive CD11b/CFSE

population, representing macrophages with phagocytosed tumor cells, was quantified by FACS analysis. Percentage of phagocytosis was calculated according to the formula:

$$\% \text{ phagocytosis} = \left(\frac{\% \text{ double positives}}{\% \text{ double positives} + \% \text{ free targets}} \right) \times 100$$

4 Recombinant human adenovirus methods

Most experiments with HAdVs were performed in DMEM containing only 2 % (*v/v*) fetal calf serum or in microarray growth medium as described in paragraph V, 3.2.

4.1 Production and purification of viral particles

A total amount of 6 µg adenoviral genomes were linearized through PacI digest for 5 hours or overnight at 37 °C. Digested DNA was precipitated by first adding a final concentration of 800 mM lithium chloride and then 2.5× volumes of 100 % ethanol. Precipitates were recovered by centrifugation at 17000 g for 30 minutes and resuspended in 20 µl bi-distilled water. After analyzing linear adenoviral DNA by gel electrophoresis (*see section V, 1.1*), a T25 flask of relevant production cell line was transfected using Lipofectamine™ (*see chapter V, 3.5.1*). For the generation of replication-competent adenoviruses, A549 cells were used while replication-deficient adenoviruses were produced in E1-complementing HEK293 cells. Upon complete cell lysis on day 10 to day 12, infected cells were collected by centrifugation at 225 g for 15 minutes. Afterwards, cells were lysed in 5 ml growth medium by three freeze thaw cycles at -80 °C and 37 °C and cellular debris removed by centrifugation at 3080 g for 10 minutes and 4 °C. Infectious supernatants were amplified by three subsequent rounds of infection and virus recovery from rising cell quantities. When complete lysis during the last amplification round was seen, viruses were purified via cesium chloride density gradients. Therefore, supernatants were transferred onto gradients composed of 3 ml cesium chloride solution 1.41 overlaid with 5 ml cesium chloride 1.27 in sterile ultracentrifugation tubes (*Herolab, Wiesloch*). Following ultracentrifugation for 2 h at ~125000 g and 4 °C resulting in separation of complete and empty virus particle bands, viruses were aspirated using a syringe equipped with a 21 G needle. Virus

suspension was buffered with 5 mM HEPES solution and purified by a second round of cesium chloride gradient density ultracentrifugation overnight at ~125000 g and 4 °C. The next day, viruses were aspirated again and desalted via PD10 columns (*Amersham, Munich*) in a final volume of 2.5 ml DPBS according to the manufacturer's instructions. Pure viruses were eluted in fractions of 0.5 ml DPBS. Fractions two and three containing the highest virus yield were combined and supplemented with 10 % (*v/v*) glycerol. Virus stock was divided in aliquots of 50 µl each and put at -80 °C for long term storage. Each virus stock was analyzed by PCR (*see section V, 1.9.1*) to verify introduced modifications and rule out contaminations with wild type adenovirus.

4.2 Determination of viral particle and infectious particle concentrations

4.2.1 Physical virus titer

Virus stocks were diluted in VL buffer with varying concentrations and lysed by incubation at 56 °C for 10 minutes. For each sample, optical absorption of DNA was determined at 260 nm wavelength using a NanoDrop ND-1000 UV/VIS spectrophotometer (*Peqlab, Erlangen*). Viral particle concentration was determined accordingly [256,257]:

$$\text{virus particles/ml} = OD_{260} \times \text{viral dilution} \times 1.1\times10^{12}$$

4.2.2 Tissue culture infectious dose 50 (*$TCID_{50}$*)-assay

For measuring infectious particle amounts, 1×10^4 HEK293 cells per well were seeded in 96-well plates in a total volume of 100 µl DMEM-2 %. The next day, adenovirus stocks were tenfold serially diluted in DMEM-2 % up to 10-12 and used for infection of ten replicates per dilution by adding 100 µl virus suspension to each well. Uninfected cells served as control and assays were done in duplicates for each virus stock. After 12 days incubation, cytopathic effects were determined by light microscopy and wells were evaluated as positive if one or more plaques were visible. The virus titer was calculated according to Kärber's statistical method [258]:

$$TCID_{50}/\text{ml} = 10^{1 + 1 \times (\text{sum of positive wells}-0.5)}$$

Ratios between physical and infectious virus titers were 5-100 depending on the virus type and preparation.

4.3 Infection of human cell lines

4.3.1 For cytotoxicity assays using crystal violet staining

To determine virus mediated cytotoxicity, 3×10^4 cells/well were seeded in 48 well plates. The following day, cells were infected in 200 µl DMEM-2 % containing tenfold serially diluted adenovirus with concentrations from 0.001-100 $TCID_{50}$/cell. Mock infected cells or infection with serially diluted replication-incompetent viruses served as negative controls. The next day, 500 µl growth medium was added and cells incubated until cytopathic effects could be observed in wells containing low viral inoculums. Cell lysis was documented by aspirating the cell culture supernatants and staining of live cells by addition of 100 µl crystal violet solution for 30 minutes at room temperature. Afterwards, plates were rinsed twice in water to remove excessive dye, air-dried, and scanned to obtain digital images.

4.3.2 For determination of transduction rates in living cells

Infection levels in different human cell lines were normalized through reporter gene quantification. Therefore, 1×10^6 cells were thawed in a water bath at 37 °C for one minute (*see section V, 3.3*), transferred to a 15 ml falcon tube, and washed once in their respective microarray growth medium. Afterwards, ~15800 cells/cm^2 were seeded in pre-warmed and CO_2 equilibrated microarray growth media into 24 well plates. The next day, growth medium was exchanged and cells incubated for another day. After two days, various $TCID_{50}$ titers of HAdV-5 CMV-gfp were serially diluted in 500 µl microarray growth medium and incubated on the cells for one hour at 37 °C. Subsequently, medium was aspirated and replaced by 1 ml fresh microarray growth medium. Cells were harvested 48 hours post infection by trypsinization and transgene levels in living cells measured by flow cytometry (*see paragraph V, 3.7.1*). Similar experiments including A549, Mel888, or Colo-829 were carried out with permanently cultured infected in DMEM-2 %. Transduction rate normalization of cells devoid for CAR receptor expression like A375M, C8161, pMel A, pMel A2, or pMel L was done with wild type HAdV-5/3

and microscopic analysis of cytopathic effects over several days. Titers for high transduction efficacy were deduced from Wells containing over 80 % of floating cells.

4.3.3 For microarray experiments, viral gene expression, and replication assays

Cells were plated as described above and infected 48 hours later with equivalent titers of HAdV-5 wild type diluted in microarray growth medium. For microarray experiments samples were upscaled accordingly to 6 well plates. Thereafter, total RNA and genomic DNA was harvested at relevant time points as indicated in the respective experiments and purified (*see sections V, 1.7.4 and V, 1.7.3*). Samples were analyzed for viral gene expression, genome replication, and cellular gene expression by quantitative real time PCR (*see chapter V, 1.9.2*).

4.3.4 For quantification of infectious progeny particles

Experiments were carried out in triplicates but were identical as in chapter V, 4.3.2 using equivalent titers of HAdV-5 wild type diluted in microarray growth medium. In addition, virus inoculum was removed one hour post infection and cells washed twice with DPBS. Supernatants containing free adenovirus particles were harvested at given time points and cellular debris removed by centrifugation at 225 g for 5 minutes. Cell free supernatants were transferred to new reaction tubes and stored at -80 °C. Meanwhile, cell pellets were scraped off in 1 ml DPBS and subjected to three freeze thaw cycles. Cellular debris was removed by centrifugation and supernatants containing intracellular viral particles were stored at -80 °C until further use. Infectious viral particles were quantified according to section V, 4.2.2.

4.3.5 For analyses of the virus life cycle in presence of temozolomide

Similarly as in the previous paragraphs V, 4.3.3 and V, 4.3.4, experiments were performed using cells from permanent cultures. One day after seeding, cells were infected with either wild type HAdV-5 or HAdV-5/3 Δ24 T2A-luc at 1 $TCID_{50}$/cell for one hour at 37 °C. Infection medium was replaced afterwards by the respective growth medium supplemented with 650 µM (*SK-MEL-28*) or 312 µM (*Mel624*) temozolomide. At given time points, samples were harvested for qPCR

(*RNA and DNA*), luciferase assays, or for quantification of progeny virions in supernatants and cell pellets.

4.3.6 After DNA plasmid or siRNA transfection

SK-MEL-28 and Mel624 were transfected according to chapters V, 3.5.1 or V, 3.5.2 with the relevant DNA plasmids or siRNAs. After sixteen hours incubation for DNA plasmid transfections or 24 hours for siRNA transfections, cells were infected with HAdV-5 at 1 $TCID_{50}$/cell diluted in DMEM-2 % for one hour at 37 °C. Medium was replaced thereafter and infection incubated up to 72 hours. Samples of total cellular DNA or RNA were harvested at relevant time points as stated in the respective experiment, purified as described in V, 1.7.3 or V, 1.7.4, analyzed by qPCR for expression of adenoviral and cellular genes.

For analyzing S-phase entry, various cell lines and primary HBEC were transfected with either a SV40 promoter or E2F promoter/luciferase construct for 24 hours. Then, cells were infected with individual $TCID_{50}$ titers of HAdV-5 or HAdV-5 CMV-gfp resulting in 80-90 % infection of living cells. Therefore virus was diluted in the respective growth medium containing no fetal calf serum (*HBEC*) or only low amounts. Inoculums were removed after one hour at 37 °C and cells grown in their normal growth media for twenty hours before luciferase expression was quantified (*refer to V, 2.9*).

4.3.7 For expression of recombinant $scFv_{CEA}$-Fc antibodies

One day before infection, 1×10^5 cells/well were seeded into 12 well plates. The following day, cells were infected with 1 $TCID_{50}$ per cell of a relevant $scFv_{CEA}$-Fc encoding adenovirus diluted in DMEM-2 %. Alternatively, similar adenoviruses encoding a firefly luciferase transgene were used as controls. After one hour incubation at 37 °C, medium was removed by aspiration and replaced by 2 ml of the normal growth medium. To block DNA replication of adenoviruses, cells were treated with either 25 µg/ml AraC (*Sigma-Aldrich, Taufkirchen*) or a correspondent vehicle control every twelve to fourteen hours. Supernatants or cell pellets were harvested at given time points and transgene levels assessed by ELISA (*see paragraph V, 2.6*) or by luciferase reporter gene assays (*see paragraph V, 2.9*).

VI REFERENCES

[1] The World Health Organization. Cancer Fact Sheet. 2009.
Ref Type: Online Source

[2] J. H. Breasted, Tumorous ulcers in the breast,perhaps resulting from injury.In:The Edwin Smith Surgical Papyrus., University of Chicago Press, (1930) 363-369.

[3] M. Lederman, The early history of radiotherapy: 1895-1939, Int. J. Radiat. Oncol. Biol. Phys., 7 (1981) 639-648.

[4] L. S. Goodman, M. M. Wintrobe, W. Dameshek, M. J. Goodman, A. Gilman, and M. T. McLennan, Landmark article Sept. 21, 1946: Nitrogen mustard therapy. Use of methyl-bis(beta-chloroethyl)amine hydrochloride and tris(beta-chloroethyl)amine hydrochloride for Hodgkin's disease, lymphosarcoma, leukemia and certain allied and miscellaneous disorders. By Louis S. Goodman, Maxwell M. Wintrobe, William Dameshek, Morton J. Goodman, Alfred Gilman and Margaret T. McLennan, JAMA, 251 (1984).

[5] R. J. Papac, Origins of cancer therapy, Yale J. Biol. Med., 74 (2001) 391-398.

[6] B. M. Fendly, M. Winget, R. M. Hudziak, M. T. Lipari, M. A. Napier, and A. Ullrich, Characterization of murine monoclonal antibodies reactive to either the human epidermal growth factor receptor or HER2/neu gene product, Cancer Res., 50 (1990) 1550-1558.

[7] R. Nahta and F. J. Esteva, Herceptin: mechanisms of action and resistance, Cancer Lett., 232 (2006) 123-138.

[8] R. Waehler, S. J. Russell, and D. T. Curiel, Engineering targeted viral vectors for gene therapy, Nat. Rev. Genet., 8 (2007) 573-587.

[9] D. E. Dorer and D. M. Nettelbeck, Targeting cancer by transcriptional control in cancer gene therapy and viral oncolysis, Adv Drug Deliv Rev, 61 (2009).

[10] S. Pearson, H. Jia, and K. Kandachi, China approves first gene therapy, Nat. Biotechnol., 22 (2004) 3-4.

[11] J. K. Raty, J. T. Pikkarainen, T. Wirth, and S. Yla-Herttuala, Gene therapy: the first approved gene-based medicines, molecular mechanisms and clinical indications, Curr. Mol. Pharmacol., 1 (2008) 13-23.

[12] D. P. Lane, Cancer. p53, guardian of the genome, Nature, 358 (1992) 15-16.

[13] A. J. Levine and M. Oren, The first 30 years of p53: growing ever more complex, Nat. Rev. Cancer, 9 (2009) 749-758.

[14] N. Senzer and J. Nemunaitis, A review of contusugene ladenovec (Advexin) p53 therapy, Curr. Opin. Mol. Ther., 11 (2009) 54-61.

[15] J. Guo and H. Xin, Chinese gene therapy. Splicing out the West?, Science, 314 (2006) 1232-1235.

[16] J. Y. Seol, K. H. Park, C. I. Hwang, W. Y. Park, C. G. Yoo, Y. W. Kim, S. K. Han, Y. S. Shim, and C. T. Lee, Adenovirus-TRAIL can overcome TRAIL resistance and induce a bystander effect, Cancer Gene Ther., 10 (2003) 540-548.

[17] G. Dranoff, E. Jaffee, A. Lazenby, P. Golumbek, H. Levitsky, K. Brose, V. Jackson, H. Hamada, D. Pardoll, and R. C. Mulligan, Vaccination with irradiated tumor cells engineered to secrete murine granulocyte-macrophage colony-stimulating factor stimulates potent, specific, and long-lasting anti-tumor immunity, Proc. Natl. Acad. Sci. U. S. A, 90 (1993) 3539-3543.

[18] C. Y. Li, Q. Huang, and H. F. Kung, Cytokine and immuno-gene therapy for solid tumors, Cell Mol. Immunol., 2 (2005) 81-91.

[19] E. Pennisi, Training viruses to attack cancers, Science, 282 (1998) 1244-1246.

[20] E. Kelly and S. J. Russell, History of oncolytic viruses: genesis to genetic engineering, Mol Ther, 15 (2007).

[21] K. A. Parato, D. Senger, P. A. Forsyth, and J. C. Bell, Recent progress in the battle between oncolytic viruses and tumours, Nat. Rev. Cancer, 5 (2005) 965-976.

[22] R. Cattaneo, T. Miest, E. V. Shashkova, and M. A. Barry, Reprogrammed viruses as cancer therapeutics: targeted, armed and shielded, Nat. Rev. Microbiol., 6 (2008) 529-540.

[23] S. J. Russell, RNA viruses as virotherapy agents, Cancer Gene Ther., 9 (2002) 961-966.

[24] W. P. Rowe, R. J. Huebner, L. K. Gilmore, R. H. Parrott, and T. G. Ward, Isolation of a cytopathogenic agent from human adenoids undergoing spontaneous degeneration in tissue culture, Proc Soc Exp Biol Med, 84 (1953).

[25] M. R. HILLEMAN and J. H. WERNER, Recovery of new agent from patients with acute respiratory illness, Proc. Soc. Exp. Biol. Med., 85 (1954) 183-188.

[26] Harrach B. Adenoviruses: General Features, Encyclopedia of Virology. 2008.
Ref Type: Edited Book

[27] K. Hall, M. E. Blair Zajdel, and G. E. Blair, Unity and diversity in the human adenoviruses: exploiting alternative entry pathways for gene therapy, Biochem. J., 431 (2010) 321-336.

[28] M. Tebruegge and N. Curtis, Adenovirus infection in the immunocompromised host, Adv. Exp. Med. Biol., 659 (2010) 153-174.

[29] Y. YABE, J. J. TRENTIN, and G. TAYLOR, Cancer induction in hamsters by human type 12 adenovirus. Effect of age and of virus dose, Proc. Soc. Exp. Biol. Med., 111 (1962) 343-344.

[30] R. J. Huebner, W. P. Rowe, and W. T. LANE, Oncogenic effects in hamsters of human adenovirus types 12 and 18, Proc. Natl. Acad. Sci. U. S. A, 48 (1962) 2051-2058.

[31] W. Doerfler, The fate of the DNA of adenovirus type 12 in baby hamster kidney cells, Proc. Natl. Acad. Sci. U. S. A, 60 (1968) 636-643.

[32] W. Doerfler, Integration of the deoxyribonucleic acid of adenovirus type 12 into the deoxyribonucleic acid of baby hamster kidney cells, J. Virol., 6 (1970) 652-666.

[33] D. Sutter, M. Westphal, and W. Doerfler, Patterns of integration of viral DNA sequences in the genomes of adenovirus type 12-transformed hamster cells, Cell, 14 (1978) 569-585.

[34] R. M. McAllister, R. V. Gilden, and M. Green, Adenoviruses in human cancer, Lancet, 1 (1972) 831-833.

[35] S. L. Hu and J. L. Manley, DNA sequence required for initiation of transcription in vitro from the major late promoter of adenovirus 2, Proc. Natl. Acad. Sci. U. S. A, 78 (1981) 820-824.

[36] L. T. Chow, R. E. Gelinas, T. R. Broker, and R. J. Roberts, An amazing sequence arrangement at the 5' ends of adenovirus 2 messenger RNA, Cell, 12 (1977) 1-8.

[37] J. A. DeCaprio, How the Rb tumor suppressor structure and function was revealed by the study of Adenovirus and SV40, Virology, 384 (2009) 274-284.

[38] G. R. Nemerow, L. Pache, V. Reddy, and P. L. Stewart, Insights into adenovirus host cell interactions from structural studies, Virology, 384 (2009) 380-388.

[39] W. C. Russell, Adenoviruses: update on structure and function, J Gen Virol, 90 (2009).

[40] J. Vellinga, S. Van der Heijdt, and R. C. Hoeben, The adenovirus capsid: major progress in minor proteins, J. Gen. Virol., 86 (2005) 1581-1588.

[41] C. Stephens and E. Harlow, Differential splicing yields novel adenovirus 5 E1A mRNAs that encode 30 kd and 35 kd proteins, EMBO J., 6 (1987) 2027-2035.

[42] N. Jones and T. Shenk, An adenovirus type 5 early gene function regulates expression of other early viral genes, Proc. Natl. Acad. Sci. U. S. A, 76 (1979) 3665-3669.

[43] J. W. Lillie, M. Green, and M. R. Green, An adenovirus E1a protein region required for transformation and transcriptional repression, Cell, 46 (1986) 1043-1051.

[44] A. J. Berk, Recent lessons in gene expression, cell cycle control, and cell biology from adenovirus, Oncogene, 24 (2005).

[45] W. Zhang and M. J. Imperiale, Requirement of the adenovirus IVa2 protein for virus assembly, J Virol, 77 (2003).

[46] J. Kitajewski, R. J. Schneider, B. Safer, S. M. Munemitsu, C. E. Samuel, B. Thimmappaya, and T. Shenk, Adenovirus VAI RNA antagonizes the antiviral action of interferon by preventing activation of the interferon-induced eIF-2 alpha kinase, Cell, 45 (1986) 195-200.

[47] M. D. Rosa, E. Gottlieb, M. R. Lerner, and J. A. Steitz, Striking similarities are exhibited by two small Epstein-Barr virus-encoded ribonucleic acids and the adenovirus-associated ribonucleic acids VAI and VAII, Mol. Cell Biol., 1 (1981) 785-796.

[48] B. W. Hayes, G. C. Telling, M. M. Myat, J. F. Williams, and S. J. Flint, The adenovirus L4 100-kilodalton protein is necessary for efficient translation of viral late mRNA species, J. Virol., 64 (1990) 2732-2742.

[49] C. S. Young, The structure and function of the adenovirus major late promoter, Curr. Top. Microbiol. Immunol., 272 (2003) 213-249.

[50] M. C. Dechecchi, P. Melotti, A. Bonizzato, M. Santacatterina, M. Chilosi, and G. Cabrini, Heparan sulfate glycosaminoglycans are receptors sufficient to mediate the initial binding of adenovirus types 2 and 5, J Virol, 75 (2001).

[51] C. G. Nicol, D. Graham, W. H. Miller, S. J. White, T. A. Smith, S. A. Nicklin, S. C. Stevenson, and A. H. Baker, Effect of adenovirus serotype 5 fiber and penton modifications on in vivo tropism in rats, Mol Ther, 10 (2004).

[52] R. R. Vives, H. Lortat-Jacob, J. Chroboczek, and P. Fender, Heparan sulfate proteoglycan mediates the selective attachment and internalization of serotype 3 human adenovirus dodecahedron, Virology, 321 (2004) 332-340.

[53] S. Tuve, H. Wang, J. D. Jacobs, R. C. Yumul, D. F. Smith, and A. Lieber, Role of cellular heparan sulfate proteoglycans in infection of human adenovirus serotype 3 and 35, PLoS. Pathog., 4 (2008) e1000189.

[54] E. Gout, G. Schoehn, D. Fenel, H. Lortat-Jacob, and P. Fender, The adenovirus type 3 dodecahedron's RGD loop comprises an HSPG binding site that influences integrin binding, J. Biomed. Biotechnol., 2010 (2010) 541939.

[55] J. M. Bergelson, J. A. Cunningham, G. Droguett, E. A. Kurt-Jones, A. Krithivas, J. S. Hong, M. S. Horwitz, R. L. Crowell, and R. W. Finberg, Isolation of a common receptor for Coxsackie B viruses and adenoviruses 2 and 5, Science, 275 (1997).

[56] P. W. Roelvink, A. Lizonova, J. G. Lee, Y. Li, J. M. Bergelson, R. W. Finberg, D. E. Brough, I. Kovesdi, and T. J. Wickham, The coxsackievirus-adenovirus receptor protein can function as a cellular attachment protein for adenovirus serotypes from subgroups A, C, D, E, and F, J. Virol., 72 (1998) 7909-7915.

[57] J. Howitt, C. W. Anderson, and P. Freimuth, Adenovirus interaction with its cellular receptor CAR, Curr Top Microbiol Immunol, 272 (2003).

[58] A. Gaggar, D. M. Shayakhmetov, and A. Lieber, CD46 is a cellular receptor for group B adenoviruses, Nat. Med., 9 (2003) 1408-1412.

[59] H. Wang, Z. Y. Li, Y. Liu, J. Persson, I. Beyer, T. Moller, D. Koyuncu, M. R. Drescher, R. Strauss, X. B. Zhang, J. K. Wahl, III, N. Urban, C. Drescher, A. Hemminki, P. Fender, and A. Lieber, Desmoglein 2 is a receptor for adenovirus serotypes 3, 7, 11 and 14, Nat. Med., 17 (2011) 96-104.

[60] T. J. Wickham, P. Mathias, D. A. Cheresh, and G. R. Nemerow, Integrins alpha v beta 3 and alpha v beta 5 promote adenovirus internalization but not virus attachment, Cell, 73 (1993).

[61] B. Albinsson and A. H. Kidd, Adenovirus type 41 lacks an RGD alpha(v)-integrin binding motif on the penton base and undergoes delayed uptake in A549 cells, Virus Res., 64 (1999) 125-136.

[62] U. F. Greber, M. Willetts, P. Webster, and A. Helenius, Stepwise dismantling of adenovirus 2 during entry into cells, Cell, 75 (1993) 477-486.

[63] O. Meier and U. F. Greber, Adenovirus endocytosis, J Gene Med, 5 (2003).

[64] D. J. FitzGerald, R. Padmanabhan, I. Pastan, and M. C. Willingham, Adenovirus-induced release of epidermal growth factor and pseudomonas toxin into the cytosol of KB cells during receptor-mediated endocytosis, Cell, 32 (1983) 607-617.

[65] C. M. Wiethoff, H. Wodrich, L. Gerace, and G. R. Nemerow, Adenovirus protein VI mediates membrane disruption following capsid disassembly, J. Virol., 79 (2005) 1992-2000.

[66] P. L. Leopold and R. G. Crystal, Intracellular trafficking of adenovirus: many means to many ends, Adv. Drug Deliv. Rev., 59 (2007) 810-821.

[67] L. C. Trotman, N. Mosberger, M. Fornerod, R. P. Stidwill, and U. F. Greber, Import of adenovirus DNA involves the nuclear pore complex receptor CAN/Nup214 and histone H1, Nat. Cell Biol., 3 (2001) 1092-1100.

[68] Z. Arany, W. R. Sellers, D. M. Livingston, and R. Eckner, E1A-associated p300 and CREB-associated CBP belong to a conserved family of coactivators, Cell, 77 (1994) 799-800.

[69] S. M. Frisch and J. S. Mymryk, Adenovirus-5 E1A: paradox and paradigm, Nat. Rev. Mol. Cell Biol., 3 (2002) 441-452.

[70] H. M. Chan, M. Krstic-Demonacos, L. Smith, C. Demonacos, and N. B. La Thangue, Acetylation control of the retinoblastoma tumour-suppressor protein, Nat. Cell Biol., 3 (2001) 667-674.

[71] H. H. Wong, N. R. Lemoine, and Y. Wang, Oncolytic Viruses for Cancer Therapy: Overcoming the Obstacles, Viruses., 2 (2010) 78-106.

[72] J. M. Trimarchi and J. A. Lees, Sibling rivalry in the E2F family, Nat. Rev. Mol. Cell Biol., 3 (2002) 11-20.

[73] S. van den Heuvel and N. J. Dyson, Conserved functions of the pRB and E2F families, Nat. Rev. Mol. Cell Biol., 9 (2008) 713-724.

[74] D. Spitkovsky, P. Jansen-Durr, E. Karsenti, and I. Hoffman, S-phase induction by adenovirus E1A requires activation of cdc25a tyrosine phosphatase, Oncogene, 12 (1996) 2549-2554.

[75] E. Vigo, H. Muller, E. Prosperini, G. Hateboer, P. Cartwright, M. C. Moroni, and K. Helin, CDC25A phosphatase is a target of E2F and is required for efficient E2F-induced S phase, Mol. Cell Biol., 19 (1999) 6379-6395.

[76] M. A. Ikeda and J. R. Nevins, Identification of distinct roles for separate E1A domains in disruption of E2F complexes, Mol. Cell Biol., 13 (1993) 7029-7035.

[77] A. R. Fattaey, E. Harlow, and K. Helin, Independent regions of adenovirus E1A are required for binding to and dissociation of E2F-protein complexes, Mol. Cell Biol., 13 (1993) 7267-7277.

[78] N. B. La Thangue and P. W. Rigby, An adenovirus E1A-like transcription factor is regulated during the differentiation of murine embryonal carcinoma stem cells, Cell, 49 (1987) 507-513.

[79] M. J. Imperiale, L. T. Feldman, and J. R. Nevins, Activation of gene expression by adenovirus and herpesvirus regulatory genes acting in trans and by a cis-acting adenovirus enhancer element, Cell, 35 (1983) 127-136.

[80] J. R. Nevins, P. Raychaudhuri, A. S. Yee, R. J. Rooney, I. Kovesdi, and R. Reichel, Transactivation by the adenovirus E1A gene, Biochem. Cell Biol., 66 (1988) 578-583.

[81] S. D. Neill, C. Hemstrom, A. Virtanen, and J. R. Nevins, An adenovirus E4 gene product trans-activates E2 transcription and stimulates stable E2F binding through a direct association with E2F, Proc. Natl. Acad. Sci. U. S. A, 87 (1990) 2008-2012.

[82] P. Sarnow, Y. S. Ho, J. Williams, and A. J. Levine, Adenovirus E1b-58kd tumor antigen and SV40 large tumor antigen are physically associated with the same 54 kd cellular protein in transformed cells, Cell, 28 (1982).

[83] T. Dobner, N. Horikoshi, S. Rubenwolf, and T. Shenk, Blockage by adenovirus E4orf6 of transcriptional activation by the p53 tumor suppressor, Science, 272 (1996) 1470-1473.

[84] M. Moore, N. Horikoshi, and T. Shenk, Oncogenic potential of the adenovirus E4orf6 protein, Proc. Natl. Acad. Sci. U. S. A, 93 (1996) 11295-11301.

[85] E. White, R. Cipriani, P. Sabbatini, and A. Denton, Adenovirus E1B 19-kilodalton protein overcomes the cytotoxicity of E1A proteins, J Virol, 65 (1991).

[86] S. K. Chiou, C. C. Tseng, L. Rao, and E. White, Functional complementation of the adenovirus E1B 19-kilodalton protein with Bcl-2 in the inhibition of apoptosis in infected cells, J Virol, 68 (1994).

[87] N. C. Elde, S. J. Child, A. P. Geballe, and H. S. Malik, Protein kinase R reveals an evolutionary model for defeating viral mimicry, Nature, 457 (2009) 485-489.

[88] B. Thimmappaya, C. Weinberger, R. J. Schneider, and T. Shenk, Adenovirus VAI RNA is required for efficient translation of viral mRNAs at late times after infection, Cell, 31 (1982) 543-551.

[89] H. G. Burgert and S. Kvist, An adenovirus type 2 glycoprotein blocks cell surface expression of human histocompatibility class I antigens, Cell, 41 (1985) 987-997.

[90] J. H. Cox, J. R. Bennink, and J. W. Yewdell, Retention of adenovirus E19 glycoprotein in the endoplasmic reticulum is essential to its ability to block antigen presentation, J. Exp. Med., 174 (1991) 1629-1637.

[91] L. R. Gooding, T. S. Ranheim, A. E. Tollefson, L. Aquino, P. Duerksen-Hughes, T. M. Horton, and W. S. Wold, The 10,400- and 14,500-dalton proteins encoded by region E3 of adenovirus function together to protect many but not all mouse cell lines against lysis by tumor necrosis factor, J Virol, 65 (1991).

[92] J. Shisler, C. Yang, B. Walter, C. F. Ware, and L. R. Gooding, The adenovirus E3-10.4K/14.5K complex mediates loss of cell surface Fas (CD95) and resistance to Fas-induced apoptosis, J Virol, 71 (1997).

[93] H. G. Burgert, Z. Ruzsics, S. Obermeier, A. Hilgendorf, M. Windheim, and A. Elsing, Subversion of host defense mechanisms by adenoviruses, Curr. Top. Microbiol. Immunol., 269 (2002) 273-318.

[94] R. N. de Jong, P. C. van der Vliet, and A. B. Brenkman, Adenovirus DNA replication: protein priming, jumping back and the role of the DNA binding protein DBP, Curr Top Microbiol Immunol, 272 (2003).

[95] M. D. Weiden and H. S. Ginsberg, Deletion of the E4 region of the genome produces adenovirus DNA concatemers, Proc. Natl. Acad. Sci. U. S. A, 91 (1994) 153-157.

[96] T. H. Stracker, C. T. Carson, and M. D. Weitzman, Adenovirus oncoproteins inactivate the Mre11-Rad50-NBS1 DNA repair complex, Nature, 418 (2002) 348-352.

[97] D. C. Farley, J. L. Brown, and K. N. Leppard, Activation of the early-late switch in adenovirus type 5 major late transcription unit expression by L4 gene products, J. Virol., 78 (2004) 1782-1791.

[98] S. J. Morris and K. N. Leppard, Adenovirus serotype 5 L4-22K and L4-33K proteins have distinct functions in regulating late gene expression, J. Virol., 83 (2009) 3049-3058.

[99] P. Ostapchuk, M. E. Anderson, S. Chandrasekhar, and P. Hearing, The L4 22-kilodalton protein plays a role in packaging of the adenovirus genome, J. Virol., 80 (2006) 6973-6981.

[100] A. E. Tollefson, A. Scaria, T. W. Hermiston, J. S. Ryerse, L. J. Wold, and W. S. Wold, The adenovirus death protein (E3-11.6K) is required at very late stages of infection for efficient cell lysis and release of adenovirus from infected cells, J Virol, 70 (1996).

[101] A. Webster, R. T. Hay, and G. Kemp, The adenovirus protease is activated by a virus-coded disulphide-linked peptide, Cell, 72 (1993) 97-104.

[102] J. J. Cornelis, S. I. Lang, A. Y. Stroh-Dege, G. Balboni, C. Dinsart, and J. Rommelaere, Cancer gene therapy through autonomous parvovirus--mediated gene transfer, Curr. Gene Ther., 4 (2004) 249-261.

[103] J. Nemunaitis, I. Ganly, F. Khuri, J. Arseneau, J. Kuhn, T. McCarty, S. Landers, P. Maples, L. Romel, B. Randlev, T. Reid, S. Kaye, and D. Kirn, Selective replication and oncolysis in p53 mutant tumors with ONYX-015, an E1B-55kD gene-deleted adenovirus, in patients with advanced head and neck cancer: a phase II trial, Cancer Res., 60 (2000) 6359-6366.

[104] K. Toth, D. Dhar, and W. S. Wold, Oncolytic (replication-competent) adenoviruses as anticancer agents, Expert. Opin. Biol. Ther., 10 (2010) 353-368.

[105] S. Hemmi, R. Geertsen, A. Mezzacasa, I. Peter, and R. Dummer, The presence of human coxsackievirus and adenovirus receptor is associated with efficient adenovirus-mediated transgene expression in human melanoma cell cultures, Hum Gene Ther, 9 (1998).

[106] C. R. Miller, D. J. Buchsbaum, P. N. Reynolds, J. T. Douglas, G. Y. Gillespie, M. S. Mayo, D. Raben, and D. T. Curiel, Differential susceptibility of primary and established human glioma cells to adenovirus infection: targeting via the epidermal growth factor receptor achieves fiber receptor-independent gene transfer, Cancer Res, 58 (1998).

[107] Y. Li, R. C. Pong, J. M. Bergelson, M. C. Hall, A. I. Sagalowsky, C. P. Tseng, Z. Wang, and J. T. Hsieh, Loss of adenoviral receptor expression in human bladder cancer cells: a potential impact on the efficacy of gene therapy, Cancer Res, 59 (1999).

[108] J. T. Douglas, B. E. Rogers, M. E. Rosenfeld, S. I. Michael, M. Feng, and D. T. Curiel, Targeted gene delivery by tropism-modified adenoviral vectors, Nat. Biotechnol., 14 (1996) 1574-1578.

[109] P. W. Roelvink, G. Mi Lee, D. A. Einfeld, I. Kovesdi, and T. J. Wickham, Identification of a conserved receptor-binding site on the fiber proteins of CAR-recognizing adenoviridae, Science, 286 (1999).

[110] V. N. Krasnykh, G. V. Mikheeva, J. T. Douglas, and D. T. Curiel, Generation of recombinant adenovirus vectors with modified fibers for altering viral tropism, J Virol, 70 (1996).

[111] S. N. Waddington, J. H. McVey, D. Bhella, A. L. Parker, K. Barker, H. Atoda, R. Pink, S. M. Buckley, J. A. Greig, L. Denby, J. Custers, T. Morita, I. M. Francischetti, R. Q. Monteiro, D. H. Barouch, R. N. van, C. Napoli, M. J. Havenga, S. A. Nicklin, and A. H. Baker, Adenovirus serotype 5 hexon mediates liver gene transfer, Cell, 132 (2008) 397-409.

[112] R. Alba, A. C. Bradshaw, A. L. Parker, D. Bhella, S. N. Waddington, S. A. Nicklin, R. N. van, J. Custers, J. Goudsmit, D. H. Barouch, J. H. McVey, and A. H. Baker, Identification of coagulation factor (F)X binding sites on the adenovirus serotype 5 hexon: effect of mutagenesis on FX interactions and gene transfer, Blood, 114 (2009) 965-971.

[113] F. Kreppel and S. Kochanek, Modification of adenovirus gene transfer vectors with synthetic polymers: a scientific review and technical guide, Mol. Ther., 16 (2008) 16-29.

[114] D. A. Einfeld, D. E. Brough, P. W. Roelvink, I. Kovesdi, and T. J. Wickham, Construction of a pseudoreceptor that mediates transduction by adenoviruses expressing a ligand in fiber or penton base, J. Virol., 73 (1999) 9130-9136.

[115] I. P. Dmitriev, E. A. Kashentseva, and D. T. Curiel, Engineering of adenovirus vectors containing heterologous peptide sequences in the C terminus of capsid protein IX, J. Virol., 76 (2002) 6893-6899.

[116] I. Dmitriev, V. Krasnykh, C. R. Miller, M. Wang, E. Kashentseva, G. Mikheeva, N. Belousova, and D. T. Curiel, An adenovirus vector with genetically modified fibers demonstrates expanded tropism via utilization of a coxsackievirus and adenovirus receptor-independent cell entry mechanism, J Virol, 72 (1998).

[117] Y. Yoshida, A. Sadata, W. Zhang, K. Saito, N. Shinoura, and H. Hamada, Generation of fiber-mutant recombinant adenoviruses for gene therapy of malignant glioma, Hum Gene Ther, 9 (1998).

[118] D. M. Shayakhmetov, T. Papayannopoulou, G. Stamatoyannopoulos, and A. Lieber, Efficient gene transfer into human CD34(+) cells by a retargeted adenovirus vector, J Virol, 74 (2000).

[119] A. Hesse, D. Kosmides, R. E. Kontermann, and D. M. Nettelbeck, Tropism modification of adenovirus vectors by peptide ligand insertion into various positions of the adenovirus serotype 41 short-fiber knob domain, J. Virol., 81 (2007) 2688-2699.

[120] T. J. Vanderkwaak, M. Wang, J. Gomez-Navarro, C. Rancourt, I. Dmitriev, V. Krasnykh, M. Barnes, G. P. Siegal, R. Alvarez, and D. T. Curiel, An advanced generation of adenoviral vectors selectively enhances gene transfer for ovarian cancer gene therapy approaches, Gynecol Oncol, 74 (1999).

[121] K. Kasono, J. L. Blackwell, J. T. Douglas, I. Dmitriev, T. V. Strong, P. Reynolds, D. A. Kropf, W. R. Carroll, G. E. Peters, R. P. Bucy, D. T. Curiel, and V. Krasnykh, Selective gene delivery to head and neck cancer cells via an integrin targeted adenoviral vector, Clin Cancer Res, 5 (1999).

[122] J. Grill, V. W. Van Beusechem, P. Van Der Valk, C. M. Dirven, A. Leonhart, D. S. Pherai, H. J. Haisma, H. M. Pinedo, D. T. Curiel, and W. R. Gerritsen, Combined targeting of adenoviruses to integrins and epidermal growth factor receptors increases gene transfer into primary glioma cells and spheroids, Clin Cancer Res, 7 (2001).

[123] J. G. Wesseling, P. J. Bosma, V. Krasnykh, E. A. Kashentseva, J. L. Blackwell, P. N. Reynolds, H. Li, M. Parameshwar, S. M. Vickers, E. M. Jaffee, K. Huibregtse, D. T. Curiel, and I. Dmitriev, Improved gene transfer efficiency to primary and established human pancreatic carcinoma target cells via epidermal growth factor receptor and integrin-targeted adenoviral vectors, Gene Ther, 8 (2001).

[124] A. A. Rivera, J. Davydova, S. Schierer, M. Wang, V. Krasnykh, M. Yamamoto, D. T. Curiel, and D. M. Nettelbeck, Combining high selectivity of replication with fiber chimerism for effective adenoviral oncolysis of CAR-negative melanoma cells, Gene Ther, 11 (2004).

[125] H. J. Haisma, J. Grill, D. T. Curiel, S. Hoogeland, V. W. Van Beusechem, H. M. Pinedo, and W. R. Gerritsen, Targeting of adenoviral vectors through a bispecific single-chain antibody, Cancer Gene Ther., 7 (2000) 901-904.

[126] D. M. Nettelbeck, D. W. Miller, V. Jerome, M. Zuzarte, S. J. Watkins, R. E. Hawkins, R. Muller, and R. E. Kontermann, Targeting of adenovirus to endothelial cells by a bispecific single-chain diabody directed against the adenovirus fiber knob domain and human endoglin (CD105), Mol Ther, 3 (2001).

[127] K. W. Peng, K. A. Donovan, U. Schneider, R. Cattaneo, J. A. Lust, and S. J. Russell, Oncolytic measles viruses displaying a single-chain antibody against CD38, a myeloma cell marker, Blood, 101 (2003) 2557-2562.

[128] A. D. Bucheit, S. Kumar, D. M. Grote, Y. Lin, M. von, V, R. B. Cattaneo, and A. K. Fielding, An oncolytic measles virus engineered to enter cells through the CD20 antigen, Mol. Ther., 7 (2003) 62-72.

[129] D. M. Nettelbeck, Cellular genetic tools to control oncolytic adenoviruses for virotherapy of cancer, J Mol Med, 86 (2008).

[130] A. Ahmed, J. Thompson, L. Emiliusen, S. Murphy, R. D. Beauchamp, K. Suzuki, R. Alemany, K. Harrington, and R. G. Vile, A conditionally replicating adenovirus targeted to tumor cells through activated RAS/P-MAPK-selective mRNA stabilization, Nat. Biotechnol., 21 (2003) 771-777.

[131] M. A. Stoff-Khalili, A. A. Rivera, A. Nedeljkovic-Kurepa, A. DeBenedetti, X. L. Li, Y. Odaka, J. Podduturi, D. A. Sibley, G. P. Siegal, A. Stoff, S. Young, Z. B. Zhu, D. T. Curiel, and J. M. Mathis, Cancer-specific targeting of a conditionally replicative adenovirus using mRNA translational control, Breast Cancer Res. Treat., 108 (2008) 43-55.

[132] E. J. Kelly, E. M. Hadac, S. Greiner, and S. J. Russell, Engineering microRNA responsiveness to decrease virus pathogenicity, Nat. Med., 14 (2008) 1278-1283.

[133] R. Rodriguez, E. R. Schuur, H. Y. Lim, G. A. Henderson, J. W. Simons, and D. R. Henderson, Prostate attenuated replication competent adenovirus (ARCA) CN706: a selective cytotoxic for prostate-specific antigen-positive prostate cancer cells, Cancer Res, 57 (1997).

[134] P. L. Hallenbeck, Y. N. Chang, C. Hay, D. Golightly, D. Stewart, J. Lin, S. Phipps, and Y. L. Chiang, A novel tumor-specific replication-restricted adenoviral vector for gene therapy of hepatocellular carcinoma, Hum Gene Ther, 10 (1999).

[135] N. S. Banerjee, A. A. Rivera, M. Wang, L. T. Chow, T. R. Broker, D. T. Curiel, and D. M. Nettelbeck, Analyses of melanoma-targeted oncolytic adenoviruses with tyrosinase enhancer/promoter-driven E1A, E4, or both in submerged cells and organotypic cultures, Mol Cancer Ther, 3 (2004).

[136] T. Kurihara, D. E. Brough, I. Kovesdi, and D. W. Kufe, Selectivity of a replication-competent adenovirus for human breast carcinoma cells expressing the MUC1 antigen, J Clin Invest, 106 (2000).

[137] Y. Li, D. C. Yu, Y. Chen, P. Amin, H. Zhang, N. Nguyen, and D. R. Henderson, A hepatocellular carcinoma-specific adenovirus variant, CV890, eliminates distant human liver tumors in combination with doxorubicin, Cancer Res, 61 (2001).

[138] C. L. Hsieh, L. Yang, L. Miao, F. Yeung, C. Kao, H. Yang, H. E. Zhau, and L. W. Chung, A novel targeting modality to enhance adenoviral replication by vitamin D(3) in androgen-independent human prostate cancer cells and tumors, Cancer Res., 62 (2002) 3084-3092.

[139] R. Hernandez-Alcoceba, M. Pihalja, D. Qian, and M. F. Clarke, New oncolytic adenoviruses with hypoxia- and estrogen receptor-regulated replication, Hum. Gene Ther., 13 (2002) 1737-1750.

[140] X. Li, Y. P. Zhang, H. S. Kim, K. H. Bae, K. M. Stantz, S. J. Lee, C. Jung, J. A. Jimenez, T. A. Gardner, M. H. Jeng, and C. Kao, Gene therapy for prostate cancer by controlling adenovirus E1a and E4 gene expression with PSES enhancer, Cancer Res., 65 (2005) 1941-1951.

[141] L. Hatfield and P. Hearing, Redundant elements in the adenovirus type 5 inverted terminal repeat promote bidirectional transcription in vitro and are important for virus growth in vivo, Virology, 184 (1991).

[142] V. J. Miralles, P. Cortes, N. Stone, and D. Reinberg, The adenovirus inverted terminal repeat functions as an enhancer in a cell-free system, J Biol Chem, 264 (1989).

[143] D. Hoffmann, C. Jogler, and O. Wildner, Effects of the Ad5 upstream E1 region and gene products on heterologous promoters, J Gene Med, 7 (2005).

[144] A. Hurtado Pico, X. Wang, I. Sipo, U. Siemetzki, J. Eberle, W. Poller, and H. Fechner, Viral and nonviral factors causing nonspecific replication of tumor- and tissue-specific promoter-dependent oncolytic adenoviruses, Mol Ther, 11 (2005).

[145] G. Vassaux, H. C. Hurst, and N. R. Lemoine, Insulation of a conditionally expressed transgene in an adenoviral vector, Gene Ther, 6 (1999).

[146] P. Martin-Duque, S. Jezzard, L. Kaftansis, and G. Vassaux, Direct comparison of the insulating properties of two genetic elements in an adenoviral vector containing two different expression cassettes, Hum Gene Ther, 15 (2004).

[147] A. G. West, M. Gaszner, and G. Felsenfeld, Insulators: many functions, many mechanisms, Genes Dev, 16 (2002).

[148] D. S. Steinwaerder and A. Lieber, Insulation from viral transcriptional regulatory elements improves inducible transgene expression from adenovirus vectors in vitro and in vivo, Gene Ther, 7 (2000).

[149] M. Yamamoto, J. Davydova, K. Takayama, R. Alemany, and D. T. Curiel, Transcription initiation activity of adenovirus left-end sequence in adenovirus vectors with e1 deleted, J Virol, 77 (2003).

[150] I. Horikawa, P. L. Cable, C. Afshari, and J. C. Barrett, Cloning and characterization of the promoter region of human telomerase reverse transcriptase gene, Cancer Res., 59 (1999) 826-830.

[151] J. R. Bischoff, D. H. Kirn, A. Williams, C. Heise, S. Horn, M. Muna, L. Ng, J. A. Nye, A. Sampson-Johannes, A. Fattaey, and F. McCormick, An adenovirus mutant that replicates selectively in p53-deficient human tumor cells, Science, 274 (1996).

[152] C. C. O'Shea, L. Johnson, B. Bagus, S. Choi, C. Nicholas, A. Shen, L. Boyle, K. Pandey, C. Soria, J. Kunich, Y. Shen, G. Habets, D. Ginzinger, and F. McCormick, Late viral RNA export, rather than p53 inactivation, determines ONYX-015 tumor selectivity, Cancer Cell, 6 (2004).

[153] C. C. O'Shea, Viruses - seeking and destroying the tumor program, Oncogene, 24 (2005).

[154] J. Fueyo, M. C. Gomez, R. Alemany, P. S. Lee, T. J. McDonnell, P. Mitlianga, Y. X. Shi, V. A. Levin, W. K. Yung, and A. P. Kyritsis, A mutant oncolytic adenovirus targeting the Rb pathway produces anti- glioma effect in vivo., Oncogene, 19 (2000).

[155] C. C. Heise, A. Williams, J. Olesch, and D. H. Kirn, Efficacy of a replication-competent adenovirus (ONYX-015) following intratumoral injection: intratumoral spread and distribution effects, Cancer Gene Ther, 6 (1999).

[156] R. Strauss and A. Lieber, Anatomical and physical barriers to tumor targeting with oncolytic adenoviruses in vivo, Curr. Opin. Mol. Ther., 11 (2009) 513-522.

[157] T. Tanaka, N. Yamanaka, T. Oriyama, K. Furukawa, and E. Okamoto, Factors regulating tumor pressure in hepatocellular carcinoma and implications for tumor spread, Hepatology, 26 (1997).

[158] C. M. Southam and A. E. Moore, Clinical studies of viruses as antineoplastic agents with particular reference to Egypt 101 virus, Cancer, 5 (1952).

[159] V. Juillard, P. Villefroy, D. Godfrin, A. Pavirani, A. Venet, and J. G. Guillet, Long-term humoral and cellular immunity induced by a single immunization with replication-defective adenovirus recombinant vector, Eur. J. Immunol., 25 (1995) 3467-3473.

[160] N. K. Green and L. W. Seymour, Adenoviral vectors: systemic delivery and tumor targeting, Cancer Gene Ther, 9 (2002).

[161] H. Fechner, A. Haack, H. Wang, X. Wang, K. Eizema, M. Pauschinger, R. Schoemaker, R. Veghel, A. Houtsmuller, H. P. Schultheiss, J. Lamers, and W. Poller, Expression of coxsackie adenovirus receptor and alphav-integrin does not correlate with adenovector targeting in vivo indicating anatomical vector barriers, Gene Ther, 6 (1999).

[162] K. M. Bernt, S. Ni, A. Gaggar, Z. Y. Li, D. M. Shayakhmetov, and A. Lieber, The effect of sequestration by nontarget tissues on anti-tumor efficacy of systemically applied, conditionally replicating adenovirus vectors, Mol Ther, 8 (2003).

[163] Q. Liu and D. A. Muruve, Molecular basis of the inflammatory response to adenovirus vectors, Gene Ther, 10 (2003).

[164] T. D. McKee, P. Grandi, W. Mok, G. Alexandrakis, N. Insin, J. P. Zimmer, M. G. Bawendi, Y. Boucher, X. O. Breakefield, and R. K. Jain, Degradation of fibrillar collagen in a human melanoma xenograft improves the efficacy of an oncolytic herpes simplex virus vector, Cancer Res, 66 (2006).

[165] W. Mok, Y. Boucher, and R. K. Jain, Matrix metalloproteinases-1 and -8 improve the distribution and efficacy of an oncolytic virus, Cancer Res, 67 (2007).

[166] R. Bilbao, M. Bustos, P. Alzuguren, M. J. Pajares, M. Drozdzik, C. Qian, and J. Prieto, A blood-tumor barrier limits gene transfer to experimental liver cancer: the effect of vasoactive compounds, Gene Ther, 7 (2000).

[167] A. Rahman, V. Tsai, A. Goudreau, J. Y. Shinoda, S. F. Wen, M. Ramachandra, R. Ralston, D. Maneval, D. LaFace, and P. Shabram, Specific depletion of human anti-adenovirus antibodies facilitates transduction in an in vivo model for systemic gene therapy, Mol. Ther., 3 (2001) 768-778.

[168] K. Ikeda, T. Ichikawa, H. Wakimoto, J. S. Silver, T. S. Deisboeck, D. Finkelstein, G. R. Harsh, D. N. Louis, R. T. Bartus, F. H. Hochberg, and E. A. Chiocca, Oncolytic virus therapy of multiple tumors in the brain requires suppression of innate and elicited antiviral responses, Nat. Med., 5 (1999) 881-887.

[169] S. Roy, P. S. Shirley, A. McClelland, and M. Kaleko, Circumvention of immunity to the adenovirus major coat protein hexon, J. Virol., 72 (1998) 6875-6879.

[170] D. M. Roberts, A. Nanda, M. J. Havenga, P. Abbink, D. M. Lynch, B. A. Ewald, J. Liu, A. R. Thorner, P. E. Swanson, D. A. Gorgone, M. A. Lifton, A. A. Lemckert, L. Holterman, B. Chen, A. Dilraj, A. Carville, K. G. Mansfield, J. Goudsmit, and D. H. Barouch, Hexon-chimaeric adenovirus serotype 5 vectors circumvent pre-existing anti-vector immunity, Nature, 441 (2006) 239-243.

[171] G. Chinnadurai, Adenovirus 2 Ip+ locus codes for a 19 kd tumor antigen that plays an essential role in cell transformation, Cell, 33 (1983).

[172] H. Sauthoff, S. Heitner, W. N. Rom, and J. G. Hay, Deletion of the adenoviral E1b-19kD gene enhances tumor cell killing of a replicating adenoviral vector, Hum Gene Ther, 11 (2000).

[173] M. Schmitz, C. Graf, T. Gut, D. Sirena, I. Peter, R. Dummer, U. F. Greber, and S. Hemmi, Melanoma cultures show different susceptibility towards E1A-, E1B-19 kDa- and fiber-modified replication-competent adenoviruses, Gene Ther, 13 (2006).

[174] S. Rohmer, C. Quirin, A. Hesse, S. Sandmann, W. Bayer, C. Herold-Mende, Y. S. Haviv, O. Wildner, A. H. Enk, and D. M. Nettelbeck, Transgene expression by oncolytic adenoviruses is modulated by E1B19K deletion in a cell type-dependent manner, Virology, 395 (2009).

[175] K. Doronin, K. Toth, M. Kuppuswamy, P. Ward, A. E. Tollefson, and W. S. Wold, Tumor-specific, replication-competent adenovirus vectors overexpressing the adenovirus death protein, J Virol, 74 (2000).

[176] M. Kuppuswamy, J. F. Spencer, K. Doronin, A. E. Tollefson, W. S. Wold, and K. Toth, Oncolytic adenovirus that overproduces ADP and replicates selectively in tumors due to hTERT promoter-regulated E4 gene expression, Gene Ther, 12 (2005).

[177] M. Chase, R. Y. Chung, and E. A. Chiocca, An oncolytic viral mutant that delivers the CYP2B1 transgene and augments cyclophosphamide chemotherapy, Nat. Biotechnol., 16 (1998) 444-448.

[178] O. Wildner, R. M. Blaese, and J. C. Morris, Therapy of colon cancer with oncolytic adenovirus is enhanced by the addition of herpes simplex virus-thymidine kinase, Cancer Res, 59 (1999).

[179] A. Merron, I. Peerlinck, P. Martin-Duque, J. Burnet, M. Quintanilla, S. Mather, M. Hingorani, K. Harrington, R. Iggo, and G. Vassaux, SPECT/CT imaging of oncolytic adenovirus propagation in tumours in vivo using the Na/I symporter as a reporter gene, Gene Ther., 14 (2007) 1731-1738.

[180] J. A. Bristol, M. Zhu, H. Ji, M. Mina, Y. Xie, L. Clarke, S. Forry-Schaudies, and D. L. Ennist, In vitro and in vivo activities of an oncolytic adenoviral vector designed to express GM-CSF, Mol. Ther., 7 (2003) 755-764.

[181] Y. S. Lee, J. H. Kim, K. J. Choi, I. K. Choi, H. Kim, S. Cho, B. C. Cho, and C. O. Yun, Enhanced antitumor effect of oncolytic adenovirus expressing interleukin-12 and B7-1 in an immunocompetent murine model, Clin. Cancer Res., 12 (2006) 5859-5868.

[182] P. Sova, X. W. Ren, S. Ni, K. M. Bernt, J. Mi, N. Kiviat, and A. Lieber, A tumor-targeted and conditionally replicating oncolytic adenovirus vector expressing TRAIL for treatment of liver metastases, Mol. Ther., 9 (2004) 496-509.

[183] J. H. Kim, Y. S. Lee, H. Kim, J. H. Huang, A. R. Yoon, and C. O. Yun, Relaxin expression from tumor-targeting adenoviruses and its intratumoral spread, apoptosis induction, and efficacy, J. Natl. Cancer Inst., 98 (2006) 1482-1493.

[184] F. Puhler, J. Willuda, J. Puhlmann, D. Mumberg, A. Romer-Oberdorfer, and R. Beier, Generation of a recombinant oncolytic Newcastle disease virus and expression of a full IgG antibody from two transgenes, Gene Ther., 15 (2008) 371-383.

[185] O. H. Brekke and I. Sandlie, Therapeutic antibodies for human diseases at the dawn of the twenty-first century, Nat. Rev. Drug Discov., 2 (2003) 52-62.

[186] S. Dubel, Recombinant therapeutic antibodies, Appl. Microbiol. Biotechnol., 74 (2007) 723-729.

[187] N. Congy-Jolivet, A. Probst, H. Watier, and G. Thibault, Recombinant therapeutic monoclonal antibodies: mechanisms of action in relation to structural and functional duality, Crit Rev. Oncol. Hematol., 64 (2007) 226-233.

[188] P. Carter, Improving the efficacy of antibody-based cancer therapies, Nat. Rev. Cancer, 1 (2001) 118-129.

[189] A. M. Wu and P. D. Senter, Arming antibodies: prospects and challenges for immunoconjugates, Nat. Biotechnol., 23 (2005) 1137-1146.

[190] T. E. Witzig, C. A. White, G. A. Wiseman, L. I. Gordon, C. Emmanouilides, A. Raubitschek, N. Janakiraman, J. Gutheil, R. J. Schilder, S. Spies, D. H. Silverman, E. Parker, and A. J. Grillo-Lopez, Phase I/II trial of IDEC-Y2B8 radioimmunotherapy for treatment of relapsed or refractory CD20(+) B-cell non-Hodgkin's lymphoma, J. Clin. Oncol., 17 (1999) 3793-3803.

[191] Illumina. Product Guide. 2009.
Ref Type: Online Source

[192] Illumina. Technical Bulletin: Gene Expression Profiling with Sentrix® Focused Arrays. 2009.
Ref Type: Online Source

[193] A. L. Volk, A. A. Rivera, G. P. Page, J. F. Salazar-Gonzalez, D. M. Nettelbeck, Q. L. Matthews, and D. T. Curiel, Employment of microarray analysis to characterize biologic differences associated with tropism-modified adenoviral vectors: utilization of non-native cellular entry pathways, Cancer Gene Ther., 12 (2005) 162-174.

[194] H. Zhao, F. Granberg, L. Elfineh, U. Pettersson, and C. Svensson, Strategic attack on host cell gene expression during adenovirus infection, J. Virol., 77 (2003) 11006-11015.

[195] H. Zhao, F. Granberg, and U. Pettersson, How adenovirus strives to control cellular gene expression, Virology, 363 (2007) 357-375.

[196] Z. C. Hartman, A. Kiang, R. S. Everett, D. Serra, X. Y. Yang, T. M. Clay, and A. Amalfitano, Adenovirus infection triggers a rapid, MyD88-regulated transcriptome response critical to acute-phase and adaptive immune responses in vivo, J. Virol., 81 (2007) 1796-1812.

[197] F. Granberg, C. Svensson, U. Pettersson, and H. Zhao, Modulation of host cell gene expression during onset of the late phase of an adenovirus infection is focused on growth inhibition and cell architecture, Virology, 343 (2005) 236-245.

[198] K. B. Spurgers, K. R. Coombes, R. E. Meyn, D. L. Gold, C. J. Logothetis, T. J. Johnson, and T. J. McDonnell, A comprehensive assessment of p53-responsive genes following adenoviral-p53 gene transfer in Bcl-2-expressing prostate cancer cells, Oncogene, 23 (2004) 1712-1723.

[199] H. Hao, Y. B. Dong, M. T. Bowling, H. S. Zhou, and K. M. McMasters, Alteration of gene expression in melanoma cells following combined treatment with E2F-1 and doxorubicin, Anticancer Res., 26 (2006) 1947-1956.

[200] T. Sato, H. Odagiri, S. K. Ikenaga, M. Maruyama, and M. Sasaki, Chemosensitivity of human pancreatic carcinoma cells is enhanced by IkappaBalpha super-repressor, Cancer Sci., 94 (2003) 467-472.

[201] M. Rajecki, H. T. af, T. Hakkarainen, P. Nokisalmi, S. Hautaniemi, A. I. Nieminen, M. Tenhunen, V. Rantanen, R. A. Desmond, D. T. Chen, K. Guse, U. H. Stenman, R. Gargini, M. Kapanen, J. Klefstrom, A. Kanerva, S. Pesonen, L. Ahtiainen, and A. Hemminki, Mre11 inhibition by oncolytic

adenovirus associates with autophagy and underlies synergy with ionizing radiation, Int. J. Cancer, 125 (2009) 2441-2449.

[202] V. Monsurro, S. Beghelli, R. Wang, S. Barbi, S. Coin, P. G. Di, S. Bersani, M. Castellucci, C. Sorio, S. Eleuteri, A. Worschech, J. A. Chiorini, P. Pederzoli, H. Alter, F. M. Marincola, and A. Scarpa, Anti-viral state segregates two molecular phenotypes of pancreatic adenocarcinoma: potential relevance for adenoviral gene therapy, J. Transl. Med., 8 (2010) 10.

[203] K. R. Spindler, C. Y. Eng, and A. J. Berk, An adenovirus early region 1A protein is required for maximal viral DNA replication in growth-arrested human cells, J. Virol., 53 (1985) 742-750.

[204] K. Fellenberg, N. C. Hauser, B. Brors, A. Neutzner, J. D. Hoheisel, and M. Vingron, Correspondence analysis applied to microarray data, Proc. Natl. Acad. Sci. U. S. A, 98 (2001) 10781-10786.

[205] Yoav Benjamini and Yosef Hochberg, Controling the False Discovery Rate: A practical and powerful approach to multiple testing, Journal of the Royal Statistical Society, Series B (Methodological), (1995) 289-300.

[206] S. M. Elbashir, J. Harborth, W. Lendeckel, A. Yalcin, K. Weber, and T. Tuschl, Duplexes of 21-nucleotide RNAs mediate RNA interference in cultured mammalian cells, Nature, 411 (2001) 494-498.

[207] J. C. Clemens, C. A. Worby, N. Simonson-Leff, M. Muda, T. Maehama, B. A. Hemmings, and J. E. Dixon, Use of double-stranded RNA interference in Drosophila cell lines to dissect signal transduction pathways, Proc. Natl. Acad. Sci. U. S. A, 97 (2000) 6499-6503.

[208] P. J. Paddison, J. M. Silva, D. S. Conklin, M. Schlabach, M. Li, S. Aruleba, V. Balija, A. O'Shaughnessy, L. Gnoj, K. Scobie, K. Chang, T. Westbrook, M. Cleary, R. Sachidanandam, W. R. McCombie, S. J. Elledge, and G. J. Hannon, A resource for large-scale RNA-interference-based screens in mammals, Nature, 428 (2004) 427-431.

[209] M. Shiina, M. D. Lacher, C. Christian, and W. M. Korn, RNA interference-mediated knockdown of p21(WAF1) enhances anti-tumor cell activity of oncolytic adenoviruses, Cancer Gene Ther., 16 (2009) 810-819.

[210] K. M. Bernt, D. S. Steinwaerder, S. Ni, Z. Y. Li, S. R. Roffler, and A. Lieber, Enzyme-activated Prodrug Therapy Enhances Tumor-specific Replication of Adenovirus Vectors, Cancer Res., 62 (2002) 6089-6098.

[211] M. M. Alonso, C. Gomez-Manzano, H. Jiang, N. B. Bekele, Y. Piao, W. K. Yung, R. Alemany, and J. Fueyo, Combination of the oncolytic adenovirus ICOVIR-5 with chemotherapy provides enhanced anti-glioma effect in vivo, Cancer Gene Ther., 14 (2007) 756-761.

[212] C. Quirin, A. Mainka, A. Hesse, and D. M. Nettelbeck, Combining adenoviral oncolysis with temozolomide improves cell killing of melanoma cells, Int J Cancer, 121 (2007).

[213] S. K. Jang, H. G. Krausslich, M. J. Nicklin, G. M. Duke, A. C. Palmenberg, and E. Wimmer, A segment of the 5' nontranslated region of encephalomyocarditis virus RNA directs internal entry of ribosomes during in vitro translation, J. Virol., 62 (1988) 2636-2643.

[214] E. Martinez-Salas, Internal ribosome entry site biology and its use in expression vectors, Curr. Opin. Biotechnol., 10 (1999) 458-464.

[215] A. A. Rivera, M. Wang, K. Suzuki, T. G. Uil, V. Krasnykh, D. T. Curiel, and D. M. Nettelbeck, Mode of transgene expression after fusion to early or late viral genes of a conditionally replicating adenovirus via an optimized internal ribosome entry site in vitro and in vivo, Virology, 320 (2004).

[216] G. E. UNDERWOOD, Activity of 1-beta-D-arabinofuranosylcytosine hydrochloride against herpes simplex keratitis, Proc. Soc. Exp. Biol. Med., 111 (1962) 660-664.

[217] S. S. Cohen, The mechanisms of lethal action of arabinosyl cytosine (araC) and arabinosyl adenine (araA), Cancer, 40 (1977) 509-518.

[218] S. A. Weston and C. R. Parish, New fluorescent dyes for lymphocyte migration studies. Analysis by flow cytometry and fluorescence microscopy, J. Immunol. Methods, 133 (1990) 87-97.

[219] Y. Wang, S. A. Xue, G. Hallden, J. Francis, M. Yuan, B. E. Griffin, and N. R. Lemoine, Virus-associated RNA I-deleted adenovirus, a potential oncolytic agent targeting EBV-associated tumors, Cancer Res., 65 (2005) 1523-1531.

[220] T. C. Liu, G. Hallden, Y. Wang, G. Brooks, J. Francis, N. Lemoine, and D. Kirn, An E1B-19 kDa gene deletion mutant adenovirus demonstrates tumor necrosis factor-enhanced cancer selectivity and enhanced oncolytic potency, Mol. Ther., 9 (2004) 786-803.

[221] D. Oberg, E. Yanover, V. Adam, K. Sweeney, C. Costas, N. R. Lemoine, and G. Hallden, Improved potency and selectivity of an oncolytic E1ACR2 and E1B19K deleted adenoviral mutant in prostate and pancreatic cancers, Clin. Cancer Res., 16 (2010) 541-553.

[222] D. M. Nettelbeck, A. A. Rivera, C. Balague, R. Alemany, and D. T. Curiel, Novel oncolytic adenoviruses targeted to melanoma: specific viral replication and cytolysis by expression of E1A mutants from the tyrosinase enhancer/promoter, Cancer Res, 62 (2002).

[223] F. Granberg, C. Svensson, U. Pettersson, and H. Zhao, Adenovirus-induced alterations in host cell gene expression prior to the onset of viral gene expression, Virology, 353 (2006) 1-5.

[224] C. Johansson, H. Zhao, E. Bajak, F. Granberg, U. Pettersson, and C. Svensson, Impact of the interaction between adenovirus E1A and CtBP on host cell gene expression, Virus Res., 113 (2005) 51-63.

[225] D. L. Miller, C. L. Myers, B. Rickards, H. A. Coller, and S. J. Flint, Adenovirus type 5 exerts genome-wide control over cellular programs governing proliferation, quiescence, and survival, Genome Biol., 8 (2007) R58.

[226] X. M. Rao, X. Zheng, S. Waigel, W. Zacharias, K. M. McMasters, and H. S. Zhou, Gene expression profiles of normal human lung cells affected by adenoviral E1B, Virology, 350 (2006) 418-428.

[227] D. G. Johnson, K. Ohtani, and J. R. Nevins, Autoregulatory control of E2F1 expression in response to positive and negative regulators of cell cycle progression, Genes Dev., 8 (1994) 1514-1525.

[228] M. J. Parr, Y. Manome, T. Tanaka, P. Wen, D. W. Kufe, W. G. Kaelin, Jr., and H. A. Fine, Tumor-selective transgene expression in vivo mediated by an E2F-responsive adenoviral vector, Nat. Med., 3 (1997) 1145-1149.

[229] W. Yan, G. Kitzes, F. Dormishian, L. Hawkins, A. Sampson-Johannes, J. Watanabe, J. Holt, V. Lee, T. Dubensky, A. Fattaey, T. Hermiston, A. Balmain, and Y. Shen, Developing novel oncolytic adenoviruses through bioselection, J Virol, 77 (2003).

[230] A. Gros, J. Martinez-Quintanilla, C. Puig, S. Guedan, D. G. Mollevi, R. Alemany, and M. Cascallo, Bioselection of a gain of function mutation that enhances adenovirus 5 release and improves its antitumoral potency, Cancer Res, 68 (2008).

[231] T. G. Uil, J. Vellinga, V. J. de, S. K. van den Hengel, M. J. Rabelink, S. J. Cramer, J. J. Eekels, Y. Ariyurek, G. M. van, and R. C. Hoeben, Directed adenovirus evolution using engineered mutator viral polymerases, Nucleic Acids Res., (2010).

[232] C. A. Moody and L. A. Laimins, Human papillomavirus oncoproteins: pathways to transformation, Nat. Rev. Cancer, 10 (2010) 550-560.

[233] E. W. Verschuren, N. Jones, and G. I. Evan, The cell cycle and how it is steered by Kaposi's sarcoma-associated herpesvirus cyclin, J. Gen. Virol., 85 (2004) 1347-1361.

[234] P. Saha, Q. Eichbaum, E. D. Silberman, B. J. Mayer, and A. Dutta, p21CIP1 and Cdc25A: competition between an inhibitor and an activator of cyclin-dependent kinases, Mol. Cell Biol., 17 (1997) 4338-4345.

[235] G. Makin and C. Dive, Recent advances in understanding apoptosis: new therapeutic opportunities in cancer chemotherapy, Trends Mol. Med., 9 (2003) 251-255.

[236] F. Al-Ejeh, R. Kumar, A. Wiegmans, S. R. Lakhani, M. P. Brown, and K. K. Khanna, Harnessing the complexity of DNA-damage response pathways to improve cancer treatment outcomes, Oncogene, 29 (2010) 6085-6098.

[237] K. Homicsko, A. Lukashev, and R. D. Iggo, RAD001 (everolimus) improves the efficacy of replicating adenoviruses that target colon cancer, Cancer Res., 65 (2005) 6882-6890.

[238] C. Fuerer and R. Iggo, 5-Fluorocytosine increases the toxicity of Wnt-targeting replicating adenoviruses that express cytosine deaminase as a late gene, Gene Ther., 11 (2004).

[239] E. Bajetta, V. M. Del, C. Bernard-Marty, M. Vitali, R. Buzzoni, O. Rixe, P. Nova, S. Aglione, S. Taillibert, and D. Khayat, Metastatic melanoma: chemotherapy, Semin. Oncol., 29 (2002) 427-445.

[240] B. Yamini, X. Yu, G. Y. Gillespie, D. W. Kufe, and R. R. Weichselbaum, Transcriptional targeting of adenovirally delivered tumor necrosis factor alpha by temozolomide in experimental glioblastoma, Cancer Res, 64 (2004).

[241] B. Kaur, T. P. Cripe, and E. A. Chiocca, "Buy one get one free": armed viruses for the treatment of cancer cells and their microenvironment, Curr. Gene Ther., 9 (2009) 341-355.

[242] E. Kievit, E. Bershad, E. Ng, P. Sethna, I. Dev, T. S. Lawrence, and A. Rehemtulla, Superiority of yeast over bacterial cytosine deaminase for enzyme/prodrug gene therapy in colon cancer xenografts, Cancer Res., 59 (1999) 1417-1421.

[243] D. Portsmouth, J. Hlavaty, and M. Renner, Suicide genes for cancer therapy, Mol. Aspects Med., 28 (2007) 4-41.

[244] A. H. Greenberg, L. Hudson, L. Shen, and I. M. Roitt, Antibody-dependent cell-mediated cytotoxicity due to a "null" lymphoid cell, Nat. New Biol., 242 (1973) 111-113.

[245] P. Perez, R. W. Hoffman, S. Shaw, J. A. Bluestone, and D. M. Segal, Specific targeting of cytotoxic T cells by anti-T3 linked to anti-target cell antibody, Nature, 316 (1985) 354-356.

[246] P. A. Baeuerle and C. Reinhardt, Bispecific T-cell engaging antibodies for cancer therapy, Cancer Res., 69 (2009) 4941-4944.

[247] J. J. Cody and J. T. Douglas, Armed replicating adenoviruses for cancer virotherapy, Cancer Gene Ther., 16 (2009) 473-488.

[248] D. M. Underhill and A. Ozinsky, Phagocytosis of microbes: complexity in action, Annu. Rev. Immunol., 20 (2002) 825-852.

[249] J. Davydova, L. P. Le, T. Gavrikova, M. Wang, V. Krasnykh, and M. Yamamoto, Infectivity-enhanced cyclooxygenase-2-based conditionally replicative adenoviruses for esophageal adenocarcinoma treatment, Cancer Res, 64 (2004).

[250] A. L. Szymczak, C. J. Workman, Y. Wang, K. M. Vignali, S. Dilioglou, E. F. Vanin, and D. A. Vignali, Correction of multi-gene deficiency in vivo using a single 'self-cleaving' 2A peptide-based retroviral vector, Nat. Biotechnol., 22 (2004) 589-594.

[251] C. Chartier, E. Degryse, M. Gantzer, A. Dieterle, A. Pavirani, and M. Mehtali, Efficient generation of recombinant adenovirus vectors by homologous recombination in Escherichia coli, J Virol, 70 (1996).

[252] J. Sambrook and D. W. Russell, Molecular cloning : a laboratory manual, Cold Spring Harbor Laboratory Press, Cold Spring Harbor, N.Y. 2001.

[253] J. Eberwine, H. Yeh, K. Miyashiro, Y. Cao, S. Nair, R. Finnell, M. Zettel, and P. Coleman, Analysis of gene expression in single live neurons, Proc. Natl. Acad. Sci. U. S. A, 89 (1992) 3010-3014.

[254] P. Simon, Q-Gene: processing quantitative real-time RT-PCR data, Bioinformatics., 19 (2003) 1439-1440.

[255] U. K. Laemmli, Cleavage of structural proteins during the assembly of the head of bacteriophage T4, Nature, 227 (1970).

[256] W. C. Lawrence and H. S. Ginsberg, Intracellular uncoating of type 5 adenovirus deoxyribonucleic acid, J. Virol., 1 (1967) 851-867.

[257] J. V. Maizel, Jr., D. O. White, and M. D. Scharff, The polypeptides of adenovirus. I. Evidence for multiple protein components in the virion and a comparison of types 2, 7A, and 12, Virology, 36 (1968) 115-125.

[258] G. Karber, 50% end-point calculation, Arch. Exp. Pathol. Pharmak, 162 (1931).

ACKNOWLEDGEMENTS

This work is dedicated to my parents Michael and Charlotte to whom I owe my deepest gratitude. Without their sacrifice, support, and faith in me throughout all the years of my life this would not have been possible. In the same way, my beloved Kathrin and my brother Benjamin helped me to keep up my spirits in difficult times and made everything so much easier than it might have been.

Furthermore, I would like to thank all my friends, in particular Jeffrey Berks, Richard Bueti, Luis Bernando González, Maximilian Mangel, David Kroeger, Thorsten Pflanzner, and the Heidelberg Hedgehogs who are like a second family to me. It is an honor to be among such people.

I am also obliged to those who made this thesis possible in the first place. Foremost, Dirk Nettelbeck who gave me the opportunity to work in his lab as well as Roland Kontermann and Jean Rommelaere who were part of my thesis advisory committee. They all provided excellent supervision and challenging scientific discussions throughout my work. Further, I am indebted to my many of my colleagues for supporting me. Special thanks go to all lab members, particularly Sarah Engelhardt for outstanding technical assistance, as well as Frank Holtrup, Kurt Fellenberg, and Jörg Hoheisel who enabled the microarray project and data interpretation.

Last but not least, I offer my regards and blessings to all of those who helped me in any respect during the completion of the project.

PUBLICATIONS

Targeting cancer by transcriptional control in cancer gene therapy and viral oncolysis.
Dorer DE, Nettelbeck DM.
Advanced Drug Delivery Reviews 2009 Jul 2;61(7-8):554-71

Kaposi's sarcoma-associated herpesvirus gH/gL: glycoprotein export and interaction with cellular receptors.
Hahn A, Birkmann A, Wies E, **Dorer D**, Mahr K, Stürzl M, Titgemeyer F, Neipel F.
Journal of Virology 2009 Jan;83(1):396-407

Lymphatic tracing and T cell responses following oral vaccination with live Mycobacterium bovis (BCG).
Dorer DE, Czepluch W, Lambeth MR, Dunn AC, Reitinger C, Aldwell FE, McLellan AD.
Cellular Microbiology 2007 Feb;9(2):544-53